UNIVERSIDAD MICHOACANA DE SAN NICOLÁS DE HIDALGO

DIVISION OF GRADUATE STUDIES

FACULTY OF ELECTRICAL ENGINEERING

THESIS

NONLINEAR OPTIMAL CONTROL IN COMBINATION WITH SLIDING MODES: APPLICATION TO UNDERACTUATED MECHANICAL SYSTEMS

In partial fulfillment of the requirements for the degree of

MASTER OF SCIENCE IN ELECTRICAL ENGINEERING

Presents

Serafín Ramos Paz

Thesis Advisor

Dr. Fernando Ornelas Tellez

Doctor of Philosophy

Morelia, Michoacán, August 2017

UNIVERSIDAD MICHOACANA DE SAN NICOLÁS DE HIDALGO

DIVISIÓN DE ESTUDIOS DE POSGRADO

FACULTAD DE INGENIERÍA ELÉCTRICA

TESIS

NONLINEAR OPTIMAL CONTROL IN COMBINATION WITH SLIDING MODES: APPLICATION TO UNDERACTUATED MECHANICAL SYSTEMS

Que para obtener el Título de

MAESTRO EN CIENCIAS EN INGENIERÍA ELÉCTRICA

Presenta

Serafín Ramos Paz

Director de Tesis

Dr. Fernando Ornelas Tellez

Doctor en Ciencias

Morelia, Michoacán, Agosto 2017

NONLINEAR OPTIMAL CONTROL IN COMBINATION WITH SLIDING MODES: APPLICATION TO UNDERACTUATED MECHANICAL SYSTEMS

Los Miembros del Jurado de Examen de Grado aprueban la **Tesis de Maestría en Ciencias en Ingeniería Eléctrica** de ***Serafín Ramos Paz***

Dr. J. Jesús Rico Melgoza
Presidente del Jurado

Dr. Fernando Ornelas Téllez
Director de Tesis

Dr. Roberto Tapia Sánchez
Vocal

Dr. Juan Anzurez Marín
Vocal

Dr. Salvador González García
Revisor Externo (ITESM)

Dr. Félix Calderón Solorio
Jefe de la División de Estudios de Posgrado de la Facultad de Ingeniería Eléctrica. UMSNH
(Por reconocimiento de firmas)

UNIVERSIDAD MICHOACANA DE SAN NICOLÁS DE HIDALGO
Agosto 2017

NONLINEAR OPTIMAL CONTROL IN COMBINATION WITH SLIDING MODES: APPLICATION TO UNDERACTUATED MECHANICAL SYSTEMS

THESIS

In partial fulfillment of the requirements for the degree of

MASTER OF SCIENCE IN ELECTRICAL ENGINEERING

Presents

Serafin Ramos Paz

Dr. Fernando Ornelas Tellez

Thesis Advisor

Universidad Michoacana de San Nicolás de Hidalgo

August 2017

Acknowledgments

To my Mother Elsa Mirella Paz Garibay and my father Antonio Ramos Yépez.

I would like to express my sincere gratitude to my teacher and thesis advisor Dr. Fernando Ornelas Tellez and to Dr. Alexander G. Loukianov from CINVESTAV for the continuous support of my Msc. study and related research, for their patience, motivation, and immense knowledge.

My sincere thanks also goes to Dr. Juan Anzurez Marin, Dr. Roberto Sanchez Tapia, who were my control teachers, to Dr. Jesus Rico Melgoza for his continuous observations throughout the development of this thesis, also to Dr. Felix Calderon Solorio, who gave me the opportunity to join the Electrical Engineering Graduate Studies Division of the UMSNH.

I would like to express my gratitude to my teachers from ITESM, M.c. Miguel Angel García Ruiz, M.c. Rubén Belmonte Izquierdo, M.Sc. Christian David Schindler, Dr. Enrique Aguayo Lara (Campus Guadalajara), Dr. Rosalino Rodriguez Calderon, Prof. Frank Donald Stonehouse and specially to Dr. Salvador Gonzalez García, who was my first control teacher and served as external reviewer of this work.

Special thanks to Dr. Antonio Ramos Paz, who has been always an example for me.

I would like to thank my sisters Beatriz Ramos Paz, Elsa Mireya Ramos Paz and Celia Maria Ramos Paz for supporting me throughout writing this thesis and my my life in general.

Thank you to my cousin Laura Arias and my aunt Laura Paz who helped me by providing me accomodation during my research stay at CINVESTAV Guadalajara.

Last but not the least, to Nuria Cortes Silva.

† This research as well as my Master of Science studies were funded by the Mexican Government CONACYT.

Resumen

Esta tesis, aborda la metodología de síntesis de un controlador óptimo no lineal robusto, con el fin de lograr la estabilización y seguimiento de trayectoria para una clase de sistemas mecánicos subactuados. La metodología de control estada basada en el uso de la factorización en coeficientes dependientes del estado, en donde la ecuación de Riccati dependiente del estado es usada para resolver el problema de control óptimo; de hecho, este enfoque podría ser considerado como la extensión no lineal del regulador cuadratico lineal. A posteriori, con la finalidad de mejorar la robustez del controlador, el control óptimo es combinado con modos deslizantes, para el diseño de una superficie de deslizamiento óptima para aquellos sistemas no lineales que puedan ser representados en la llamada forma regular, después la superficie de deslizamiento es utilizada para sintetizar un controlador de super-twisting. La efectividad de la técnica de control óptimo no lineal, es demostrada a través de simulaciones para el caso del Pendubot y a través de simulaciones y resultados de tiempo real para el caso del péndulo invertido rotacional, siendo ambos sistemas no lineales de fase no mínima. Sin embargo la metodología de control puede ser aplicada para el caso general de sistemas mecánicos subactuados. Cabe mencionar que a diferencia de trabajos relacionados para el control de sistemas subactuados, esta tesis presenta un mayor rango de control óptimo de seguimiento de trayectoria para la variable a controlar, lo que es logrado a través de la solución en línea de las ecuaciones diferenciales derivadas de la ecuación de Hamilton-Jacobi-Bellman (HJB), cuya solución es suficiente para resolver el problema de control óptimo no lineal.

Palabras clave: Control no lineal, sistemas subactuados, control óptimo, modos deslizantes, seguimiento de trayectoria.

Abstract

This thesis addresses the synthesis of a robust nonlinear optimal control methodology for achieving stabilization and trajectory tracking in underactuated mechanical system (UAMS). The control methodology is based in using the state-dependent coefficient factorization (SDCF) for nonlinear systems, in which the state-dependent Riccati equation SDRE is associated to solve the nonlinear optimal control; indeed, this approach can be described as the nonlinear extension of the linear quadratic regulator. A posteriori, with the aim of enhancing the control strategy robustness, the optimal controller is combined with sliding mode control for designing an optimal sliding surface for those nonlinear systems which can be presented into the so-called regular form, then the sliding surface is used to synthesize a super-twisting controller. The effectiveness of the nonlinear optimal control technique is proven via simulations for the Pendubot, and through simulations and in real time for the rotary inverted pendulum, being both systems non-minimum phase and nonlinear ones; nonetheless, the control methodology can be applied for general UAMS. It is worth mentioning that compared to related works for controlling UAMS, this thesis presents a larger operation range of the optimal trajectory tracking for the controlled variable, which is achieved by solving on-line the associated differential equations derived from the Hamilton-Jacobi-Bellman (HJB) equation, whose solution is sufficient to solve the nonlinear optimal control.

Table of Content

List of Figures

List of Tables

List of Symbols

$\mathbb{R}$	Set of real numbers
$\mathcal{O}$	Observability matrix
$\mathcal{C}$	Controllability matrix
$\mathcal{K}$	Kinetic energy
$\mathcal{P}$	Potential energy
$\mathcal{L}$	Lagrangian function
$\mathcal{H}$	Hamiltonian function
τ	Applied torque
δ	Bounded disturbance
μ	Friction coefficient
φ	Diffeomorphism (nonlinear transformation)
σ	Sliding surface
Λ	Motor gear-box dynamics
η_g	Gear box efficiency
K_g	High-gear total gear ratio
η_m	Motor efficiency
k_t	Motor current-toque constant
B_r	RIP first joint viscous friction
B_p	RIP second joint viscous friction
V_m	Applied motor voltage
R_m	Armature resistance
x_i	State variable
y_i	System output
J	Performance index
J_i	Inertia moment
I	Link inertia moment
l	Link length
$V(x)$	Lyapunov's function
$*$	Optimal value
$L_g L_f$	Lie derivate

List of Acronyms

DC	Direct current
DOF	Degree of freedom
DRE	Differential Riccati equation
FIB	Francis-Isidori-Byrnes
HJB	Hamilton-Jacobi-Bellman
HOSM	High-order sliding modes
LQR	Linear quadratic regulator
OSMC	Optimal sliding mode controller
RIP	Rotary inverted pendulum
SDCF	State-dependent coefficient factorized
SDRE	State-dependent Riccati equation
SMC	Sliding mode controller
UAMS	Underactuared mechanical system

Chapter 1

Introduction

Throughout history, man has been a protagonist in the development of new technologies, which have allowed him to satisfy his own needs or even guarantee his own existence. New technological developments have created difficult engineering challenges that require the use of sophisticated theoretical concepts, which are developed based on the contributions of great mathematicians, scientists and engineers. A control system is an interconnection of components forming a system configuration that will provide a desired system response [Dorf08]. Control systems have taken a leading role in the advent of new technologies, where the control of mechanical systems is currently among of the most active fields of research due to diverse applications of mechanical systems, from the development of production tools to means of transportation and defense systems. As a result, the efforts of engineers and scientist together led to the creation of different control schemes (e.g. linear control, optimal control, adaptive control and nonlinear control theory). More recently, robust control theory has been added to the control theories because of an inevitable need to deal with the presence of parametric uncertainties and external disturbances of the systems on real-life applications [Saber01].

The optimal control is one particular branch of modern control theory, which has

the objective of determine the control signals that will cause a process to satisfy the physical constraints and at the same time minimize or maximize a performance index [Kirk04]. Linear optimal control is a special sort of optimal control, where the plant is assumed to be linear as well as the controller, which is obtained by working with quadratic performance indices. Methods that achieve linear optimal control are named linear quadratic regulator (LQR) [Anderson90]. A solution to the optimal control problem is obtained by using the method of dynamic programming developed by Bellman [Bellman57], which leads to a nonlinear partial differential equation named the Hamilton-Jacobi-Bellman equation (HJB) [Kirk04], whose solution in general is complicated for nonlinear systems. The application of this technique is well stablished in solving the optimal control problem for linear systems, where its formulation results in the solution given by the differential Riccati equation (DRE); hence, optimal control for linear systems is considered to be a solved problem; however, the nonlinear optimal control is an open issue.

In this sense, the state-dependent Riccati equation (SDRE) [Cloutier02], extends the LQR approach to the nonlinear case by allowing the matrices involved to be functions of state variables and transforming an input-affine nonlinear system into the so-called state-dependent coefficient factorized (SDCF) nonlinear systems [Cloutier97], [Ornelas-Tellez13],[Cimen10], a linear like representation for nonlinear systems used to solve the associated HJB equation. In essence, the SDCF nonlinear control technique is a systematic way for synthesizing optimal nonlinear feedback controllers, which mimics the controller synthesis as done for the linear case, by exploiting the nature of the nonlinear behavior throughout the state space. Notice that by using the SDCF technique the system is not being linearized around an equilibrium point, therefore the nonlinear system is completely considered; thus, the controller has a larger operation range over the system in comparison with the linear controllers; in addition, the nonlinear inherit nature of the system is exploited.

In the other hand, sliding mode control (SMC) [Fridman02],[Utkin92], provides robustness properties against uncertainties in system parameters and external disturbances; however, sliding modes has a drawback: due to their associated discontinuous control laws, high frequency switching may lead to actuator damage for the plant, or may cause system resonance via excitation of neglected unmodeled dynamics, these dangerous vibrations are called the "chattering-effect" [Bartolini98]. An ideal sliding mode does not exist in practice since it would imply that switches can work at an infinite frequency. The sliding mode controllers are typically designed for the worst scenario, in which the system uncertainties and external disturbances are dominant [Utkin92]. For such circumstance the stability is the main concern of the controller; nevertheless, there are systems where it is possible to known or to be sure about some of their parameters or structure; thus, the system becomes more or less transparent in a certain degree and the nominal part of the system will be dominant, therefore the robustness is no longer the only concern of the controller, also it is of concern to design a controller able to minimize a criteria as it can be the convergence time, the control effort or the energy expenditure. In this sense, optimal control provides a systematic design procedure able to design a controller according to a performance index; however, optimal control theory requires a complete knowledge of the system, hence this type of controllers are not considered to be robust in the sense of parametric uncertainties. A possible solution to this problem is to introduce the so-called optimal sliding mode control (OSMC) [Feng16]. A controller based on optimal sliding modes, allows to take advantage of a robust controller that does not depend on the parameters of the system to be controlled, along with the advantages of an optimal controller which allows to minimize a certain performance index [Utkin92].

1.1. Problem Statement

For this thesis, it is of interest the controller design for dynamical systems, whe-

re the nonlinear components can not be neglected, for instance the motion control of underactuated mechanical systems [Mullhaupt09], actuated by DC drives, where besides the intrinsic nonlinear operation of the DC motor, a linear model of the mechanical system cannot capture the behavior of the system under fast motions. This thesis deals with the problem of nonlinear optimal control for a class of underactuated mechanical systems, which have a highly nonlinear model. This kind of systems are of interest, due to the great variety of nonlinear phenomena that present. Indeed most cases, these systems are not feedback linearizable, and an internal instability appears, which is the reflection of an input-output property namely in the presence of what is called the non-minimum phase property; therefore, sophisticated control methodologies need to be employed [Mullhaupt09]. In this sense, the nonlinear optimal control theory is proposed in order to deal with the non-minimum phase problem associated with this class of nonlinear systems. The class of underactuated mechanical systems is rich in both applications and control problems, in this sense inverted-pendulum type systems (e.g. the Pendubot and the rotary inverted pendulum), have been extensively used in order to test novel control strategies.

1.2. Background

As there is an increase in the applications of the control systems, there is an increase in the requirements for the designed controller, which means that these systems become more and more complex. Nonlinear control is an important area in control, due to the fact that virtually all systems are nonlinear, it is possible to obtain approximated linear models of the systems, however; when the required operation range is large, a linear model may result inaccurate or even inadequate. In this sense nonlinear controllers take a leading role because they are capable of handling nonlinearities in large operation ranges. It cannot be said, that there exist a single nonlinear control strategy which might be considered to be the best of all, there are pros and cons

between them, and the use of one particular control scheme depends mainly from the plant the be controlled and the desired requirements. Within the popular nonlinear control strategies, the followings can be mentioned:

- ◇ **Feedback Linearization** [Kokotovic97], Transforms the nonlinear system into an equivalent linear system by introducing a feedback control law; however, feedback linearization may result in wasteful controllers and also in nonrobust systems, due to the fact that feedback linearization often destroys stabilizing nonlinear terms and replaces them with destabilizing ones.

- ◇ **Takagi-Sugeno Fuzzy Controller** [Chang12], It is a design procedure for nonlinear controllers, based on the representation of a nonlinear system into a set of linear subsystems, where by doing so, it is possible to apply a linear control strategy for each subsystem, which are related by a fuzzy implication rule. The Takagi-Sugeno fuzzy models are said to be universal approximators, however; this approach implies the linearization of the system and then the use of a linear controller.

- ◇ **Sliding Mode** [Utkin92], Is a nonlinear control method which alters the dynamics of a nonlinear system by the application of a discontinuous control law. The main advantages of this method are: the robustness against a large class of perturbations or model uncertainties and the need for a reduced amount of information in comparison to classical control techniques.

- ◇ **Lyapunov Redesign** [Khalil02], Refers to the design of a state feedback controller based on the prior knowledge of the Lyapunov function, which is used to stabilized the system, one of the major disadvantages for this method is the difficulty of finding the associated Lyapunov function for a nonlinear system.

- ◇ **Backstepping** [Khalil02], Is a nonlinear control technique for the design of stabilizing controllers, where the system is built from subsystems that radiate

out from a irreducible subsystem which can be stabilized using some other method.

- ◇ **Neural Networks** [Nguyen03], Refers both to a methodology in which the controller itself is a neural network, and to a methodology in which controllers are designed based on a neural network model of the plant.

- ◇ **Optimal Control** [Kirk04], Deals with the problem of finding a control law for a given system, such that a certain optimality criterion is achieved. Optimal control requires a complete knowledge of the system to be controlled as well as the measurement of the state variables.

The applied controllers for inverted-pendulum like systems are chiefly based on swing-up and balancing controllers [Saber01], as a subset of the balancing controller, it can be considered the tracking and stabilization problem. Within the latest related works for this class of underactuated mechanical systems, it is worth mentioning the following:

In [Furuta93], a new type of pendulum on a rotating arm fixed to a rotating shaft and a swing up controller is presented. This work supports the statement that inverted pendulum systems have been used for the verification of designed control systems and control laboratory experiments in control education. Later as seen in [Spong95], the Pendubot is introduced as a mechatronic device for use in control engineering education and for research in nonlinear control and robotics. In this work the Pendubot is considered to be a mechatronic system such as the Acrobot and the the inverted pendulum of Furuta. Different nonlinear control strategies have been applied to this class of systems, in [Erdem01], the SDRE is used to regulate the Pendubot, results show that SDRE control outperforms the LQR control. However, the SDRE controller proposed solves a nonlinear algebraic Riccati equation at each sampling time, which requires of a great computational effort for real time implementations. In the

work carried out by [Cai03], by combining optimal control theory and linear regulator theory, the Takagi-Sugeno fuzzy methodology is used in order to obtain a global stable fuzzy controller applied to the Pendubot. Later, in more recent works such as done by [Rivera08], the nonlinear optimal regulation for the Pendubot is presented. The theory is revisited for nonlinear systems presented into the so-called nonlinear systems regular form. In [Serrano-Heredia11], the problem of nonlinear regulation of the Pendubot is treated by means of sliding mode continuous control action combined with block control. Similar work as done by [Galicia12], presents an approach to solve the output regulation problem for a class of nonlinear discrete non-minimum phase systems, based on feedback linearization and sliding mode control applied to the Pendubot.

For the rotary inverted pendulum, in [Jadlovská13], the application of a nonlinear optimal control design technique based on the SDRE on generalized (n link) pendulum systems is presented; however, the nonlinear optimal tracking control is not considered. In [Dang14] and [Farooq15], an experimental study of optimal control Takagi-Sugeno fuzzy controller for a rotary inverted pendulum is presented. More recently in [Kathpal17] by the used of SimMechanics® and Matlab® toolbox, a LQR control is implemented to the rotary inverted pedulum.

1.3. Motivation

The interest of controlling underactuated mechanical systems (UAMS), is motivated by a large number of applications which present this phenomenon; given the nature of the system such as robotics systems, aerospace and marine vehicles, or together with a design optimization factor, which is reflected in a simpler mechanical design, derived into an economic profit in the manufacturing process. Given the complexity of underactuated mechanicals systems, they represent a challenge for

any control scheme, which makes them attractive for the use of novel nonlinear and optimal control strategies.

1.4. Hypotesis

It is possible to design a nonlinear optimal controller, in order to stabilize and track time varying reference signals for a class of underactuated mechanical systems, where the controller deals with the problem of non-minum phase associated with this class of systems. In addition, it is possible to design a nonlinear optimal sliding mode controller able to reject parametric uncertainties and external disturbances.

1.5. Objectives

1.5.1. General Objective

Synthesis of a novel robust control strategy, by combining optimal control and sliding modes, applied a class of underactuated mechanical systems, which is able to deal with the underactuation and non-minimum phase problems, in order to track a time varying reference signal, and at the same time, to provide of robustness properties to the controller against unknown parameters and external disturbances.

1.5.2. Particular Objectives

- ◇ Design of a nonlinear optimal tracking control scheme for a class of UAMS based on the SDCF technique.
- ◇ To combine the nonlinear optimal control theory with the sliding modes in order to provide of additional robustness properties to the optimal controller.
- ◇ Real-time application of the nonlinear optimal controller.

1.6. Contributions

As a result of this thesis, the following contributions are given:

- ◇ The novel optimal sliding mode controller, which is extended to the nonlinear case for a class of nonlinear systems which can be represented in the so-called regular form, by combining sliding modes with the nonlinear optimal control theory based on the state-dependent coefficient factorized form (SDCF), in order to obtain an optimal manifold used for a sliding mode controller, this is considered to be the main contribution of the thesis.

- ◇ Nonlinear optimal tracking control error analysis. An analysis of the convergence of the error for the optimal nonlinear control based on the state dependent coefficient factorization, which determines that the error is ultimately bounded.

- ◇ Nonlinear optimal control design based on the state-dependent coefficient factorized form, extended to the tracking problem for a time-varying reference signal, which is applied to the Pendubot and for the rotary inverted pendulum.

- ◇ It is worth remarking that with the proposed methodology, a wider tracking range for the controlled variable is achieved in contrast with related works.

- ◇ The nonlinear optimal tracking control for the rotary inverted pendulum, which stabilizes the system in the complete operational range of the system.

- ◇ Simulations and real-time experimental results to exhibit the effectiveness of the design nonlinear controller for the rotary inverted pendulum.

1.7. Thesis Outline

This thesis is organized as follows:

- ◇ **Chapter 2.** Details the concepts associated with nonlinear systems, as well as a modeling tool for open kinematic chains, finally the dynamic equations for a class of mechanical systems are obtained.

- ◇ **Chapter 3.** Describes the design of nonlinear optimal and sliding modes controllers, after that a nonlinear control scheme which combines the capabilities of both optimal control and sliding modes is presented.

- ◇ **Chapter 4.** Presents the application of the designed controllers in chapter 3, for a class of underactuated mechanical systems, the effectiveness of the designed controllers is proven for the Pendubot and the rotary inverted pendulum by simulation and real-time experimental results.

- ◇ **Chapter 5.** Concludes this thesis, where the final comments of this work are presented, also proposals for future work are proposed.

Figure 1.1, depicts the thesis outline and the application of the control strategies developed within this thesis.

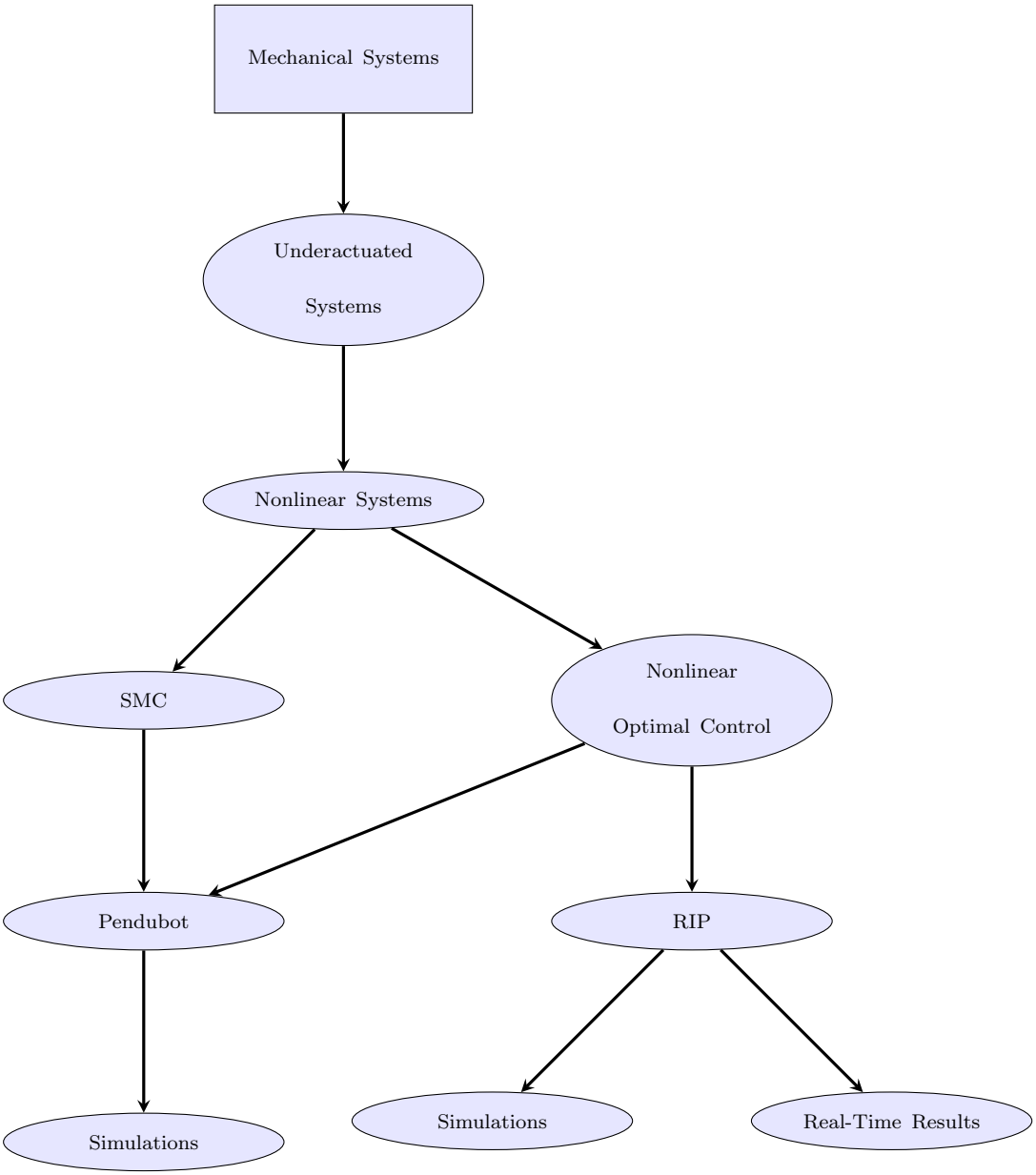

Figure 1.1: General flow chart of the modeling and control techniques developed within this thesis.

Chapter 2

Modeling of Mechanical Systems

In this chapter the concept of nonlinear systems is introduced; then the main concepts related with the mathematical modeling principles for open kinematic chains, are developed based on the Euler-Lagrange equations for the generalized case, applied to robotic systems with n links. Finally, the use of the modeling methodology is applied for the Pendubot and the Rotary Inverted Pendulum, deriving into the equations of motion for the these UAMS in the state space framework.

2.1. Nonlinear Systems

Physical systems are inherently nonlinear in nature, thus all control systems are nonlinear to certain extent [Slotine91]. A nonlinear system can usually be represented by a set of differential equations in the form

$$\begin{aligned} \dot{x}_i &= f_i\left(x_i, u_p\right) \\ y_i &= h_i\left(x_i, u_p\right) \end{aligned} \tag{2.1}$$

where $x_i \in \mathbb{R}^n$ denotes the state variable, $u_p \in \mathbb{R}^m$ are the input variables, and $y \in \mathbb{R}^p$ is the output vector that comprises the variables of particular interest, f_i and h_i are smooth maps of appropriate dimension. A particular value of the state

vector is also called a point because it corresponds to a point in the state-space, and the number of n states is called the order of the system. Nonlinearities can be classified as inherent (natural) and intentional (artificial) [Slotine91], where the inherent nonlinearities are those which comes with the system's hardware and motion (e.g. centripetal forces in rotational motion or the Coulomb's friction). On the other hand intentional nonlinearities are those which are introduced by the designer.

Equilibrium Points of Nonlinear Systems

An important concept related with nonlinear systems is the concept of equilibrium points. Nonlinear systems frequently have more than one equilibrium point [Slotine91].

Definition 1 *[Khalil02] A point $x = x^*$ in the state-space is said to be an equilibrium point of (2.1), if it has the property that whenever the state of the system starts at x^*, it will remain at x^* for all future time, for autonomous systems, the equilibrium points are given by the real roots of the equation*

$$f(x^*) = 0. \tag{2.2}$$

Lyapunov Stability

Given a control system, the first and most important question about its various properties is whether it is stable [Slotine91]. There are several well-developed techniques for analyzing nonlinear feedback systems, as they are: the phase-plane method [Isidori95], the Popov's criterion and passivity analysis [Ortega98]. For this thesis the Lyapunov stability analysis will be used, which is stated in the following theorem:

Theorem 1 *[Khalil02] Let $x = 0$ be an equilibrium point for (2.1) and $D \in \mathbb{R}^n$ be a domain containing $x = 0$. Let $V : D \to \mathbb{R}$, be a continuous differentiable map such that*

$$V(0) = 0 \ \wedge \ V(x) > 0 \in D - \{0\} \tag{2.3}$$

$$\dot{V}(x) \leq 0 \in D \tag{2.4}$$

then $x = 0$ *is stable. If*

$$\dot{V}(x) < 0 \in D - \{0\} \tag{2.5}$$

then $x = 0$ *is asymptotically stable.* ■

The basic philosophy of the Lyapnunov's method is the mathematical extension of a fundamental physics observation: if the total energy of a mechanical system (or electrical) is continuously dissipated, then the system whether linear or nonlinear, must eventually settle down to an equilibrium point [Slotine91]. Qualitative, a system is described as stable, if starting the system somewhere near its desired operating point, implies that it will stay around the point ever after.

2.1.1. A Class of Nonlinear Systems SDCF

Extended linearization [Friedland.96], also known as apparent linearization [Wernli75], or state-dependent coefficient factorization (SDCF) [Cloutier02],[Ornelas-Tellez13] is the process of factorizing a nonlinear system into a linear-like structure, which contains state-dependent matrices. From (2.1), consider a class of input-affine nonlinear system described as

$$\begin{aligned} \dot{x} &= f(x) + B(x)u, \quad x(t_0) = 0 \\ y &= h(x) \end{aligned} \tag{2.6}$$

where $x \in \mathbb{R}^n$ is the state vector, $u \in \mathbb{R}^m$ is the control input and $y \in \mathbb{R}^p$ is the system output; the functions $f(x)$, $B(x)$ and $h(x)$ are sufficiently smooth to make the system well-defined, and it is assumed that they can be decomposed in the state-dependent coefficient factorization. Under the assumptions $f(\cdot) \in C_1(\Omega)$ and $f(0) = 0$, a continuous nonlinear matrix-valued function exist such that $f(x) = A(x)x$ and $h(x) = C(x)x$, respectively, [Shamma03]. Then, system (2.6) can be rewritten as

$$\begin{aligned} \dot{x} &= A(x)x + B(x)u \\ y &= C(x)x. \end{aligned} \tag{2.7}$$

Remark 1 *From now on system (2.7) will be named in this thesis as the SDCF nonlinear system, and it will be used for analysis and control purposes.*

Remark 2 *The factorizations $A(x)x$ and $C(x)x$ are not unique; then, in order to obtain well-defined control schemes, these factorizations must be chosen in order to fulfilled the state-dependent controllability and observability properties as seen in [Hammett98] and [Ornelas-Tellez13].*

Associated with the SDCF, the following definitions are stated:

Definition 2 *[Antsaklis07] A state x_1 is called reachable if there exist an input that transfers the state of the system $x(t)$ from the zero state to x_1 in a finite time T. In addition a state x_0 is called controllable if there exist an input that transfers the state from x_0 to the zero state in finite time T.*

Definition 3 *[Antsaklis07] The concept of observability refers to the ability of determining the present state x_0 of a given system, from the knowledge of the current and past outputs $y(t)$ and present inputs $u(t)$.*

Definition 4 *[Cimen10] The SDCF is a stabilizable parametrization of the nonlinear system in a region Ω if the pair $[A(x),\ B(x)]$ is pointwise stabilizable (respectively controllable) in the linear sense $\forall\, x\ \in \Omega$.*

Definition 5 *[Cimen10] The SDCF is a detectable parametrization of the nonlinear system in a region Ω if the pair $[C(x),\ A(x)]$ is pointwise detectable (respectively observable) in the linear sense $\forall\, x\ \in \Omega$.*

The SDCF controllability matrix must satisfy

$$rank\{\mathcal{C}(x)\} = n \,\forall\, x \tag{2.8}$$

with

$$\mathcal{C}(x) = \begin{bmatrix} B(x) & A(x)B(x) & \dots & A^{n-1}(x)B(x) \end{bmatrix} \tag{2.9}$$

while the observability matrix must fulfill

$$rank\{\mathcal{O}(x)\} = n \,\forall\, x \tag{2.10}$$

$$\mathcal{O}(x) = \begin{bmatrix} C(x) \\ C(x)A(x) \\ \vdots \\ C(x)A^{n-1}(x) \end{bmatrix}. \tag{2.11}$$

2.1.2. Nonlinear Systems Regular Form

For a given nonlinear system, which is not represented into a canonical form [Su83], with the purpose of analyzing certain properties of the nonlinear system or in order to design a nonlinear controller (e.g. sliding mode, block control, feedback linearization or backstepping), it is often more convenient to transform the nonlinear system (2.6) via diffeomorphism (nonlinear transformation) into the so-called nonlinear system regular form [Loukianov80]. Consider an appropriate state vector such that system (2.6) can be presented as

$$\begin{aligned} \dot{x}_1 &= f_1(x_1, x_2) + B_1(x_1, x_2)u \\ \dot{x}_2 &= f_2(x_1, x_2) + B_2(x_1, x_2)u \end{aligned} \tag{2.12}$$

where $x_1 \in \mathbb{R}^{n-m}$, $x_2 \in \mathbb{R}^m$, $u \in \mathbb{R}^p$, $f_1(x)$ and $f_2(x)$ are smooth functions of appropriate dimension. If it is possible to find a nonlinear transformation $\varphi(x)$ applied to

(2.12) such that $B_1(x_1, x_2) = 0$, then system (2.12) is represented in the transformed coordinates by two blocks as

$$\begin{aligned} \dot{x}'_1 &= f_1(x'_1, x'_2) \\ \dot{x}'_2 &= f_2(x'_1, x'_2) + B_2(x'_1, x'_2)u. \end{aligned} \tag{2.13}$$

Hereafter a system like (2.13) will be called the regular form of system (2.12), the regular form (2.13) consists of two blocks, where the first block does not depend on the control input, and the dimension of the second block coincides with the dimension of the control. In order to find the nonlinear system regular form, a vector of new state variables $x' = (x'_1, \ldots, x'_n)^T$ is introduced, which is related with the original variables by a diffeomorphism $\varphi(x)$, where $x'_1 = \varphi(x)$ and $x'_2 = x_2$ [Loukianov80].

Definition 6 *[Khalil02] Let $\dot{x}$=f(x), where $f : \mathbb{R}^n \to \mathbb{R}^n$. Consider the change of variables $z = \varphi(x)$, where $\varphi(0) = 0$ and $\varphi : \mathbb{R}^n \to \mathbb{R}^n$ is a diffeomorphisim in the neighborhood of the origin; that is, the inverse map $\varphi^{-1}(\cdot)$ exists, and both $\varphi(\cdot)$ and $\varphi^{-1}(\cdot)$ are continuously differentiable.*

Considering the existence of the diffeomorphism $\varphi(x)$, the equations with respect to x'_1 are given by

$$\dot{x}'_1 = \left[\frac{\partial \varphi(x)}{\partial x}\right] f(x) + \left[\frac{\partial \varphi(x)}{\partial x}\right] B(x)u. \tag{2.14}$$

Notice that (2.14) will not depend on the control input if the diffeomorphism $\varphi(x)$ is the solution of the matrix equation in partial derivates

$$\left[\frac{\partial \varphi(x)}{\partial x}\right] B(x) = 0. \tag{2.15}$$

The solution of (2.15), is reduced to the problem of finding the $m-$ dimensional integral manifold that correspond to the Pfaffian system [Hermann83],[Loukianov80].

2.2. Non-minimun Phase Nonlinear Systems

Linear non-minimum phase systems have been extensively studied in literature [Isidori13]. Non-minimum phase is an input-output property and is linked to the positions of the zeros of a transfer function; if there is existence of zeros with positive real part, the linear system is said to be non-minimum phase between the corresponding input-output pairs [Mullhaupt09]. However, the problem with the position of the zeros in the transfer function, is that they, can not be extended to the nonlinear case. Then for the nonlinear case, the non-minimum phase property is defined in terms of the existence of the so-called zero dynamics. Prior to the introduction of the concept of zero dynamics it is necessary to define the concept of relative degree.

Relative Degree

Definition 7 *[Isidori95] The nonlinear system is said to have relative degree* $\bar{r}$, $1 \leq \bar{r} \leq n$ *in a region* $D_0 \subset D$ *if*

$$L_g L_f^{i-1} h(x) = 0, \quad i = 1, 2, \ldots, \bar{r} - 1; \quad L_g L_f^{\bar{r}-1} h(x) \neq 0. \tag{2.16}$$

Where $L_g L_f$ denotes the Lie derivate of the functions $g(x)$ and $f(x)$. In other words the relative degree $\bar{r}$ of an input affine nonlinear system (2.6), given the input u and the output $y = h(x)$, is the number of times the output should be differentiated before the input explicitly appears.

Zero Dynamics

Consider the nonlinear system (2.6) with $\bar{r}$ strictly less than n, such that $L_g h(x) \neq 0 \ \forall x$. Then system (2.6) is transformed via diffeomorphism as

$$\begin{aligned} \dot{z} &= f(z, \xi) \\ \dot{\xi} &= q(z, \xi) + b(z, \xi) u \\ y &= \xi \end{aligned} \tag{2.17}$$

in this coordinates the state ξ produces a zero output under a certain input, then the system is constrained to obey

$$\dot{z} = f(z, 0). \tag{2.18}$$

This phenomenon leads to the concept of zero dynamics and non-minimum phase [Isidori13]. The nonlinear system (2.6) is said to be globally non-minimum phase if it has a relative degree $\bar{r}$, such that $n < \bar{r}$, and if (2.18) have a globally asymptotically stable equilibrium point at $z = 0$. on the other hand when the dynamics of (2.18) are unstable, system (2.6) is said to be non-minimum phase.

2.3. Mechanical Systems Description

Classical mechanics is the branch of physics which describes the motion of bodies. This field of study is divided in two subsets, statics and dynamics. The first one studies the rigid bodies under the equilibrium conditions, and dynamics studies the bodies under movement and the causes of movement. At the same time, the dynamics is divided in two subsets the kinematics and kinetics. The major interest of kinematics is the study of the geometric characteristics of movement and the kinetic studies the causes of movement related with the applied forces [Norton98].

In order to understand the kinematic chains modeling, it is necessary to state the following definitions:

Definition 8 *(Mechanism) [Norton98] A mechanism is a device which transforms motion into some desirable pattern.*

Definition 9 *(Link) [Norton98] A link is a rigid body which possesses at least two nodes, which are points for attachments to other links.*

Definition 10 *(Joint) [Reinholtz98] A joint is a connection between two or more links which allows some motion.*

Definition 11 *(Kinematic Chain) [Reinholtz98] A kinematic chain refers to an assembly of rigid bodies connected by joints to provide constrained motion.*

2.3.1. Types of Motion

Pure Rotation

A body has pure rotational motion when one point of the body is attached and all the other points rotate around it.

Pure Translation

Translational motion is the movement of object without a change of orientation relative to a fixed point, as opposed to rotational motion, in which the object is turning about an axis.

Complex motion

A complex movement is a combination of the simultaneous rotational and translational movements.

2.3.2. Degrees of Freedom DOF

Any mechanical system can be classified according to the number of degrees of freedom (DOF) which it posses. The DOF is equal to the number of independent parameters which are needed to uniquely define its position at any instant of time [Norton98]. In order to determine the DOF for a mechanism, it is necessary to consider the number of links, joints and their relations between them. The DOF of a mechanism is determined by applying the Gruebler condition [Gruebler17] stated as follows:

$$\bar{M} = 3\bar{L} - 2\bar{J} - 3\bar{G} \tag{2.19}$$

where $\bar{M}$ is the degree of freedom of the mechanism, $\bar{L}$ is the number of links, $\bar{J}$ the number of joints and $\bar{G}$ the number of grounded joints.

2.3.3. Generalized Coordinates

Generalized coordinates, are called to any set of numerical parameters that serve to uniquely describe the configuration of a mechanism, with a finite number of degrees of freedom. The minimum number of generalized coordinates to define the state of a system is known as independent coordinates, so the coordinates can be absolute (where the system's motion is referenced to a fixed point) or relative to another element of the mechanism.

Example 1 *Figure 2.1, shows a mechanical arm with two degrees of freedom, which can be determined using the Gruebler's equation. The system is composed by three links, two joints and a fixed reference link therefore the DOF is computed as follows:*

$$\bar{M} = 3(3) - 2(2) - 3(1) = 2. \tag{2.20}$$

Thus, the number of generalized coordinates is equal to the DOF of the system. For Figure 2.1, the coordinates (x_1, y_1) *and* (x_2, y_2) *define the position of center of mass for links* 1 *and* 2 *respectively, and* (θ_1, θ_2) *define the links angle. Therefore, the* 6 *parameters set can be described by* d_1 *and* d_2*, which represent the distance to the centre of mass for each link.*

$$x_1 = d_1 cos\theta_1 \tag{2.21}$$

$$y_1 = d_1 sin\theta_1 \tag{2.22}$$

$$x_2 = L_1 cos\theta_1 + d_2 cos\theta_{12} \tag{2.23}$$

$$y_2 = L_1 sin\theta_1 + d_2 sin\theta_{12} \tag{2.24}$$

where $\theta_{12} = \theta_1 + \theta_2$.

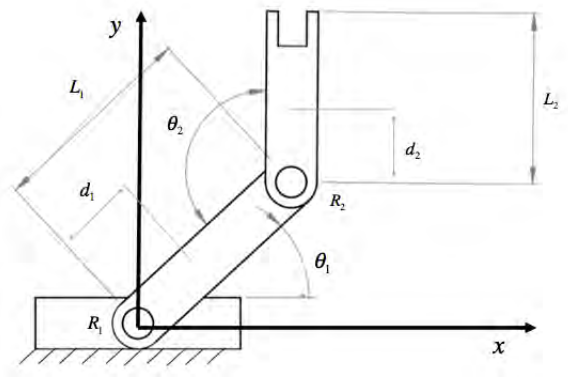

Figure 2.1: Generalized coordinates for a 2 DOF mechanical arm

2.4. The Euler-Lagrange Model

An accurate model of robotic systems is useful for the design of motion control systems and analysis of mechanical design. There exist two different approaches in order to obtain the mathematical model for open kinematic chains or manipulator robots, these approaches are the recursive Newton-Euler approximation [Yang16] based on a force balance and the mechanical equilibrium conditions of the body under study, and the second approach is the Euler-Lagrange model based on an energy or passivity model of the system [Ortega98], both are equivalent as both describe the dynamic behavior of the robotic motion. The most important reason for singling out the study of the Euler-Lagrange systems is that they capture a large class of contemporary engineering problems, specially some which are intractable with linear control tools [Ortega98]. An Euler-Lagrange system is a system whose motion is described by the Euler-Lagrange equations, from the mathematical point of view the Euler-Lagrange equations are a set of nonlinear differential equations with a certain specific structure.

Euler-Lagrange equations are important because they are the outcome of a powerful modeling technique which describes the behavior of a large class of physical systems [Ortega98]. Prior to the introduction of the Euler-Lagrange equations, the following concepts must be stated:

Kinetic energy for a $n-$link robotic chain

Definition 12 *[Vidyasagar89] The kinetic energy of an object is the energy which it possesses due to its motion. In classical mechanics the kinetic energy $\mathcal{K}$ of a non-rotating object is defined as*

$$\mathcal{K} = \frac{1}{2}mv^2 \tag{2.25}$$

where m is the mass of the body and v its speed.

The kinetic energy of a system conceived as a kinematic chain made up n links is defined as follows:

$$\mathcal{K} = \frac{1}{2}\dot{q}^T \sum_{i=1}^{n} \left[m_i J_{vi}(q)^T J_{vi}(q) + J_{wi}(q)^T R_i(q) I_i R_i(q)^T J_{wi}(q) \right] \dot{q} \tag{2.26}$$

where q is the vector of generalized coordinates of the system, the mass of the link i is denoted by m_i, I_i is the inertia matrix, R_i is transformation matrix between the body attached frame and the inertial frame, $J_{\omega i}$ and J_{vi} are the corresponding Jacobian matrices for the angular acceleration and velocity respectively, for appropriate Jacobian matrices it is follows that

$$v_i = J_{vi}(q)\dot{q} \qquad \omega_i = J_{\omega}(q)\dot{q} \tag{2.27}$$

in a compact form the expression (2.26) can be reduced into

$$\mathcal{K} = \frac{1}{2}\dot{q}^T D(q)\dot{q} \tag{2.28}$$

where $D(q) \in \mathbb{R}^{n\times n}$ is the generalized inertia matrix which satisfies $D(q) = D(q)^T > 0$ [Ortega98]

Potential energy for a $n-$link robotic chain

Definition 13 *[Vidyasagar89] The potential energy of a body is the energy that it possesses as a result of it's position, in classical mechanics the kinetic energy $\mathcal{P}$ of an object is defined as*

$$\mathcal{P} = mgh \tag{2.29}$$

where m is the mass of the body under study, g is the gravitational term and h is the altitude of the object with respect to their inertial reference frame. The potential energy $\mathcal{P}$ for a kinematic chain is described as

$$\mathcal{P}_i = g^T r_{ci} m_{i.} \tag{2.30}$$

where g is a vector which represents the gravitational force in the inertial reference frame, r_{ci} are the coordinates of the centre of mass for the link i, and m_i is the mass of the link i, such that the potential energy of the system can be represented as

$$\mathcal{P} = \sum_{i=1}^{n} \mathcal{P}_i = \sum_{i=1}^{n} g^T r_{ci} m_i. \tag{2.31}$$

2.4.1. The Euler-Lagrange Equations

A mechanical system with n degrees of freedom with generalized coordinates $q \in \mathbb{R}^n$ and external applied forces $Q \in \mathbb{R}^n$, it is described by the Euler-Lagrange equations as

$$\frac{d}{dt}\frac{\partial \mathcal{L}}{\partial \dot{q}_k} - \frac{\partial \mathcal{L}}{\partial q_k} = Q \tag{2.32}$$

where the Lagrangian function $\mathcal{L}$ is defined as the difference between the kinetic and the potential energy of the system as

$$\mathcal{L} = \mathcal{K} - \mathcal{P}. \tag{2.33}$$

The Euler-Lagrange model consider three types of external forces: the control actions, dissipation and the interaction of the system with the environment, assuming that the controls enter linearly as $\mathcal{M}u \in \mathbb{R}^n$, where $\mathcal{M}$ is a column matrix relating the external inputs to the generalized coordinates, $u \in \mathbb{R}^n$ is the control vector, which represents the applied input torques τ_k, dissipative forces are of the form $\frac{\partial \mathcal{F}}{\partial \dot{q}}$, where $\mathcal{F}$ is the Rayleigh dissipation function which satisfies

$$\dot{q}\frac{\partial \mathcal{F}}{\partial \dot{q}}(\dot{q}) \geq 0. \tag{2.34}$$

In summary the external forces presented in the Euler-Lagrange systems are defined by

$$Q = -\frac{\partial \mathcal{F}}{\partial \dot{q}}(\dot{q}) + \mathcal{M}\tau_k. \tag{2.35}$$

Therefore the Euler-Lagrange equation is defined as

$$\frac{d}{dt}\left(\frac{\partial \mathcal{L}}{\partial \dot{q}_k}(q,\dot{q})\right) - \frac{\partial \mathcal{L}}{\partial q_k}(q,\dot{q}) + \frac{\partial \mathcal{F}}{\partial \dot{q}}(\dot{q}) = \mathcal{M}\tau_k. \tag{2.36}$$

Once the kinetic and the potential energy are obtained and the Lagrangian is found, then the task is to compute various derivates in order to get the equations of motion, after going through this process, from (2.32) and (2.35), the Euler-Lagrange equation is obtained into it's matrix form

$$D(q)\ddot{q} + C(q,\dot{q})\dot{q} + G(q) + F(\dot{q}) = \tau_k \tag{2.37}$$

where $D(q)$ is the proper inertia matrix of the corresponding robotic configuration, $C(q,\dot{q})$ is the vector of Coriolis and centripetal torques, $G(q)$ is the gravitational terms matrix, $F(\dot{q})$ is the vector of viscous frictional terms, τ_k is the vector of applied torques. Hereinafter, a mechanical system described by (2.37) will be called an Euler-Lagrange system.

2.4.2. Actuated and Underactuated Mechanical Systems

According to the structure of matrix $\mathcal{M}$ from (2.35), it is convenient to distinguish two classes of Euler-Lagrange systems: fully actuated and underactuated mechanical systems, described as follows:

Fully-actuated Mechanical System

Definition 14 *[Ortega98] An Euler-Lagrange system is said to be fully actuated if it has equal number of degrees of freedom as available control inputs, otherwise, if* $rank(\tau_k) < n$ *it is said that the system is underactuated.*

Underactuated Mechanical System

A Mechanical system satisfying the Euler-Lagrange equation (2.32), with $rank(\tau_k) < n$ is called an underactuated mechanical system, which have fewer actuators than configuration variables. This property does not allow the exact feedback linearization [Mullhaupt09], therefore sophisticated control techniques must be applied to this certain class of systems, which is the main topic of this thesis. Underactuated mechanical systems appear in a wide range of applications including robotics, aerospace systems, marine systems applications and locomotion. The interest of controlling UAMS is motivated mainly by the following reasons [Spong95]:

- ◇ Dynamics of the system: There are systems that by their very nature are underactuated and need to be controlled, such as helicopters, airplanes, space vehicles, submarine vehicles and locomotion systems for robots.

- ◇ Design optimization: For practical purposes in many mechanical systems it is possible to carry out a process of optimization in the design, which allows to reduce the number of actuators, this way has a reduction of the manufacturing costs and the weight of the system. As in the case of manipulator robots with flexible links or satellites with two propellers.

- ◇ Failure of actuators: In a fault tolerant control scheme, it is possible to have a control strategy where due to the failure of an actuator, the system can continue operating but underactuated, where a control action compensates the actuator failure and the system continues operating, as could be the case in aerospace systems.

Keeping in the palm of the hand a rod of a certain length in it's vertical position as seen in Figure 2.2, it is an example of an underactuated system. This system has 5 degrees of freedom (three corresponding to the translational movements along the axes x, and, z and two rotational movements characteristic of the wrist). Examples of less obvious underactuated systems are bipedal robots, submarine vehicles, manipulators with flexible structure, missiles, satellites, space rockets, among others. The underactuated mechanical systems involve more challenges than the fully actuated mechanical systems because its control inputs are less that their degrees of freedom.

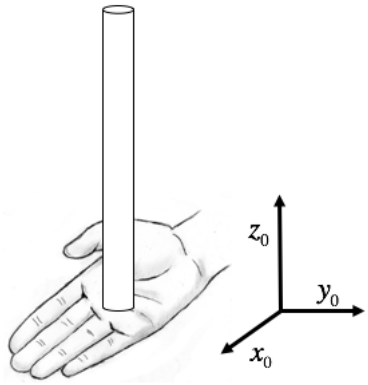

Figure 2.2: Underactuated system

2.4.3. Examples of Underactuated Mechanical Systems

The following are examples, among a vast of underactuated mechanical systems, which will be used within this thesis for analysis and control purposes.

The Pendubot

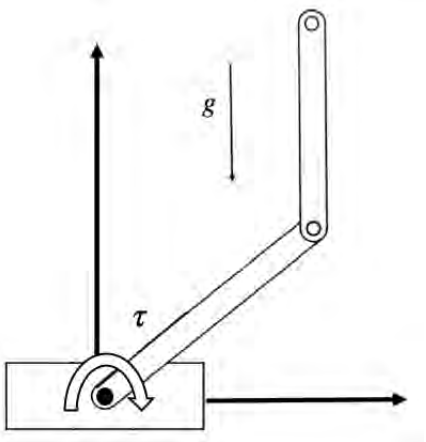

Figure 2.3: Pendubot

The Pendubot [Spong95], shown in Figure 2.3, is a mechatronic device used in control engineering education and for research in nonlinear control and robotics. This device is a two-link robot with an actuator at the shoulder but not at the elbow. The Pendubot inertia matrix is defined as

$$D(q) = \begin{bmatrix} J_1 + 2J_3 cos(q_2) & J_2 + J_3 cos(q_2) \\ J_2 + J_3 cos(q_2) & J_2 \end{bmatrix}. \tag{2.38}$$

Where J_i us the inertia moment for the i-th arm respectively, and the internal dynamics are

$$\ddot{q}_1 = -\frac{J_3 sin(q_2)}{J_2 + J_3 cos(q_2)} \dot{q}_1^2. \tag{2.39}$$

Notice that these dynamics are well defined and unstable therefore this systems are considered to be nonminimum phase [Mullhaupt98].

Pendubot Equations of Motion

Consider the following Pendubot's representation as seen in Figure 2.4

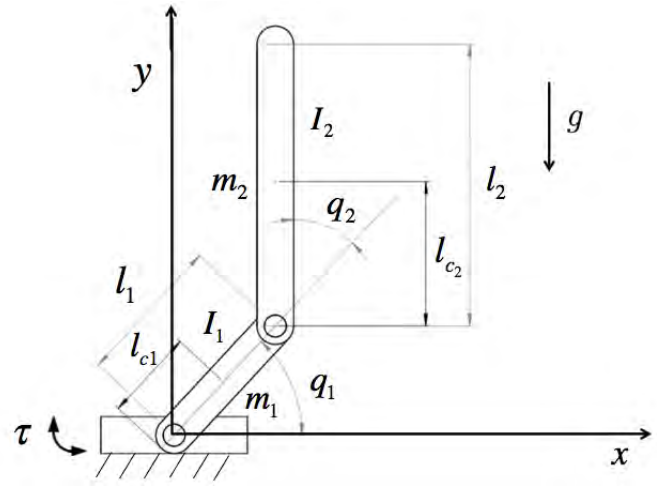

Figure 2.4: Schematic diagram of the Pendubot

with m_1 and m_2 as the mass of the first and second link of the Pendubot respectively, l_1 and l_2 are the length of the first and second link respectively, l_{c1} and l_{c2} are the distance to the center of mass of link one and two respectively, g is the gravitational term, I_1 and I_2 are the moment of inertia of the first and the second link respectively about its centroids, μ_1 and μ_2 are the viscous drag coefficients for the first and second joint of the system, q_1 and q_2 are the actuated and underactuated joints respectively and τ is the applied input torque. The dynamics of the Pendubot can be derived from the Euler-Lagrange principle (2.33) and (2.32), as seen in [Vidyasagar89], where $q = \begin{bmatrix} q_1 & q_2 \end{bmatrix}^T \in \mathbb{R}^2$ are vectors of generalized coordinates; q_1 and q_2 are actuated and unactuated variables, and $\tau_k = \begin{bmatrix} \tau & 0 \end{bmatrix}^T$ is the control input. From the Pendubot's inertia matrix (2.38) and (2.36), the equations of motion for the system become

$$\begin{aligned} \tau - \dot{q}_1\mu_1 &= g\theta_4 cos(q_1) + \ddot{q}_2(\theta_2 + \theta_3 cos(q_2)) + \ddot{q}_1(\theta_1 + \theta_2 + 2\theta_3 cos(q_2)) \\ &\quad + g\theta_5 cos(q_1 + q_2) - 2\dot{q}_1\dot{q}_2\theta_3 sin(q_2) - \dot{q}_2^2\theta_3 sin(q_2) \\ -\dot{q}_2\mu_2 &= \ddot{q}_2\theta_2 + \ddot{q}_1(\theta_2 + \theta_3 cos(q_2)) + g\theta_5 cos(q_1 + q_2) + \dot{q}_1^2\theta_3 sin(q_2) \end{aligned} \tag{2.40}$$

where the masses and link lengths are grouped into five system parameters $\theta_1, \ldots, \theta_5$ as [Eom15], with $\theta_1 = m_1 l_{c1}^2 + m_2 l_1^2 + I_1$, $\theta_2 = m_2 l_{c2}^2 + I_2$, $\theta_3 = m_2 l_1 l_{c2}$, $\theta_4 = m_1 l_{c1} + m_2 l_1$ and $\theta_5 = m_2 l_{c2}$.

Then the nominal Pendubot's dynamics (2.40) can be rewritten in the matrix form (2.37), where $D(q)$ is the inertia matrix, $C(q)$ is the vector of Coriolis and centripetal forces, $G(q)$ is the gravitational terms matrix, and $F(\dot{q})$ is the vector of viscous frictional terms, given respectively as

$$D(q) = \begin{bmatrix} D_{11} & D_{12} \\ D_{21} & D_{22} \end{bmatrix}; \qquad C(q, \dot{q}) = \begin{bmatrix} C_1 \\ C_2 \end{bmatrix}$$

$$G(q) = \begin{bmatrix} G_1 \\ G_2 \end{bmatrix}; \qquad F(\dot{q}) = \begin{bmatrix} F_1 \\ F_2 \end{bmatrix}$$

where $D_{11} = \theta_1 + \theta_2 + 2\theta_3 cos(q_2)$, $D_{12} = \theta_2 + \theta_3 cos(q_2)$, $D_{21} = \theta_2 + \theta_3 cos(q_2)$, $D_{22} = \theta_2$, $C_1 = -2\theta_3 \dot{q}_1 \dot{q}_2 sin(q_2) - \theta_3 \dot{q}_2^2 sin(q_2)$, $C_2 = \theta_3 sin(q_2) \dot{q}_1^2$, $G_1 = \theta_4 g cos(q_1) + \theta_5 g cos(q_1 + q_2) + \theta_6 cos(q_1)$, $G_2 = \theta_5 g cos(q_1 + q_2)$, $F_1 = \mu_1 \dot{q}_1$ and $F_2 = \mu_2 \dot{q}_2$. Thus the system (2.40) can be described as

$$\begin{bmatrix} D_{11} & D_{12} \\ D_{21} & D_{22} \end{bmatrix} \begin{bmatrix} \ddot{q}_1 \\ \ddot{q}_2 \end{bmatrix} + \begin{bmatrix} C_1 \\ C_2 \end{bmatrix} + \begin{bmatrix} G_1 \\ G_2 \end{bmatrix} + \begin{bmatrix} F_1 \\ F_2 \end{bmatrix} = \begin{bmatrix} \tau \\ 0 \end{bmatrix}. \tag{2.41}$$

Pendubot SDCF

With state $x \in \mathbb{R}^4$ of the origin and $u \in \mathbb{R}^1$, $y \in \mathbb{R}^1$. Choosing $(x_1 \quad x_2 \quad x_3 \quad x_4)^T = (q_1 + \frac{\pi}{2} \quad q_2 \quad \dot{q}_1 \quad \dot{q}_2)^T$ as the state vector, with $u = \tau$ as the control input and x_2 as the system output, the system (2.41) can be represented into the space state form (2.6), and then apply the state dependent coefficient factorization. Therefore, the Pendubot's Euler-Lagrange mode into the SDCF is described as

$$\dot{x} = \begin{bmatrix} 0 & 0 & 1 & 0 \\ 0 & 0 & 0 & 1 \\ a_{31} & a_{32} & a_{33} & a_{34} \\ a_{41} & a_{42} & a_{43} & a_{44} \end{bmatrix} \begin{bmatrix} x_1 \\ x_2 \\ x_3 \\ x_4 \end{bmatrix} + \begin{bmatrix} 0 \\ 0 \\ b_3 \\ b_4 \end{bmatrix} u \tag{2.42}$$

$$y = \begin{bmatrix} 0 & 1 & 0 & 0 \end{bmatrix} \begin{bmatrix} x_1 \\ x_2 \\ x_3 \\ x_4 \end{bmatrix}$$

where the entries of matrices $A(x)$ and $B(x)$ are defined as follows:

$$\begin{aligned}
a_{31} &= \alpha \frac{sin(x_1)}{x_1} \left(g\theta_2\theta_4 - g\theta_3\theta_5 cos^2(x_2) \right) \\
a_{32} &= \alpha \frac{sin(x_2)}{x_2} (\theta_2\theta_3 x_3^2 + 2\theta_2\theta_3 x_3 x_4 + \theta_2\theta_3 x_4^2 + \theta_3^2 x_3^2 cos(x_2) - g\theta_3\theta_5 cos(x_1) cos(x_2)) \\
a_{33} &= -\alpha\mu_1\theta_2 \\
a_{34} &= \alpha \left(\mu_2\theta_2 + \mu_2\theta_3 cos(x_2) \right) \\
a_{41} &= \alpha \frac{sin(x_1)}{x_1} (-g\theta_2\theta_4 - g\theta_3\theta_4 cos(x_2) + g\theta_1\theta_5 cos(x_2) + g\theta_3\theta_5 cos^2(x_2)) \\
a_{42} &= \alpha \frac{sin(x_2)}{x_2} (-\theta_1\theta_3 x_3^2 - \theta_2\theta_3 x_3^2 - 2\theta 2\theta_3 x_3 x_4 - \theta_2\theta_3 x_4^2 + g\theta_1\theta_5 cos(x_1) \\
&\quad - 2\theta_3^2 x_3^2 cos(x_2) - 2\theta_3^2 x_3 x_4 cos(x_2) - \theta_3^2 x_4^2 cos(x_2) + g\theta_3\theta_5 cos(x_1) cos(x_2)) \\
a_{43} &= \alpha \left(\mu_1\theta_2 + \mu_1\theta_3 cos(x_2) \right) \\
a_{44} &= \alpha(-\mu_2\theta_1 - \mu_2\theta_2 - 2\mu_2\theta_3 cos(x_2)) \\
\alpha &= \frac{-1}{(\theta_2 + \theta_3 cos(x2))^2 + \theta_2(\theta_1 + \theta_2 + 2\theta_3 cos(x_2))} \\
b_3 &= \frac{\theta_2}{\theta_1\theta_2 - \theta_3^2 cos^2(x_2)} \\
b_4 &= -\frac{\theta_2 + \theta_3 cos(x_2)}{\theta_1\theta_2 - \theta_3^2 cos^2(x_2)}.
\end{aligned}$$

Notice that the entries of $A(x)$ are always continuous and bounded in x since

$$\lim_{x \to 0} \frac{sin(x)}{x} = 1.$$

2.4.4. The Rotary Inverted Pendulum

The rotary inverted pendulum or Furuta pendulum [Furuta93] is a system composed by two rigid links, a rotary arm pivot attached actuated at the base and a simple pendulum which is underactuated. Consider the following rotary inverted pendulum model shown in Figure 2.5. The inertia matrix for the rotational inverted pendulum is given by (2.43) as seen in [Mullhaupt98].

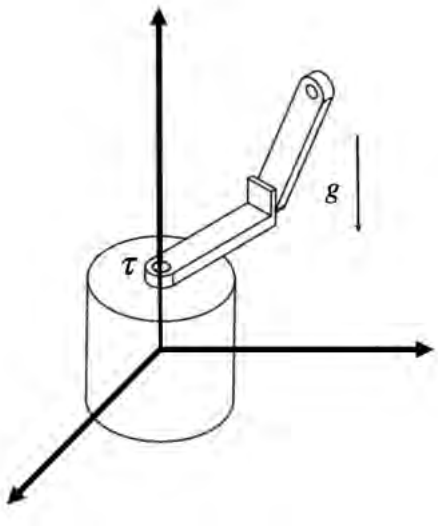

Figure 2.5: Rotary inverted pendulum

$$D(\theta, \alpha) = \begin{bmatrix} J_1 + J_3 cos(2\alpha) & -J_4 sin(\alpha) \\ -J_4 sin(\alpha) & J_2 \end{bmatrix} \tag{2.43}$$

where J_i us the inertia moment for the i-th arm respectively. From the inertia matrix, this system has a singularity when $\alpha \neq 0$ the zero dynamics are $\ddot{\theta} = 2cos(\alpha)\dot{\theta}^2$, if the system happens to be in the position where $\alpha = 0$ or $\alpha = \pi$ with zero velocity, singularity occurs and the system becomes uncontrollable [Mullhaupt98].

Equations of Motion

Consider a system composed by two rigid links, a rotary arm pivot attached to the actuated link at the base, and a simple pendulum, which is underactuated, as shown in Figure 2.6.

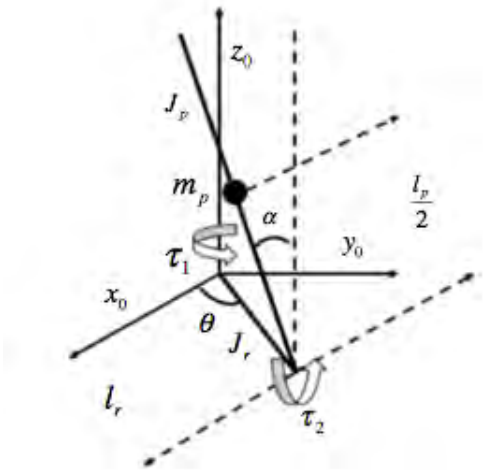

Figure 2.6: Schematic diagram of the Rotary Inverted Pendulum

where l_r is the rotary arm length, l_p the pendulum length, $\frac{l_p}{2}$ Pendulum length to the center of mass, m_p the pendulum mass, J_p and J_r are the moment of inertia of the pendulum link and the moment of inertia of the rotary arm link respectively, τ_1 is the applied input torque, θ and α are the rotary arm angle and the pendulum angle respectively. The dynamics of the rotary inverted pendulum are derived from the Euler-Lagrange principle (2.33) and (2.32), where $q = \begin{bmatrix} q_i & q_j \end{bmatrix} = \begin{bmatrix} \theta & \alpha \end{bmatrix}^T \in \mathbb{R}^2$ is a vector of the so-called generalized coordinates of the system, where θ and α are the actuated and underactuated variables respectively, $\tau_k = \begin{bmatrix} \tau_1 & 0 \end{bmatrix}^T$ is the control input, g is the gravity vector, r_{ci} is a vector of generalized coordinates of the center of mass of the i, j links, $m_{i,j}$ is the mass of the i, j links, $D(q)$ is the inertia matrix. Thus the system equations of motion are given by

$$\begin{aligned}\tau - B_r\dot{\theta} = &\left(m_pL_r^2 + \frac{1}{4}m_pL_p^2 - \frac{1}{4}m_pL_p^2cos(\alpha)^2 + J_r\right)\ddot{\theta} \\ &- \left(\frac{1}{2}m_pL_pL_rcos(\alpha)\right)\ddot{\alpha} + \left(\frac{1}{2}m_pL_pL_rsin(\alpha)\right)\dot{\alpha}^2 \\ &+ \left(\frac{1}{2}m_pL_p^2sin(\alpha)cos(\alpha)\right)\dot{\theta}\dot{\alpha}\end{aligned} \tag{2.44}$$

$$\begin{aligned}-B_p\dot{\alpha} = &-\frac{1}{2}m_pL_pL_rcos(\alpha)\ddot{\theta} - \frac{1}{2}m_pL_pgsin(\alpha) \\ &+ \left(J_p + \frac{1}{4}m_pL_p^2\right)\ddot{\alpha} - \frac{1}{4}m_pL_p^2cos(\alpha)\sin(\alpha)\dot{\theta}^2.\end{aligned} \tag{2.45}$$

Then the nominal dynamics of the rotary inverted pendulum can be rewritten into the Euler-Lagrange matrix form as (2.37), with

$$D(q) = \begin{bmatrix} D_{11} & D_{12} \\ D_{21} & D_{22} \end{bmatrix}; \qquad C(q,\dot{q}) = \begin{bmatrix} C_1 \\ C_2 \end{bmatrix};$$

$$G(q) = \begin{bmatrix} G_1 \\ G_2 \end{bmatrix}; \qquad F(\dot{q}) = \begin{bmatrix} F_1 \\ F_2 \end{bmatrix}$$

where: $D_{11} = \Delta_1 + \Delta_2 - \Delta_2 cos(\alpha)^2$, $D_{12} = -\Delta_3 cos(\alpha)$, $D_{21} = -\Delta_3 cos(\alpha)$, $D_{22} = \Delta_4$, $C_1 = 2\Delta_2 sin(\alpha)cos(\alpha)\dot{\theta}\dot{\alpha} + \Delta_3 sin(\alpha)\dot{\alpha}^2$, $C_2 = -\Delta_2 sin(\alpha)cos(\alpha)\dot{\theta}^2$, $G_1 = 0$, $G_2 = -\Delta_5 gsin(\alpha)$, $F_1 = B_{eq}\dot{\theta}$, and $F_2 = B_p\dot{\alpha}$, with: $\Delta_1 = m_pL_r^2 + J_r$, $\Delta_2 = \frac{1}{4}m_pL_p^2$, $\Delta_3 = \frac{1}{2}m_pL_pL_r$, $\Delta_4 = \frac{1}{4}m_pL_p^2 + J_p$, $\Delta_5 = \frac{1}{2}m_pL_p$.

Rotary Inverted Pendulum SDCF

Consider the rotary inverted pendulum equations of motion (2.44) and (2.45), notice that the control variable for the nonlinear model is the applied torque; however, for the real-time implementation, the torque is not directly controlled , the servo motor

input voltage is the controlled variable; therefore, the applied torque at the base of the rotary arm is generated by the servo motor gear-box given by

$$\tau = \frac{\eta_g K_g \eta_m k_t (V_m - K_g k_m \dot{\theta})}{R_m} \tag{2.46}$$

where η_g is the gear box efficiency, K_g high-gear total gear ratio, η_m is the motor efficiency, k_t motor current-torque constant, V_m is the applied voltage and R_m is the armature resistance (The servo motor gear-box model is described in detail in appendix C). Substituting (2.46) into (2.44), the Euler-Lagrange model of the system is defined as follows:

$$\begin{aligned} \Lambda V_m &= D_{11}\ddot{\theta} + D_{12}\ddot{\alpha} + C_1 + G_1 + F_1 \\ 0 &= D_{21}\ddot{\theta} + D_{22}\ddot{\alpha} + C_2 + G_2 + F_2 \end{aligned} \tag{2.47}$$

where

$$\Lambda = \frac{\eta_g K_g \eta_m k_t}{R_m} \tag{2.48}$$

Then defining a state vector $x = \begin{bmatrix} \theta & \alpha & \dot{\theta} & \dot{\alpha} \end{bmatrix}^T$, it is possible to represent the nonlinear equations of motion into the nonlinear input affine representation as (2.6), where the system output is defined as $h(x) = x_1 + x_2$. Therefore the Rotary Inverted Pendulum can be represented into the SDCF form as

$$\dot{x} = \begin{bmatrix} 0 & 0 & 1 & 0 \\ 0 & 0 & 0 & 1 \\ a_{31} & a_{32} & a_{33} & a_{34} \\ a_{41} & a_{42} & a_{43} & a_{44} \end{bmatrix} \begin{bmatrix} x_1 \\ x_2 \\ x_3 \\ x_4 \end{bmatrix} + \begin{bmatrix} 0 \\ 0 \\ b_3 \\ b_4 \end{bmatrix} u \tag{2.49}$$

$$h(x) = \begin{bmatrix} 1 & 0 & 0 & 0 \\ 0 & 1 & 0 & 0 \end{bmatrix} \begin{bmatrix} x_1 \\ x_2 \\ x_3 \\ x_4 \end{bmatrix}. \tag{2.50}$$

Where the entries of matrix $A(x)$ and $B(x)$ are defined as follows:

$$a_{31} = 0$$

$$a_{32} = \Gamma \frac{sin(x_2)}{x_2}(-\theta_3\theta_4 x_4^2 + g\theta_3\theta_5 cos(x_2) - 2\theta_2\theta_4 x_3 x_4 cos(x_2) + \theta_2\theta_3 x_3^2 cos^2(x_2))$$

$$a_{33} = -\Gamma(B_{eq}\theta_4)$$

$$a_{34} = -\Gamma(B_p\theta_3 cos(x_2))$$

$$a_{41} = 0$$

$$a_{42} = \Gamma \frac{sin(x_2)}{x_2}(g\theta_1\theta_5 + g\theta_2\theta_5 + \theta_1\theta_2 x_3^2 cos(x_2) + \theta_2^2 x_3^2 cos(x_2) - \theta_3^2 x_4^2 cos(x_2) - g\theta_2\theta_5 cos^2(x_2)$$
$$- 2\theta_2\theta_3 x_3 x_4 cos^2(x_2) - \theta_2^2 x_3^2 cos^3(x_2)) - \theta_3^2 x_4^2 cos(x_2) + g\theta_3\theta_5 cos(x_1)cos(x_2))$$

$$a_{43} = -\Gamma(B_{eq}\theta_3 cos(x_2))$$

$$a_{44} = \Gamma(-B_p\theta_1 - B_{eq}\theta_2 + B_{eq}\theta_2 cos^2(x_2))$$

$$\Gamma = \frac{1}{(\theta_1 + \theta_2)\theta_4 - (\theta_3^2 + \theta_2\theta_4)cos^2(x_2)}$$

$$b_3 = \Lambda \frac{\theta_4}{(\theta_1 + \theta_2)\theta_4 - (\theta_3^2 + \theta_2\theta_4)cos(x_2)^2}$$

$$b_4 = \Lambda \frac{\theta_3 cos(x_2)}{(\theta_1 + \theta_2)\theta_4 - (\theta_3^2 + \theta_2\theta_4)cos(x_2)^2}$$

$$B_{eq} = \left[\frac{\eta_g \eta_m K_g^2 k_t k_m}{R_m} + B_r\right]$$

2.5. Conclusions

In this chapter the main concepts related to the dynamics and modeling of open cinematic chains are presented, making use of the methodology known as the Euler-Lagrange model, from which the equations of motion for the Pendubot and rotary inverted pendulum are obtained. Finally different representations that can be given for a class of nonlinear systems, such as the state dependent coefficient factorization and the regular form, are stated. The state-space models obtained for both the Pendubot and the rotary inverted pendulum. Particularly the SDCF will be used in the incoming chapters for control purposes.

Chapter 3

Nonlinear Optimal Control and Sliding Modes Design

In this chapter, two control strategies for nonlinear systems are presented; the optimal control based on SDCF and the sliding modes. Then it is proposed the design of a control algorithm which combines the capabilities of optimal control in the sense of minimization of a performance index, along with the sliding modes, which allows to add elements of robustness to the controller.

3.1. Optimal Control for SDCF Systems

The state-dependent Riccati equation (SDRE) [Cimen10], entails factorization of the nonlinear dynamics of a system into the product of a matrix-valued function (dependent on the state), and a state vector. By doing so the SDRE algorithm fully captures the nonlinearities of the system, and in the context of optimal control, it allows the minimization of a quadratic performance index, having a linear-like structure. As a result of the SDCF of the involved matrices, the non-unique parametrization of the system gives extra degrees of freedom, which can be used in order to enhance the controller performance. Therefore, the SDRE solves online the optimal problem. SDRE

has emerged as a general design methodology, which provides a systematic means of designing nonlinear controllers observers and filters, this include missiles, aircraft, unmanned aerial vehicles, satellites, spacecraft ships, under water vehicles, biomedical systems and robotics [Cimen10]. According with the existence of the SDRE solution the following considerations are stated:

Remark 3 *If matrices $A(x)$, $B(x)$, $C(x)$ are bounded and piecewise continuous and, if the pair $\left[\ A(x),\ \ C(x)\ \right]$, is observable, then the solution of the SDRE is positive definite and upper bounded.*

Remark 4 *If the pairs $\left[\ A(x),\ \ B(x)\ \right]$ and $\left[\ A(x),\ \ C(x)\ \right]$ are stabilizable and detectable $\forall x$, then the SDRE has a unique and asymptotically stable solution.*

The above considerations are derived from the properties of linear systems in terms of the Riccati equation as seen in [Kalman59], and for this thesis, these properties are considered to be inherited to SDCF systems due to their linear-like structure.

3.1.1. Optimal Control for Nonlinear Systems Stabilization

Problem statement

Consider a nonlinear system described by (2.6) and (2.7). The objective of the nonlinear optimal stabilizing controller is to provide an optimal control law $u^*(x)$ such that it stabilizes the system (2.7). The nonlinear optimal controller is introduced by the following theorem:

Theorem 2 *[Ornelas-Tellez13] Assume that system (2.7) is state-dependent controllable and state-dependent observable, then it is possible to compute an optimal control law $u^*(x)$ such that it provides asymptotic stability of the system in close loop:*

$$u^*(x) = -R^{-1}B^T(x)P(x)x \tag{3.1}$$

which minimizes the following performance index described by

$$J = \frac{1}{2}\int_0^\infty \left(x^T Q x + u^T R u\right) dt \tag{3.2}$$

where Q and R are symmetric and positive define weighting matrices, and $P(x)$ is the solution of State-dependent Riccati matrix differential equation (SDRE) given by

$$\dot{P}(x) = -Q + P(x)B(x)R^{-1}B^T(x)P(x) - A^T(x)P(x) - P(x)A(x) \tag{3.3}$$

With the boundary condition $P(x(\infty)) = 0$ ■

According with Theorem 2, the stabilization of (2.7) is achieved.

3.1.2. Nonlinear Optimal Tracking Control

Nonlinear optimal tracking control [Ornelas-Tellez13], extends the nonlinear optimal control methodology by using the SDCF in order to track time varying reference signals. The problem considered is the infinite-horizon tracking control [Carlson87] of nonlinear systems, derived from the state-regulation problem [Athans07], which has the objective of "keeping the state near zero", then the minimum principle is used in order to obtain the necessary conditions for the optimal control.

Problem Statement

Consider a nonlinear system affine in the input as (2.6), which can be described into the SDCF given by (2.7). Considering the output of the system y and a reference signal r, the objective of the nonlinear optimal tracking control is to make the system output to track the desired reference signal and at the same time minimize a performance index given as

$$J = \frac{1}{2}\int_0^\infty (e^T Q e + u^T R u) dt \tag{3.4}$$

with a trajectory tracking error defined as

$$\begin{aligned} e &= r - y \\ &= r - C(x)x \end{aligned} \tag{3.5}$$

where r is the reference to be tracked. Vector r can be considered to be the desired output for the system, as seen in [Athans07]; Q and R are symmetric and positive definite matrices. The optimal tracking scheme deals with the problem of determining an optimal control law $u(x)^*$ which forces the output of system (2.7) to track a desire reference r, in the optimal sense of minimizing a given performance index (3.4), so that the tracking error e is minimized [Athans07]. It is assumed that the optimal control law $u(x)^*$ is not constrained in magnitude, thus there may be cases in which the control signal is extremely large; therefore, there exist a tradeoff between the control expenditure and the error magnitude; in one hand it is desired to keep the error "small", but on the other hand it is desired not to use unnecessary "large" controls. Matrix Q is a matrix weighting the performance of the state vector, while R is a matrix weighting the control effort expenditure, if more importance is given to the system state performance, a higher value for Q could be selected or reducing the value of R. Matrix Q can be also selected as $Q(x)$ in order to gain flexibility on the entries of Q, in such a way that they can be defined as error functions in order to weight the controller perfomance in terms of the error. Different methodologies are reported in which the optimal values of matrix Q are computed, as seen in [Ornelas-Tellez14] where a particule swarm optimization method is used, a different approach might be the use of the so-called Bryson rules for linear systems, thus the entries of matrix Q might be selected as

$$q_n = \frac{\alpha}{\beta|e|+\gamma}. \tag{3.6}$$

Therefore, it is guaranteed that for "small" errors the element of matrix Q will be a

constant defined by $\lim_{e\to 0}(q_n) = \frac{\alpha}{\gamma}$, and for the case of "large" errors $\lim_{e\to\infty}(q_n) = 0$, which reduces the control input expenditure. The following theorem establishes the solution to the optimal tracking control problem for SDCF systems:

Theorem 3 *[Ornelas-Tellez13] Assume that system (2.7) is state-dependent controllable and state-dependent observable, then the nonlinear optimal control law*

$$u^*(x) = -R^{-1}B^T(x)\left(P(x)x - z(x)\right) \tag{3.7}$$

achieves trajectory tracking for system (2.7), along a desired trajectory r, where $P(x)$ is the solution of the SDRE and $z(x)$ is the solution of a vector differential equation, respectively, where

$$\dot{P}(x) = -C^T(x)QC(x) + P(x)B(x)R^{-1}B^T(x)P(x) \tag{3.8}$$
$$-A^T(x)P(x) - P(x)A(x)$$

$$\dot{z}(x) = -\left[A(x) - B(x)R^{-1}B^T(x)P(x)\right]^T z(x) - C^T(x)Qr \tag{3.9}$$
$$\dot{\varphi} = -\frac{1}{4}z^T B(x)R^{-1}B(x)z(x) - r^T Qr$$

with boundary conditions $P(x(\infty)) = 0$, $z(x(\infty)) = 0$, and $\varphi(\infty) = 0$. ■

Here, for the sake of completeness, a sketch of the proof for Theorem 3 is presented. Details of the proof can be seen in [Ornelas-Tellez13].

The controller (3.7)-(3.9) is derived from the optimality conditions on the Hamiltonian function, which is defined as

$$\mathcal{H}(x,u,t) = \frac{1}{2}(r - C(x)x)^T Q(r - C(x)x) + \frac{1}{2}u^T Ru + \tag{3.10}$$
$$\frac{\partial V(x,t)}{\partial x}f(x) + \frac{\partial V(x,t)}{\partial x}g(x)u$$

where $V(x,t)$ is the optimal value function. The Hamiltonian is used to attain the control law u by applying the maximum principle condition

$$\frac{\partial \mathcal{H}(x,u,t)}{\partial u} = Ru + B^T(x)\frac{\partial V(x,t)}{\partial x} = 0 \tag{3.11}$$

and solving for u, then the optimal control law results in

$$u^* = -R^{-1}B^T(x)\frac{\partial V(x,t)}{\partial x} \tag{3.12}$$

For the optimal control solution based on (3.10) and the optimal control law (3.12) the following HJB equation must be satisfied

$$\begin{aligned} 0 = &\frac{\partial V(x,t)}{\partial t} + \frac{1}{2}r^T Q r - r^T Q C(x)x \\ &+ \frac{1}{2}x^T C^T(x) Q C(x)x - \frac{1}{2}\frac{\partial V^T(x,t)}{\partial x}B(x) \\ &\times R^{-1}B^T(x)\frac{\partial V(x,t)}{\partial x} + \frac{\partial V^T(x,t)}{\partial x}A(x)x. \end{aligned} \tag{3.13}$$

One way of solving the Hamilton-Jacobi-Bellman (HJB) equation is to propose a solution such that (3.11) satisfies itself [Kirk04]; hence, $V(x)$ is proposed as a quadratic form, as seen in [Athans07]

$$V(x,t) = \frac{1}{2}x^T P x - z^T(x)x + \varphi \qquad P = P^T > 0. \tag{3.14}$$

Using (3.14) and (3.13), equations (3.8) and (3.9) are obtained. The optimal value of the function $V(x)$ also serves as a Lyapunov function, which along with the detectability property guarantees asymptotic stability of the optimal feedback systems [Kokotovic97].

3.1.3. Nonlinear Optimal Tracking Control Error Analysis

This subsection provides the tracking error analysis of the optimal controller based on the SDCF proposed in [Ornelas-Tellez13], the following analysis results in the

conclusion that the tracking error is globally uniformly ultimately bounded, unlike the stability analysis proposed in [Ornelas-Tellez13], for this analysis it is considered the differential vector (3.9), which implies the tracking error for the controller (3.7). This result is considered to be a contribution of this thesis. Consider an input affine nonlinear system as (2.6) under the following assumptions:

Assumption 1 *The functions $f(x)$ and $h(x)$ can be decomposed into the state-dependent coefficient factorization (SDCF) as*

$$f(x) = A(x)x, \qquad h(x) = C(x)x. \tag{3.15}$$

Assumption 2 *The factorization of $A(x), B(x)$ and $C(x)$ fulfill the state-dependent controllability and observability tests*

$$rank\{\mathcal{C}\} = n \qquad \forall\, x \qquad rank\{\mathcal{O}\} = n \,\forall\, x. \tag{3.16}$$

Under assumptions 1 and 2, the following analysis can be carried out for the tracking error, defined as

$$\epsilon = x - r. \tag{3.17}$$

The close-loop behavior of the system (2.7) under optimal tracking control law (3.7) is described by

$$\begin{aligned} \dot{x} &= \left[A(x) - B(x)R^{-1}B^T(x)P\right]x + B(x)R^{-1}B^T(x)z \\ &= \bar{A}(x)x + \bar{B}(x)z \end{aligned} \tag{3.18}$$

where

$$\begin{aligned} \bar{A}(x) &= \left[A(x) - B(x)R^{-1}B^T(x)P\right] \\ \bar{B}(x) &= B(x)R^{-1}B^T(x). \end{aligned} \tag{3.19}$$

From (3.17), (3.18) and (3.9), it follows that the dynamic of the error function results in

$$\begin{aligned}\dot{\varepsilon} &= \bar{A}(x)x + \bar{B}(x)z - \dot{r} \\ &= \bar{A}(x)(\varepsilon + r) + \bar{B}(x)z(x) \\ &= \bar{A}(x)\varepsilon + \bar{A}(x)r + \bar{B}(x)z(x) - \dot{r} \\ \dot{z}(x) &= -\bar{A}(x)^T z(x) - C^T Q r.\end{aligned} \tag{3.20}$$

In order to analyze the stability of the transformed system (3.20) in terms of the tracking error (3.17), let consider the following Lyapunov candidate function

$$V = \varepsilon^T P(t)\varepsilon + z^T M z \tag{3.21}$$

where $P(t)$ and M are symmetric positive define matrices. Assume that $P(t)$ satisfies the matrix differential equation [Khalil02]

$$-\dot{P}(t) = P(t)\bar{A} + \bar{A}^T P(t) + Q_z \tag{3.22}$$

with

$$0 < c_1 I \leq P(t) \leq c_2 I, \quad \forall t \geq 0 \tag{3.23}$$

and Q_z a symmetric and positive definite matrix satisfying

$$Q_z \geq c_3 I > 0. \tag{3.24}$$

Thus, the time derivate of V is calculated as

$$
\begin{aligned}
\dot{V} &= \varepsilon^T \dot{P}\varepsilon + \dot{\varepsilon}^T P\varepsilon + \varepsilon^T P\dot{\varepsilon} + z^T \dot{M} z + \dot{z}^T M z + z^T M \dot{z} \\
&= \varepsilon^T \dot{P}\varepsilon + (\bar{A}\varepsilon + \bar{B}z + \bar{A}r - \dot{r})^T P\varepsilon + \varepsilon^T P(\bar{A} + \bar{B}z + \bar{A}r - \dot{r}) \\
&+ z^T \dot{M} z + (-\bar{A}^T z - C^T Q r)^T M z + z^T M(-\bar{A}^T z - C^T Q r) \\
&= \varepsilon^T \dot{P}\varepsilon + \varepsilon^T \bar{A}^T P\varepsilon + \varepsilon^T P\bar{A}\varepsilon + 2z^T \bar{B}^T P\varepsilon + 2(\bar{A}r - \dot{r})^T P\varepsilon \\
&+ z^T \dot{M} z - z^T \bar{A} M z - z^T M \bar{A}^T z - 2rQCMz \\
&= \varepsilon^T \left[\dot{P} + \bar{A}^T P + P\bar{A}\right] \epsilon + z^T \left[\dot{M} - \bar{A}M - M\bar{A}^T\right] z + 2z^T \bar{B}^T P\varepsilon \\
&+ 2(\bar{A}r - \dot{r})^T P\epsilon - 2rQCMz.
\end{aligned}
\tag{3.25}
$$

From (3.8) and (3.22), it follows that

$$
\begin{aligned}
\dot{V} &= -\varepsilon \left[C^T QC + P\bar{B}P\right] \varepsilon - z^T Q_z z + 2z^T \bar{B}^T P\varepsilon \\
&+ 2(\bar{A}r - \dot{r})^T P\varepsilon - 2rQCMz
\end{aligned}
\tag{3.26}
$$

Setting an augmented state defined as follows:

$$
x_a = \begin{bmatrix} \varepsilon \\ z \end{bmatrix}, \tag{3.27}
$$

expression (3.26) can be rewritten in terms of the augmented state x_a as follows:

$$
\begin{aligned}
\dot{V} &= -\begin{bmatrix} \varepsilon^T & z^T \end{bmatrix} \begin{bmatrix} C^T QC + P\bar{B}P & -\bar{B}^T P \\ -\bar{B}^T P & Q_z \end{bmatrix} \begin{bmatrix} \varepsilon \\ z \end{bmatrix} \\
&+ \begin{bmatrix} 2(\bar{A}r - \dot{r})^T P & -2rQCM \end{bmatrix} \begin{bmatrix} \varepsilon \\ z \end{bmatrix} \\
&= -x_a^T \bar{Q} x_a + E x_a.
\end{aligned}
\tag{3.28}
$$

By defining

$$\bar{Q} = \begin{bmatrix} C^T Q C + P\bar{B}P & -\bar{B}^T P \\ -\bar{B}^T P & Q_z \end{bmatrix} \tag{3.29}$$

$$E = \begin{bmatrix} 2(\bar{A}x_{ss} - \dot{x}_{ss})^T P & -2x_{ss}QCM \end{bmatrix} \tag{3.30}$$

then (3.28) becomes

$$\dot{V} = -x_a \bar{Q} x_a + E x_a. \tag{3.31}$$

Through Q and Q_z matrix $\bar{Q}$ can be selected as a continuous bounded positive definite differentiable matrix such that

$$0 < c_4 I \leq \bar{Q} \leq c_5 I \ \ \forall x \tag{3.32}$$

then (3.31) can be expressed as

$$\dot{V} \leq -c_4(\bar{Q})||x_a||^2 + ||E||\,||x_a|| \tag{3.33}$$

Rewriting (3.31) by adding a convenient zero

$$\begin{aligned} \dot{V} &\leq -c_4(\bar{Q})||x_a||^2 + ||E||\,||x_a|| + \theta c_4(\bar{Q})||x_a|| - \theta c_4(\bar{Q})||x_a|| \\ &= -(1-\theta)c_4(\bar{Q})||x_a||^2 + (||E|| - \theta c_4(\bar{Q})||x_a||)||x_a|| \qquad \forall ||x_a|| \geq \frac{||E||}{\theta c_4(\bar{Q})} \\ &= -(1-\theta)c_4(\bar{Q})||x_a||^2 \end{aligned} \tag{3.34}$$

where $0 < \theta < 1$. That is, the tracking error is globally uniformly ultimately bounded.

Remark 5 *Notice that as far as the values of Q and Q_z are greater the convergence quote for the state x_a will be smaller, therefore the greater the values for Q and Q_z are, the lower the tracking error will be, according to [Khalil02]. The convergence quote for the state x_a is defined as follows:*

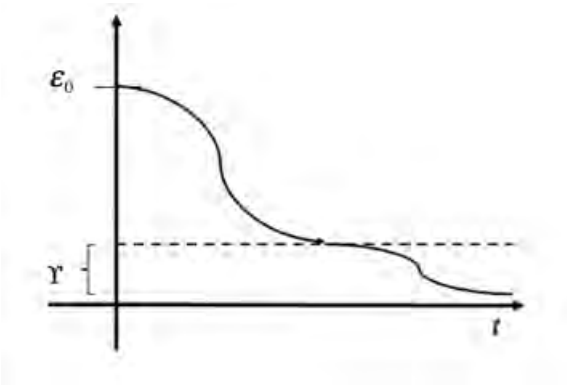

Figure 3.1: Tracking error bounded region

$$\Upsilon = \frac{||E||}{\theta c_4(\bar{Q})}\sqrt{\frac{c_2}{c_1}}. \tag{3.35}$$

That is, the tracking error remains bounded in a region Υ, as seen in Figure 3.1.

■

3.1.4. Robust Nonlinear Tracking Controller

As a result of the tracking error analysis, it was possible to demonstrate that nonlinear optimal tracking control based on the SDCF, bounds the error function in a certain region Υ. Then in order to reduce the tracking error it possible to add an integral action to the optimal controller that would enhance the controller performance and reduce the tracking error. This approach is called the robust nonlinear tracking controller, also this approach is more feasible for a real-time implementation. Consider a nonlinear disturbed system described as follows:

$$\begin{aligned} \dot{x} &= f(x) + g(x)u + D \\ y &= h(x) \end{aligned} \tag{3.36}$$

where D is a disturbances term, which is considered to be known. Consider that system (3.36) can be decomposed into the SDCF resulting in

$$\begin{aligned} \dot{x} &= A(x)x + B(x)u + D \\ y &= C(x)x. \end{aligned} \tag{3.37}$$

The main purpose of the robust nonlinear optimal tracking controller is that the controller allows the system(3.37) output to track a desired reference signal as close as possible in the presence of disturbances in the optimal sense of minimizing a performance index. Defining the trajectory tracking error as (3.5), an integral term is introduced such that disturbances can be rejected defined as

$$\dot{\Phi} = -e \tag{3.38}$$

where $\Phi \in \mathbb{R}^p$ is a vector of integrators for a system with p outputs. Therefore an augmented system can be stated, as seen in [Diaz-Sepulveda16], which includes an integrator defined as

$$\begin{aligned} \dot{x}_a &= \begin{bmatrix} \dot{\Phi} \\ \dot{x} \end{bmatrix} \\ &= \begin{bmatrix} -e \\ A(x)x + B(x)u \end{bmatrix} \\ &= \begin{bmatrix} C(x)x - r \\ A(x)x + B(x)u \end{bmatrix} \end{aligned} \tag{3.39}$$

with $x_a = [\Phi, x]^T$, therefore the augmented system (3.39) can be rewritten as

$$\begin{aligned} \dot{x}_a &= A_a(x_a) + B_a(x_a)u + D \\ y_a &= C_a(x_a)x_a \end{aligned} \tag{3.40}$$

where

$$\begin{aligned} A_a(x_a) &= \begin{bmatrix} 0 & C(x) \\ 0 & A(x) \end{bmatrix}; \quad B_a(x_a) = \begin{bmatrix} 0 \\ B(x) \end{bmatrix}; \\ C_a(x_a) &= \begin{bmatrix} 0 & C(x) \end{bmatrix}; \qquad D_a = \begin{bmatrix} -r \\ 0 \end{bmatrix}. \end{aligned} \tag{3.41}$$

With the addition integral term, the performance index is defined as

$$J = \frac{1}{2}\int_{t_0}^{\infty} (\Phi^T Q_i \Phi + e^T Q e + u^T R u) dt \tag{3.42}$$

where Q_i is a parameter weighting matrix with the integral gains. The solution of the nonlinear robust optimal tracking control is established as the following theorem.

Theorem 4 *Assume that system (3.37) is state-dependent controllable and state-dependent observable, then the nonlinear optimal control law*

$$u^*(x_a) = -R^{-1}B_a^T(x_a)(P(x_a)x_a - z_a(x_a)) \tag{3.43}$$

ensures trajectory tracking control for system (3.37) over the desired reference r, where $P(x_a)$ is the solution of the matrix Riccati differential equation (3.8), and $z(x_a)$ is the solution of the vector differential equation

$$\dot{z}(x_a) = -\left[A_a(x_a) - B_a x_a R^{-1} B_a^T(x_a) P(x_a)\right]^T z(x_a) + P(x_a)D - C_a^T(x_a)Qr \tag{3.44}$$

with boundary conditions $P(x(\infty)) = 0$ and $z(x(\infty)) = 0$ respectively. ■

Remark 6 *By using the SDCF technique, the system is not being linearized around an equilibrium point, hence the nonlinear system is completely considered, and thus the controller has a larger operation range over the system in comparison with the linear controllers; in addition, the nonlinear inherit nature of the system is exploited.*

Optimal Control Properties

In this thesis it is assumed that the previous properties are inherit for the nonlinear case for systems represented into the SDCF. These properties have been considered for the nonlinear case in [Kokotovic97].

By the use of optimal control techniques, the following properties are achieved for the case of linear systems:

- ◇ Robustness. Optimal control provides infinite gain margin $K \rightarrow \infty$, also it guarantees phase margin $\gamma \geq 60°$. The passivity connection established by [Moylan74], states that as in the linear case, optimal systems have an infinite gain margin, due to its passivity property with respect to the output [Kokotovic97].

- ◇ Behavior of closed-loop poles: Expensive control. When $R > C^T QC$, the cost function is dominated by the control effort u and the controller minimizes the control action itself.

- ◇ Behavior of closed-loop poles: Cheap control. When $R < C^T QC$, the cost function is dominated by the output errors and there is no penalty for using large values for u. (For the LQR tracking control).

3.2. Sliding Mode Control

Uncertainty in the system behavior appears as a result of the imperfection of the model, which is supposed to be idealized the real life system; nonetheless, the models fail to recognize factors as time delays, dead zones, hysteresis, inertiality of the elements, etc. [Utkin92]. Robust control is a branch of modern control theory that explicitly deals with uncertainty in its approach to controller design. Robust control methods are design to function properly so long as uncertain parameters or disturbances [Fridman14]. The sliding mode control (SMC) is considered to be a sort of robust control because it is able to deal with model uncertainties as well as external disturbances. Sliding mode control has been successfully applied to robot manipulators, underwater vehicles, automotive transmissions, engines, high performance electric motors and power systems [Slotine91].

The sliding mode control was developed in the Soviet Union in the mid $1950s$, the control technique is a particular type of variable structure control (VSC), characterized by a suite of feedback control laws and a decision rule. The decision rule, (known as the switching function), has information related with the system behavior and produces an output, which is the particular feedback control that should be used at a particular instant of time. The result is a variable structure system which consist of a combination of subsystems where each one of them have a well defined control structure, valid for specific regions of the whole system behavior.

3.2.1. Problem Statement

Consider the following nonlinear system (2.6) with the discontinuous control law

$$u_i = \begin{cases} u_i^+ & if \ \ \sigma_i(x) > 0 \\ u_i^- & if \ \ \sigma_i(x) < 0 \end{cases} \quad i = 1, 2, \ldots, m \tag{3.45}$$

where

$$\sigma(x) = [\sigma_1(x), \sigma_2(x), \ldots, \sigma_m(x)]^T = 0 \tag{3.46}$$

is the sliding mode surface.

The aim of the sliding mode control is to find a continuous function u_i^+, u_i^- and a sliding surface $\sigma(x)$ in order to drive and constrain the trajectories of system to lie inside a neighborhood of a sliding manifold. The next important aspect of the sliding mode control (SMC) is to guarantee the existence of a sliding mode. A sliding mode exist when in the neighborhood the switching function $\sigma(x) = 0$, where the velocity vector of the state trajectories is always directed toward the switching function. The advantages for obtaining such motion are firstly the system reduction order and secondly, that the sliding motion is insensitive to parameter variations; this property makes the sliding mode methodology attractive for designing robust controllers [Edward98]. Figure 3.2, illustrates sliding mode in the intersection of each of the surfaces.

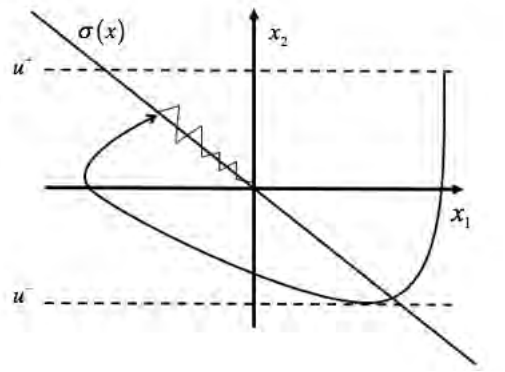

Figure 3.2: Portrait phase sliding motion

3.2.2. Existence of the Sliding Mode

The existence of the sliding mode requires the stability of the trajectories of the sliding surface $\sigma(x) = 0$. Thus, the system states must approach the sliding surface at least asymptotically. Therefore the existence of sliding mode problem can be seen as a generalized stability problem; hence, the Lyapunov's method may be used for such analysis. For single input systems, the suitable Lyapunov's function is

$$V(x) = \frac{1}{2}\sigma^2(x) \tag{3.47}$$

which is positive definite, thus the time derivate of the candidate Lyapunov's function is given by

$$\dot{V}(x) = \sigma\frac{\partial\sigma}{\partial x} < 0. \tag{3.48}$$

Condition (3.48) is called the reaching condition or the reachability condition [Utkin99], which ensures that the sliding surface is reached asymptotically. The reachability condition (3.48) is also replaced by the so-called η reachability condition defined as follows:

$$\dot{V}(x) = \sigma\frac{\partial\sigma}{\partial x} \leq -\eta|\sigma| < 0. \tag{3.49}$$

Condition (3.49) ensures finite time convergence of the sliding surface $\sigma(x) = 0$, defined by integration of (3.49) as

$$|\sigma(x(t))| - |\sigma(x(0))| \leq -\eta t. \tag{3.50}$$

From (3.50), the required time to reach the sliding surface from the initial condition, is defined as [Fridman02]:

$$t_s = \frac{|\sigma(x(0))|}{\eta}. \tag{3.51}$$

3.2.3. The Chattering Effect

Sliding mode control is an effective control methodology for nonlinear systems. The major advantage of the sliding mode control is that the uncertainties and external disturbances of the system can be handled, nevertheless sliding mode control has the following drawbacks:

- ◇ The SMC is only effectively applied to systems described in the regular form.
- ◇ Chattering: the undesirable oscillations inspired by the discontinouos control law in the presence of unmodeled dynamics.
- ◇ Basic sliding mode is invariant with respect to matched perturbations only.

One of the major disadvantages of the sliding mode controllers is that the resulting control action is a discontinuous function of time, which in practical applications may lead to actuators damage, besides to the fact that there not exist any physical device able to support a theoretical infinite switching frequency; this phenomenon will take place as the system trajectories repeatedly cross the sliding surface, this high frequency motion is described as "chattering", illustrated in Figure 3.3. In order to overcame these drawbacks, it is of interest to find a continuous control action (smooth function), robust against uncertainties and disturbances, guaranteeing the same control objectives as the discontinuous sliding mode control. The use of smooth functions in sliding modes has some advantages: reduces chattering and make sliding mode viable in real time applications due to their limited switching frequency. Hence high order sliding modes can reduce and eliminate chattering and ensure the asymptotically convergence of the system.

3.2.4. High-Order Sliding Modes

The recently proposed high-order sliding modes (HOSM), generalizes the basic sliding mode idea acting on the higher order time derivates of the system deviation

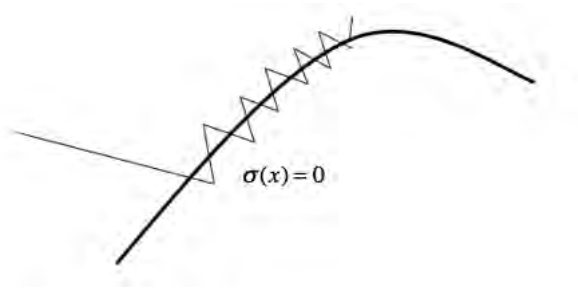

Figure 3.3: The chattering effect

from the constraint instead of influencing the first deviation as it happens in standard sliding modes [Fridman02]. The main problem in the implementation of HOSM is the increasing information demand where the only known exclusion is the so-called "Super-Twisting " [Levant93], a second order sliding mode which only need information related to the measurable elements of the sliding surface.

For the super-twisting analysis, let consider the nonlinear system

$$\dot{x} = f(x,u), \quad s = s(x) \in \mathbb{R}, \quad u = U(x) \in \mathbb{R} \tag{3.52}$$

where $x \in \mathbb{R}^n$, u is the control input, f and s are smooth functions of appropriate dimension. The main task of the controller is to constrain $s = 0$. By differentiating successively the output variable s, depending on the relative degree of the system, the following 2 different cases are considered:

1. Relative degree of the system $\bar{r} = 1$

2. Relative degree of the system $\bar{r} \geq 2$

In case 1, the variable structure problem can be solved by means of first-order sliding mode control, however second-order sliding mode control can be used to avoid the chattering effect. In this case u, will become the output of a first order dynamic system, thus a discontinuos control $\dot{u}$ steers the sliding variable s to zero, keeping $s = 0$ in a

second order sliding mode, thus the control u is continuous and the chattering effect is avoided.

Super-Twisting Algorithm

The super-twisting algorithm is a variant from the sliding mode controller used to control systems with relative degree one; thus, the chattering effect can be eliminated. The controller name refers that the trajectories of the phase plane $(\sigma, \dot{\sigma})$ are characterized by a twist around the origin as seen in Figure 3.4.

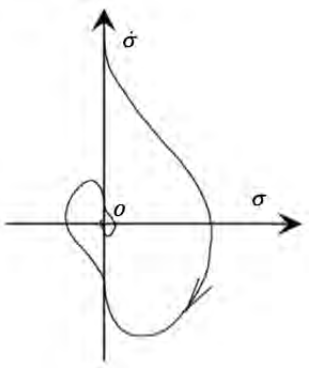

Figure 3.4: Portrait phase super-twisting

Theorem 5 *[Moreno08] Consider the system (2.6), assuming that it has relative degree one, therefore the algorithm defined by*

$$\begin{aligned} u(x) &= -M_1|\sigma|^{\frac{1}{2}} sign(\sigma) + u_1 \\ \dot{u}_1(x) &= -M_2 sign(\sigma), \quad M_1 > 0, \;\; M_2 > 0 \\ \sigma &= \lambda - \lambda_i \end{aligned} \tag{3.53}$$

with $M_1, M_2 > 0$ is able to drive the trajectories of the second order sliding mode on the sliding manifold in finite time. ■

Proof: see Appendix A, where the analysis is done based on [Moreno08]

3.3. Optimal Control with Sliding Modes

In this section a nonlinear controller which combines the capabilities of both optimal control an sliding modes is presented, in order to obtain a robust control scheme able to reject bounded external disturbances and parametric uncertainties, for nonlinear systems represented in the so-called regular form, which is the main contribution of this thesis.

Consider a nonlinear system described in the regular form (2.13), then assume that the subsystem $\dot{x}_1'$, can be decomposed into the SDCF representation as

$$\begin{aligned} \dot{x}_1' &= A(x_1')x_1' + B_1(x_1')x_2' \\ y &= C(x_1')x_1' \end{aligned} \tag{3.54}$$

where x_1' is a reduced order vector such that $x_1' \in \mathbb{R}^{n-1}$ with $A(x_1') \in \mathbb{R}^{n-1\times n-1}$ and $B(x_1')$ is a column matrix of appropriate dimension. Notice that the state x_2' becomes the control input for the subsystem (3.54). Hereinafter the state x_2' will be called "Pseudocontrol". If the resulting subsystem (3.54) is both state-dependent controllable and state-dependent observable, satisfying conditions (2.8) and (2.10), then it is possible to apply a nonlinear optimal tracking control law as (3.7) to subsystem (3.54) described as

$$x_2'^{*} = -R^{-1}B^T(x_1')\left(P(x_1')x_1' - z(x_1')\right) \tag{3.55}$$

where

$$\begin{aligned} \dot{P}(x') = &-C^T(x_1')QC(x_1') + P(x_1')B(x_1')R^{-1}B^T(x_1')P(x_1') \\ &-A^T(x_1')P(x_1') - P(x_1')A(x_1') \end{aligned} \tag{3.56}$$

$$\dot{z}(x_1') = -\left[A(x_1') - B(x_1')R^{-1}B^T(x_1')P(x_1')\right]^T z(x_1') - C^T(x_1')Qr$$

where r is a desired reference vector and e is the tracking error defined as

$$\begin{aligned} e &= r - y \\ &= r - C(x_1')x_1'. \end{aligned} \tag{3.57}$$

such that system (3.54) tracks a time varying reference signal in the optimal sense of minimizing the following performance index.

$$J = \frac{1}{2}\int_{t_s}^{\infty} (e^T Q e + x_2'^T R x_2')dt \tag{3.58}$$

where t_s is the required time to reach the sliding surface which is calculated as (3.51).

Then the optimal control law $x_2'^*$ will be considered to be the reference signal for the synthesis of a super-twisting controller (3.53), for controlling the second block (2.13), which is achieved by selecting an optimal sliding surface $\sigma(x)$ defined as

$$\sigma = x_2'^* - x_2' = 0. \tag{3.59}$$

Remark 7 *One of the major advantages of using the nonlinear optimal sliding mode controller, in contrast with the nonlinear optimal controller based on the SDCF, is firstly a reduction of the possible system factorizations of $f_1(x) = A(x_1)x_1$ for the first block (which is controlled via optimal control based on SDCF), due to the fact that only the state dependent coefficient factorization is performed for the first regular form subsystem and is considered to be a reduced-order system. Secondly since the second regular form block with the structure*

$$\dot{x}_2' = f_2(x_1', x_2') + B_2(x_1', x_2')u + \delta \tag{3.60}$$

is controlled via a super-twisting controller, it does not require the complete information of the parameters of the system, only the measurable information of the sliding

surface, which makes this control scheme to be robust against parametric uncertainties and bounded external disturbances, where δ is a bounded term of external disturbances. Since the nonlinear optimal sliding modes controller does not require neither information of the parameters nor the structure of the regular form second block, it is possible to reject such external disturbances.

Nonlinear Optimal Tracking Sliding Mode Algorithm

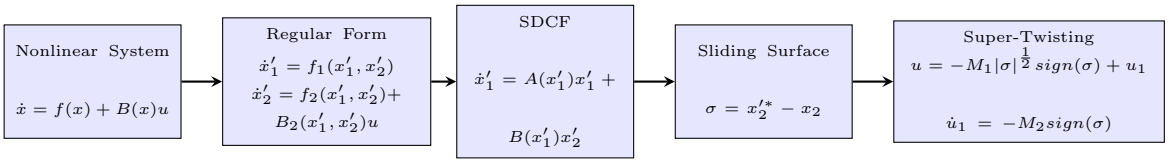

Figure 3.5: General flow chart of the nonlinear optimal sliding mode controller.

The nonlinear optimal tracking sliding modes procedure Figure 3.5, can be summarized as follows:

1. Determine the diffeomorphism $\varphi(x)$.
2. Bring the nonlinear system into the regular form.
3. Apply nonlinear optimal control theory for the reduced order subsystem (first block), from which is calculated the optimal pseudo control x_2^*.
4. Determine the optimal sliding surface $\sigma(x) = x_2^* - x_2$, for the second block.
5. Apply high order sliding mode (Super-Twisting) to drive $\sigma(x) = 0$, for the second block.

3.4. Conclusions

In this chapter the theoretical concepts for the design of optimal nonlinear controllers are presented, as well as a variant, which combines the nonlinear optimal control with

the sliding modes. The following points can be additionally addressed:

- ◇ A characterist of using a SDCF control schemes is the multiple factorizations of matrices $A(x)$ and $B(x)$, which may result in a enhance the controller performance or even cause a loss of controllability of the system.

- ◇ Nonlinear optimal control based on the SDCF needs a complete knowledge of the systems parameters, in contrast by the use of optimal sliding modes it is possible to design an optimal controller for a reduced order subsystem, which reduces the amount of information required, and then control the rest of the system by the use of a robust controller which do not require information of the system parameters.

- ◇ For use of an optimal sliding mode controller, it is necessary the prior knowledge of the diffeomorphism, which transforms the nonlinear system into the regular form.

- ◇ The design control strategies are used in the next chapter for controlling underactuated mechanical systems.

Chapter 4

Application of Optimal Control and Sliding Modes

This chapter presents the application of optimal control based on the SDCF and the nonlinear optimal sliding modes control algorithms designed in chapter 3, to the Pendubot and the rotary inverted pendulum, whose models are obtained in chapter 2. Simulations and real-time experimental results demonstrate the effectiveness of the designed control algorithms.

4.1. Application to the Pendubot

Consider the Pendubot SDCF model (2.42). Notice that this system is a particular case of input-affine nonlinear systems in the form (2.6), and therefore, the optimal tracking control technique can be applied.

4.1.1. Controllability Analysis

In accordance with Remark 2, in order to design a nonlinear optimal controller, the observability and controllability properties of the systems must be fulfilled; therefore,

the region over the space state, where the Pendubot is not controllable, is defined by the condition where $det(\mathcal{C}(x)) = 0$, that is for the following regions [Wang11]:

$$\begin{aligned} &1) \quad x_1 = \pm\pi \ \wedge \ x_2 = \pm\pi \\ &2) \quad x_1 = \pm\tfrac{\pi}{2} \ \wedge \ x_2 = \pm\tfrac{\pi}{2} \end{aligned} \tag{4.1}$$

The first uncontrollable configuration of the Pendubot corresponds with the first link being completely horizontal and the second link at $\frac{\pi}{2}\ rad$ in reference with the first link. The second configuration corresponds to the links folded over each other with the first link hanging downward.

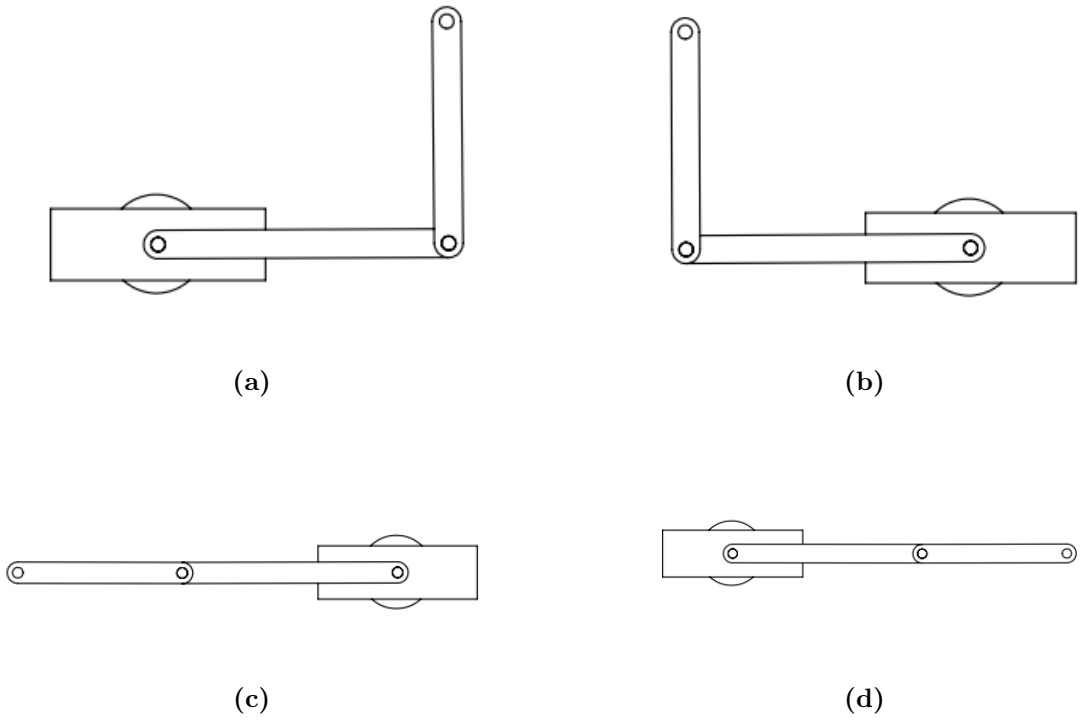

Figure 4.1: Pendubot's uncontrollable positions

Figure 4.1 depicts the Pendubot's uncontrollable positions where *a*) is the first uncontrollable position defined by $x_1 = -\frac{\pi}{2} \ \wedge x_2 = \frac{\pi}{2}$, *b*) with $x_1 = \frac{\pi}{2} \ \wedge x_2 = \frac{\pi}{2}$, *c*) with $x_1 = \pi \ \wedge x_2 = \pi$ and *d*) with $x_1 = -\pi \ \wedge x_2 = -\pi$.

4.1.2. Nonlinear Optimal Controller Design

It is worth mention that there exist a natural steady-state constraint for the Pendubot, the sum of the angles $q_1 + q_2 = \frac{\pi}{2}$, since the origin of the system was shifted up to the vertical position it follows that in the transformed coordinates system $q_1 + q_2 = 0$, using such constraint it is possible to define a reference vector r for the complete state of the system, given a time varying reference signal χ_{ref}

$$r = \begin{bmatrix} -\chi_{ref} \\ \chi_{ref} \\ -\dot{\chi}_{ref} \\ \dot{\chi}_{ref} \end{bmatrix}. \tag{4.2}$$

With the given parametrization for matrices $A(x)$ and $B(x)$ as (2.42), the optimal control law (3.7) is applied to the system, in order to track a time varying reference signal for the position of link 2 of the Pendubot. Notice that by selecting this output for the system, it becomes a nonminimum phase system. The matrices Q and R must be selected in order to obtain the desired behavior of the tracking error or the control effort respectively.

Table 4.1: Pendubot simulation parameters

Parameter	Value
l_1	$0.203m$
l_{c1}	$0.155m$
l_2	0.384
l_{c2}	$0.164m$
m_1	$0.829kg$
m_2	$0.34kg$
I_1	$0.0055kg - m^2$
I_2	$0.0041kg - m^2$
μ_1	$0.00545Ns/rad$
μ_2	$0.00047Ns/rad$
g	$9.81m/s^2$

4.1.3. Simulation Results

In order to demonstrate the performance of the nonlinear optimal tracking controller, simulations are carried out using Matlab/Simulink®, by applying the nonlinear optimal control law (3.7) to system (2.42) considering the parameters given in Table 4.1, and the following weighting matrices Q and R defined as

$$Q = \begin{bmatrix} 2000 & 0 & 0 & 0 \\ 0 & 1 & 0 & 0 \\ 0 & 0 & 10 & 0 \\ 0 & 0 & 0 & 1 \end{bmatrix}, \quad R = [1]\,. \tag{4.3}$$

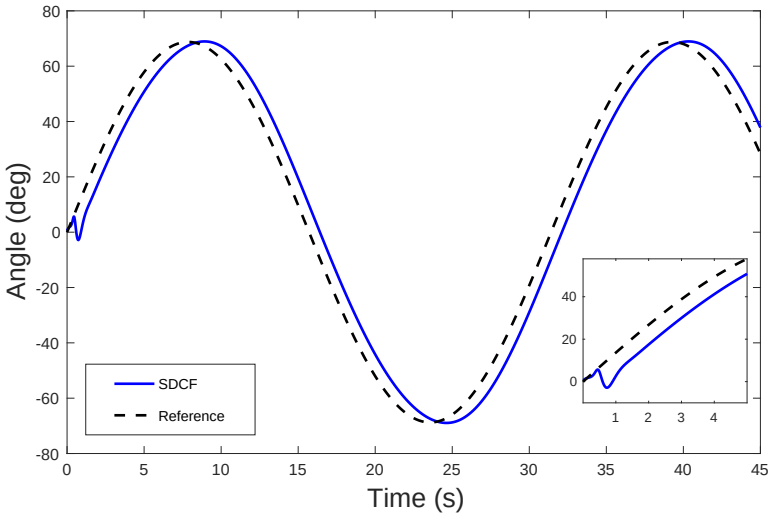

Figure 4.2: Nonlinear optimal tracking for Pendubot's link 2

The proposed controller is evaluated as follows: nonlinear optimal tracking control for x_2 is displayed in Figure 4.2, for which the desired reference is $\chi_{ref} = 1.2sin(0.2t)$, and the initial conditions for the pendubot are chosen near the equilibrium point as $x(0) = \begin{pmatrix} 1.5607, & 0.01, & 0.01, & 0.01, \end{pmatrix}^T$. In Figure 4.2, it can be seen that the output of the system, has a constant error, due to the fact that the tracking error has been bounded in a region Υ, therefore the result shown in Figure 4.2 is considered to be

the minimization of the tracking error under the optimal control (3.7), since larger values of the entries of matrix Q do not allow a decrease of the error.

4.1.4. Nonlinear Optimal Controller with Integral Action

In order to reduce the steady state error of the system as a result of the bounded error in a region Υ by the use of nonlinear optimal control based on the SDCF, an integral action is added to system (2.42), therefore it is represented as a disturbed nonlinear systems with an augmented state defined as (3.40) where

$$A_a(x_a) = \begin{bmatrix} 0 & q_2 & 0 & 0 & 0 \\ 0 & 0 & 0 & 1 & 0 \\ 0 & 0 & 0 & 0 & 1 \\ 0 & a_{31} & a_{32} & a_{33} & a_{34} \\ 0 & a_{41} & a_{42} & a_{43} & a_{44} \end{bmatrix} \quad B_a(x_a) = \begin{bmatrix} 0 \\ 0 \\ 0 \\ b_3 \\ b_4 \end{bmatrix}$$

$$C_a(x_a) = \begin{bmatrix} 0 & 0 & 0 & 0 & 0 \\ 0 & 1 & 0 & 0 & 0 \\ 0 & 0 & 1 & 0 & 0 \\ 0 & 0 & 0 & 1 & 0 \\ 0 & 0 & 0 & 0 & 1 \end{bmatrix} \quad D = \begin{bmatrix} \mathcal{X}_{ref} \\ 0 \\ 0 \\ 0 \\ 0 \end{bmatrix} \tag{4.4}$$

with $x_a = \begin{bmatrix} \Phi_2 & x_1 & x_2 & x_3 & x_4 \end{bmatrix}^T$, the given matrices $A_a(x_a), B_a, C_a(x_a)$ and D, the nonlinear optimal controller (3.43) is used. Notice that for many practical applications in most cases it is necessary the addition of an integral action in order to add robustness properties to the controller.

4.1.5. Nonlinear Optimal Sliding Mode Controller

Consider the Pendubot's nonlinear equations of motion (2.40) obtained in Chapter 2, then it is possible to represent the system dynamics into a state-space model with a more convenient structure as seen in [Serrano-Heredia11] having the form (2.6), with state $x \in \mathbb{R}^4$ of the origin and $u \in \mathbb{R}^1$, $y \in \mathbb{R}^1$. The vector $f(x)$ and the columns of $g(x)$ are smooth vector fields of appropriate dimension, choosing the variables $(x_1 \quad x_2 \quad x_3 \quad x_4)^T = (q_1 + \frac{\pi}{2} \quad q_2 \quad \dot{q}_1 \quad \dot{q}_2)^T$ as the state vector, with $u = \tau$ as the control input and x_2 as the system output, the system can be represented into the form (2.6) where

$$
\begin{aligned}
f(x) &= \begin{pmatrix} f_1(x) \\ f_2(x) \\ f_3(x) \\ f_4(x) \end{pmatrix} = \begin{pmatrix} x_3 \\ x_4 \\ g_3(x_2)p_3(x) \\ g_4(x_2)p_4(x) \end{pmatrix} \\
g(x) &= \begin{pmatrix} g_1(x) \\ g_2(x) \\ g_3(x_2) \\ g_4(x_2) \end{pmatrix} = \begin{pmatrix} 0 \\ 0 \\ \frac{D_{22}}{D_{11}D_{22}-D_{12}^2} \\ \frac{-D_{12}}{D_{11}D_{22}-D_{12}^2} \end{pmatrix} \\
h(x) &= x_2
\end{aligned}
\tag{4.5}
$$

with $p_3 = \frac{D_{12}}{D_{22}}(C_2 + G_2 + F_2) - C_1 - G_1 - F_1$, $p_4 = \frac{D_{11}}{D_{12}}(C_2 + G_2 + F_2) - C_1 - G_1 - F_1$ in a admissible region $\Omega : (-\frac{\pi}{2} \leq x_2 \leq \frac{\pi}{2})$.

Pendubot Regular Form

To design an optimal sliding mode controller for the Pendubot, it is necessary to transform the system (4.5) via differomorphism $\varphi(x)$ into the regular form (2.13)

$$x' = \begin{pmatrix} \varphi_1(x) \\ \varphi_2(x) \end{pmatrix}, \quad \varphi_1 \in \mathbb{R}^3, \quad \varphi_2 \in \mathbb{R}^1 \tag{4.6}$$

The resulting transformation (4.6) can be obtained from the condition (2.15) thus after the transformed system variables are defined as follows:

$$\begin{pmatrix} x'_1 \\ x'_2 \\ x'_3 \end{pmatrix} = \varphi_1(x) = \begin{pmatrix} x_1 \\ x_2 \\ x_3 - [g_3 g_4^{-1}] x_4 \end{pmatrix}$$
$$x'_4 = \varphi_2(x) = x_4 \tag{4.7}$$

with $g_3 g_4^{-1} = D_{22} D_{12}^{-1}$, then the regular form becomes

$$\dot{x}'_1 = \begin{pmatrix} f_1(x') \\ f_2(x') \\ f_3(x') \end{pmatrix} \tag{4.8}$$

$$\dot{x}'_2 = f_4(x') + g_4 u$$

where

$$\begin{aligned} f_1(x') &= x'_3 - D_{22} D_{12}^{-1} x'_4 \\ f_2(x') &= x'_4 \\ f_3(x') &= \Theta_1 \left(\frac{D_{12}}{D_{22}} - \frac{D_{11}}{D_{12}} \right) \Theta_2 \\ f_4(x') &= g_4 p_4 \end{aligned} \tag{4.9}$$

and $\Theta_1 = \frac{D_{22}}{D_{11} D_{22} - D_{12}^2}$, $\Theta_2 = C_2 + G_2 + F_2$.

Pendubot's Regular Form Steady State

Since for the use of the nonlinear optimal sliding mode controller, it is necessary to transform the nonlinear system into its regular form (2.13), the system reference vector for the optimal controller for the regular form first block $\dot{x}_1'$ is also affected, therefore it is necessary to compute the system's reference (steady state constraint). For a class of mechanical systems (e.g. Pendubot or rotary inverted pendulum), it is possible to define a geometrical constraint between the links angles of the system, however for a different class of nonlinear systems (e.g. biomedial, electrical) it is not possible to define a geometrical constraint in order to obtain the steady state of the system, in this sense the Francis-Isidori-Brynes equation [Isidori90] is used in order to determine the steady state for general nonlinear system in the transformed framework. For the case of the Pendubot's regular form steady state, it is obtained as follows: The output tracking error $e(x, \omega)$ is defined as the difference between the output of the system x_2' and a reference signal $r(\omega)$.

$$e = x_2 - r(\omega) \tag{4.10}$$

where the reference signal is provided by a signal generator (exosystem) described by

$$\dot{\omega} = s(\omega), \;\; s(0) \neq 0 \tag{4.11}$$

with $\omega = (\omega_1, \omega_2)^T$, and $r(\omega) = \omega_2$. Notice that an exosystem is a system with the Jacobian matrix $S = \left(\frac{\partial s}{\partial \omega}\right)$, which at the equilibrium point it has eigenvalues on the imaginary axis. For this application the exosystem is a linear system given by

$$s(\omega) = \begin{pmatrix} \alpha\omega_2 \\ -\alpha\omega_1 \end{pmatrix}, \quad \alpha > 0 \tag{4.12}$$

where ω_i and α determines the amplitude and the frequency of the signal respectively. The steady state of the system can be found in terms of the state feedback regulation problem (SFRP), which is stated in terms of the existence of a pair of mappings

$$x = \pi(\omega) \ \ and \ \ u = c(\omega) \tag{4.13}$$

which solves the partial differential Francis-Isidori-Byrnes (FIB) equations [Isidori90]

$$\begin{aligned} \frac{\partial \pi}{\partial \omega} s(\omega) &= f(\pi(\omega)) + g(\pi(\omega))c(\omega) \\ 0 &= h(\pi(\omega), \omega) \end{aligned} \tag{4.14}$$

where vector $\pi(\omega)$ is defined as $\pi'(\omega) = (\pi_1'(\omega), \pi_2'(\omega), \pi_3'(\omega), \pi_4'(\omega,))^T$. Introducing a zero output manifold and a control error defined as

$$\begin{pmatrix} e_1 \\ e_2 \\ e_3 \\ e_4 \end{pmatrix} = \begin{pmatrix} x_1' - \pi_1(\omega) \\ x_2' - \pi_2(\omega) \\ x_3' - \pi_3(\omega) \\ x_4' - \pi_4(\omega) \end{pmatrix} \tag{4.15}$$

then, $\pi(\omega)$ will be calculated with respect to system (4.8) making use of the respective regulation equations (4.14)

$$\frac{\partial \pi_1(\omega)}{\partial \omega} s(\omega) = \pi_3(\omega) \tag{4.16}$$

$$\frac{\partial \pi_2(\omega)}{\partial \omega} s(\omega) = \pi_4(\omega) \tag{4.17}$$

$$\frac{\partial \pi_3(\omega)}{\partial \omega} s(\omega) = \Theta_1 \frac{D_{12}(\pi_2(\omega))}{D_{22}} \Theta_2 - \frac{D_{11}(\pi_2(\omega))}{D_{12}(\pi_2(\omega))} \Theta_2 \tag{4.18}$$

$$0 = \pi_2(\omega) - \omega_2. \tag{4.19}$$

From (4.19), it follows that

$$\pi_2(\omega) = \omega_2 \tag{4.20}$$

replacing (4.20) in (4.17)

$$\begin{pmatrix} 0 & 1 \end{pmatrix} \begin{pmatrix} \alpha\omega_2 \\ -\alpha\omega_1 \end{pmatrix} = \pi_4(\omega)$$
$$-\alpha\omega_1 = \pi_4(\omega). \tag{4.21}$$

Notice that it is needed to known the complete vector $\pi(\omega)$; however, the values of $\pi_1(\omega)$ and $\pi_3(\omega)$ are not easy to calculate since they are part of a set of nonlinear partial differential equations, but it is possible to calculate an approximate solution based on the following power series, as seen in [J. Rivera08]:

$$\begin{aligned} \pi_1(\omega) = a_0 &+ a_1\omega_1 + a_2\omega_2 + a_3\omega_1^2 + a_4\omega_1^2 + a_4\omega_1\omega_2 \\ &+ a_5\omega_2^2 + a_6\omega_1^3 + a_7\omega_1^2\omega_2 + a_8\omega_1\omega_2^2 + a_9\omega_2^3 \\ &+ O^4(||\omega||_1) \end{aligned} \tag{4.22}$$

where $O^4(||\omega||_1)$ represents the high order terms from the approximation which are despised, then replacing (4.22) into (4.16) yields to the approximated solution for $\pi_3'(\omega)$

$$\begin{aligned} \pi_3(\omega) = \alpha(&a_1\omega_2 - a_2\omega_1 + 2a_3\omega_1\omega_2 + a_4\omega_2^2 - a_4\omega_1^2 \\ &- 2a_5\omega_1\omega_2 + 3a_6\omega_1^2\omega_2 + 2a_7\omega_1\omega_2^2 - a_7\omega_1^3 \\ &+ a_8\omega_2^3 - 2a_8\omega_1^2\omega_2 - 3_a 9\omega_1\omega_2^2 \\ &- D_{22}D_{12}^{-1}(\omega_2)\omega_1) + O^4(||\omega||_1). \end{aligned} \tag{4.23}$$

By using this Taylor series expansion on (4.18) around the equilibrium point $x = (\frac{\pi}{2}, 0, 0, 0)^T$ the values of the coefficients $a_i (i = 0, \ldots, 9)$ can be found, as shown in Table 4.2.

Figure 4.3 shows the reference steady-state vector for the Pendubot system described in the regular form, selecting $\omega = 0.2\, rad$ and $\alpha = 1\, rad$.

Table 4.2: Parameters Taylor series expansion

Coefficient	**Value**
a_0	1.570757
a_1	-0.0025944
a_2	-1.001871
a_3	0
a_4	0
a_5	0
a_6	0
a_7	0.001926
a_8	0
a_9	-0.00001588

4.1.6. Simulation Results

The proposed nonlinear optimal tracking controller, is evaluated as follows, considering the Pendubot's transformation into the regular form (4.8), the nonlinear optimal sliding mode controller (3.55) is applied for the regular form first block having the following SDCF representation

$$\dot{x}'_1 = \begin{bmatrix} 0 & 0 & 1 \\ 0 & 0 & 0 \\ a_{31} & a_{32} & a_{33} \end{bmatrix} \begin{bmatrix} x'_1 \\ x'_2 \\ x'_3 \end{bmatrix} + \begin{bmatrix} 0 \\ b_2 \\ b_3 \end{bmatrix} x'_2 \tag{4.24}$$

$$y = x'_2$$

where the entries of the matrix $A(x')$ and $B(x')$ are defined as follows

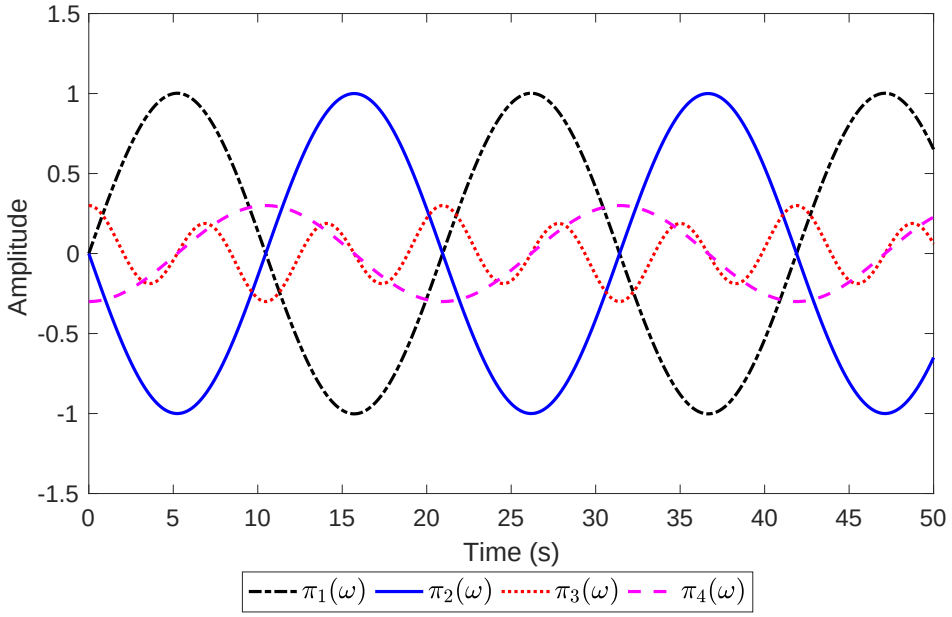

Figure 4.3: References for the Pendubot's transformed system into the regular form, generated by the solution of the Francis -Isidori equations

$$
\begin{aligned}
a_{31} &= \frac{sin(x1)}{x1}\left(\frac{g\theta_5 cos(x_2)}{\theta_2 + \theta_3 cos(x_2)}\right) \\
a_{32} &= \frac{sin(x2)}{x2}\left(\frac{-\theta_3 x_3^2}{\theta_2 + \theta_3 cos(x_2)} + \frac{g\theta_5 cos(x_1)}{\theta_2 + \theta_3 cos(x_2)}\right) \\
a_{33} &= 0 \\
b_1 &= 1 \\
b_2 &= -\frac{\mu_2}{\theta_2 + \theta_3 cos(x_2)}
\end{aligned}
$$

with a reference vector is defined as

$$
r = \begin{bmatrix} \pi_1(\omega) \\ \pi_2(\omega) \\ \pi_3(\omega) \end{bmatrix}. \tag{4.25}
$$

The effectiveness of the nonlinear optimal sliding mode controller is proven via simulation results using Matlab/Simulink® and SimMechanics/SolidWorks®. Where the initial conditions for the pendubot are chosen near the equilibrium point as selected for the SDCF controller; $x(0) = \begin{pmatrix} 1.5607, & 0.01, & 0.01, & 0.01, \end{pmatrix}^T$, the parameters given by Table (4.1) and a reference signal $\chi_{ref} = 1.2sin(0.2t)\, rad$. For the nonlinear optimal control, the entries of matrices Q and R are selected as

$$Q(x) = \begin{bmatrix} 100000 & 0 & 0 \\ 0 & \frac{1}{0.5|\chi_{ref} - x_2| + 1} & 0 \\ 0 & 0 & 10 \end{bmatrix}, \quad R = [1]\,. \tag{4.26}$$

And for the Pendubot's regular form second block x_2', the sliding modes super-twisting gains are user defined in order to fulfill the desired system response requirements, for this simulation they were chosen as: $M_1 = 10$ and $M_2 = 0.8$. Using a sampling period of $0.001s$.

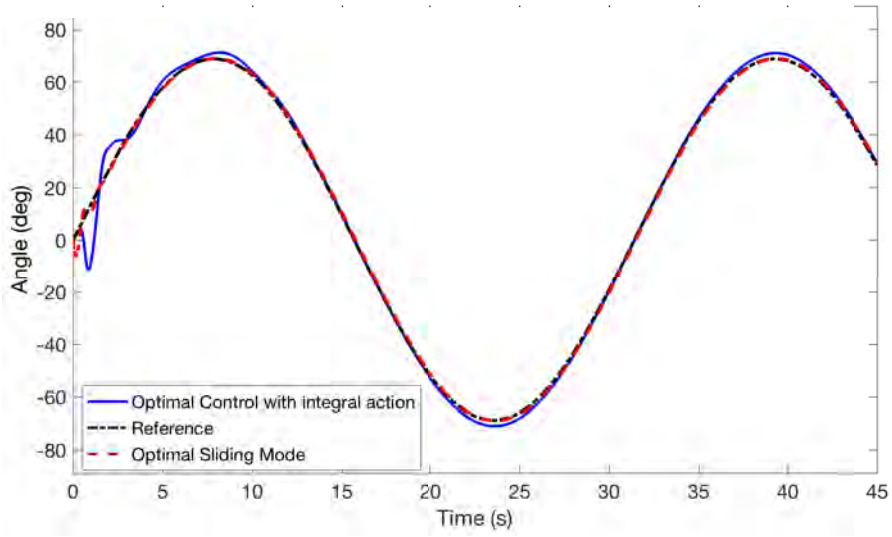

Figure 4.4: Comparison between optimal tracking based on the SDCF with integral action and optimal sliding mode for the Pendubot's link 2

Figure 4.4 displays a comparison between the optimal tracking control with an integral

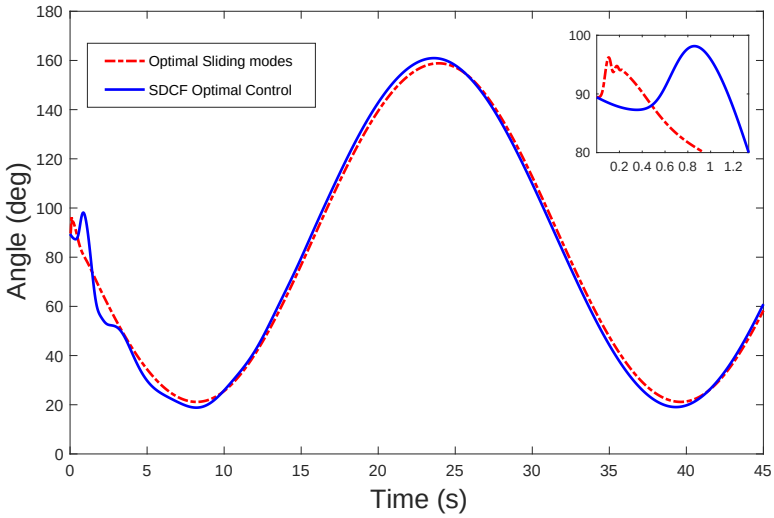

Figure 4.5: Link 1 position during the optimal tracking for link 2

action with $Q_i = 80$ and the nonlinear optimal tracking control for the Pendunbot's link 2. Simulations results depicts that by the use of the SDCF optimal control, it is possible to obtain a wider operation range for tracking a time varying signal for the Pendubot's link 2 ($\pm$ 70°), in comparison with related works, for instance [Rivera08] with $\pm$ 8° tracking range, [Serrano-Heredia11], [Cai03] with $\pm$ 60° and [Erdem01] where the use SDCF was only used for stabilization and the tracking problem not considered. Also it is possible to appreciate that with the optimal sliding modes there exists a reduction in the transient effect, in comparison with the nonlinear optimal control with integral action.

Figure 4.5 depicts the position of link 1 during both nonlinear optimal tracking control with integral action and nonlinear optimal sliding modes. Notice that simulation results fulfill the natural steady state constraint for the Pendubot.

In Figure 4.6, it can be seen that by the application of high-order sliding modes (super-twisting controller), the control action results in a smooth function rather

than a discontinuous function, which makes this controller attractive for real time applications.

In Figure 4.7, the velocities for link 1 and 2 are shown.

In Figure 4.8, it can be seen the convergence of the sliding mode controller which constrains the system over a manifold where the sliding surface is defined as $\sigma(x) = 0$. The transient effect shown in the simulation is due to the fact that the nonlinear optimal sliding mode controller requires a reaching time t_s, in order to constrain the system to lie within the manifold. And from there on the performance index will be optimized by the action of the optimal control.

Figure 4.9, depicts the "Pseudocontrol" action, which serves as a reference signal for the super-twisting controller.

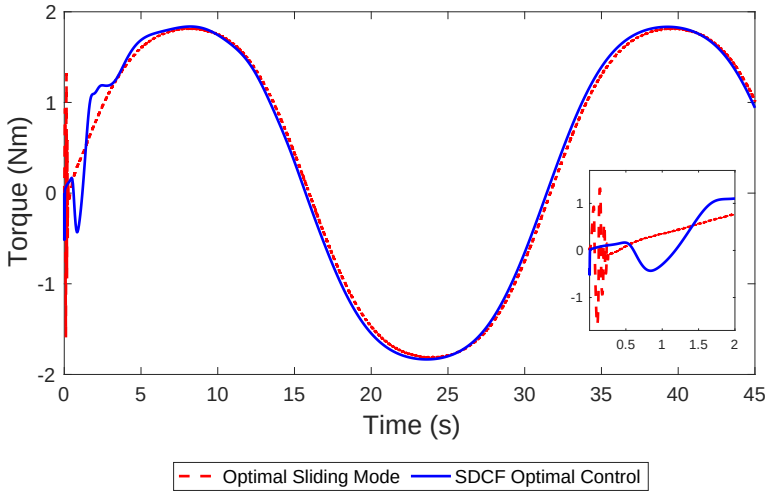

Figure 4.6: Pendubot's control law, (applied torque)

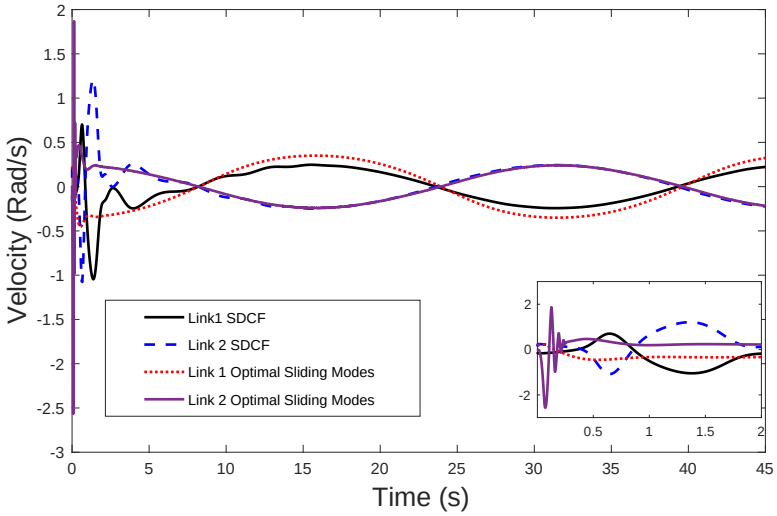

Figure 4.7: Pendubot's velocities during optimal tracking

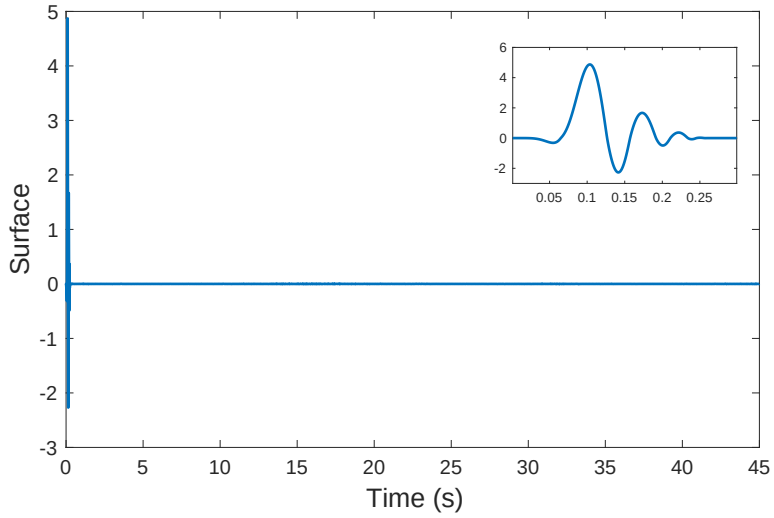

Figure 4.8: Sliding surface reaching the condition $\sigma = 0$

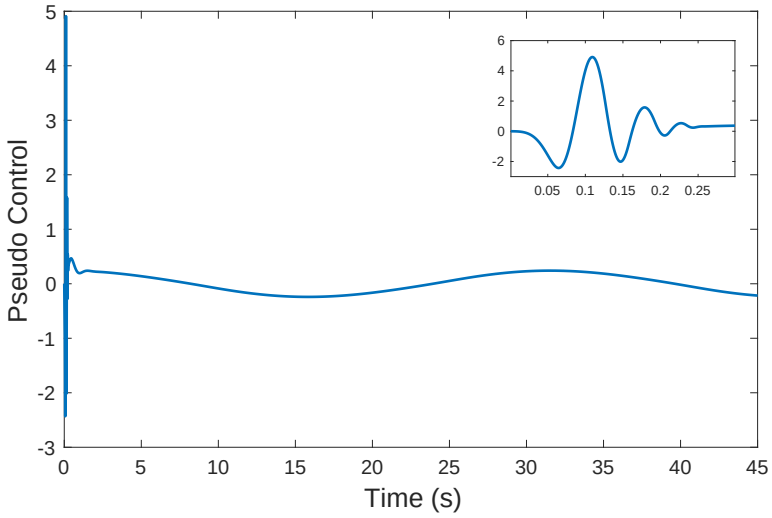

Figure 4.9: Pseudo control action x_2'

4.1.7. SolidWorks/SimMechanics® Simulation

Simscape Multibody (formerly SimMechanics®) provides a multibody simulation environment for $3D$ mechanical systems, such as robots, vehicle suspensions, construction equipment, and aircraft landing gear. It is possible to model multibody systems using blocks representing bodies, joints, constraints, force elements, and sensors. Simscape Multibody formulates and solves the equations of motion for the complete mechanical system. Due to the lack of the Pendubot's physical system in the laboratory of Faculty of Electrical Engineering of the Universidad Michoacana, this analysis tool was applied to the pendubot as shown in Figure 4.10, in order to have a complete simulation of the system dynamics under the action of the proposed controllers.

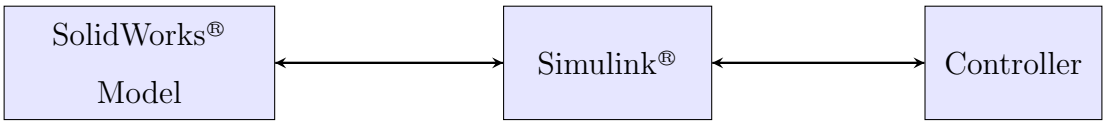

Figure 4.10: Mechanical simulation loop scheme.

In Figure 4.11 the Pendubot's mechanical simulation is depicted, during the nonli-

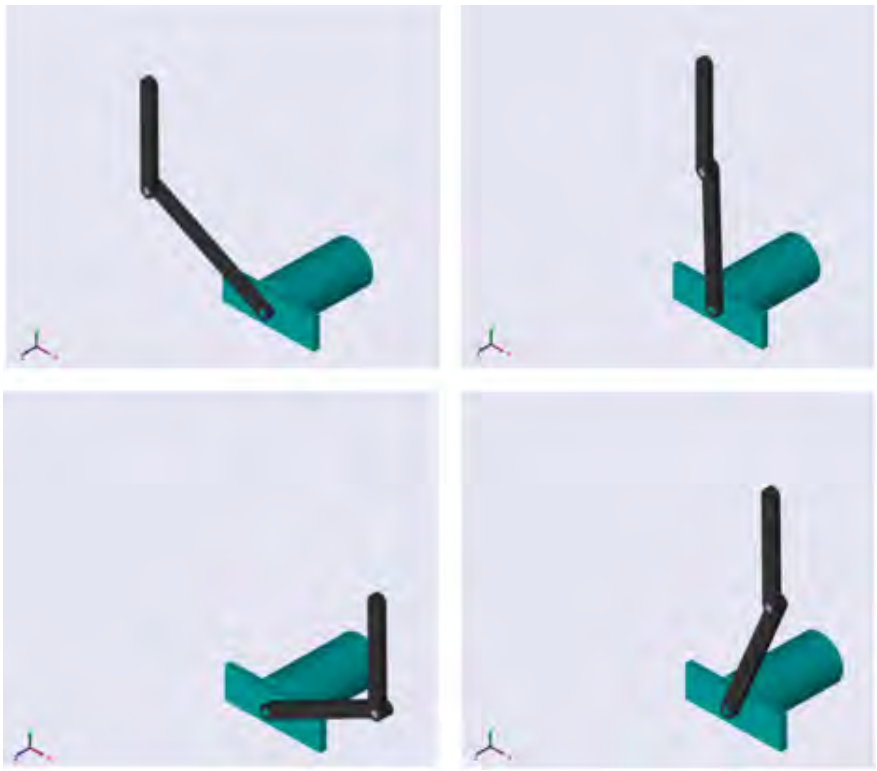

Figure 4.11: Pendubot's mechanical Simulation

near optimal sliding mode control application, tracking a time varying reference signal for the Pendubot's link 2.

4.2. Application to the Rotary Inverted Pendulum

In order to show the effectiveness of the nonlinear optimal tracking controller, simulations and a real time implementation are carried out, using the nonlinear optimal controller based on the SDCF.

4.2.1. Simulations and Real-Time Experimental Results

Consider the rotary inverted pendulum equations of motion (2.44) and (2.45), obtained from Chapter 2. Once the equation of motion are represented into the SDCF

Table 4.3: Rotary Inverted Pendulum parameters

Parameter	Value
m_p	$0.1270Kg$
L_r	$0.2159m$
L_p	$0.3365m$
J_r	$9.9829e^{-4}Kg-m^2$
J_p	$0.0012Kg-m^2$
B_r	0.0024
B_p	0.0024
η_g	0.90
η_m	0.69
K_g	70
k_t	$7.68x10^{-3}N-m/A$
k_m	$7.68x10^{-3}V/(rad/s)$
R_m	$2.6\,\Omega$

as (2.6), then it is possible to apply the nonlinear optimal tracking controller (3.7), where the vector r is defined as the desired trajectory for the complete state vector. The main objective of the controller (considering the case of the rotary inverted pendulum) is to stabilize the underactuated link over their upward vertical position, while the actuated link tracks a desired reference. Therefore the given reference for the link 2 is 0, thus vector r is defined as

$$r = \begin{bmatrix} \chi_{ref} & 0 & \dot{\chi}_{ref} & 0 \end{bmatrix}^T \tag{4.27}$$

where χ_{ref} is the desired reference to be tracked, while the values of matrices Q and R must be selected in order to obtain the desired behavior of the tracking error or the control effort respectively. The initial conditions for the rotary inverted pendulum are given as: $x_1(0) = -0.01$, $x_2(0) = 0.01$, $x_3(0) = -0.01$ and $x_4(0) = 0.01$, using a sampling period of $0.001s$. The entries of matrices Q and R are defined as

$$Q(x) = \begin{bmatrix} 500 & 0 & 0 & 0 \\ 0 & 1000 & 0 & 0 \\ 0 & 0 & 10 & 0 \\ 0 & 0 & 0 & 10 \end{bmatrix}, \quad R = [30]\,. \tag{4.28}$$

With the system parameters as shown in Table 4.3. The proposed controller is evaluated as follows. Figure 4.12, shows the stabilization of the controlled variable (link 1) over different references, then the nonlinear optimal tracking controller is applied in order to track a time varying reference signal, the controller references χ_{ref} are described as follows

$$\chi_{ref} = \begin{pmatrix} 0\ rad\ \ if\ \ 0 < t < 21s \\ 1\ rad\ \ if\ \ 21s < t < 43s \\ 0\ rad\ \ if\ \ 43s < t < 52s \\ -1\ rad\ \ if\ \ 52s < t < 62.6s \\ 0\ rad\ \ if\ \ 62.6s < t < 63s \\ 1.1sin(0.2t)\ rad\ \ if\ \ 62.6s < t < 111.67s \\ 0\ rad\ \ if\ \ t > 111.67s \end{pmatrix} \tag{4.29}$$

where clearly the tracking for the desired reference is achieved by using the proposed controller. In Figure 4.13, the pendulum stabilization over their upward vertical position is shown, notice that a swing-up controller is not considered, therefore the pendulum is manually moved from their downward vertical position to their upward vertical position where the nonlinear optimal controller is activated.

Figure 4.20 displays the applied voltage to the servo motor gear box, during the optimal tracking control.

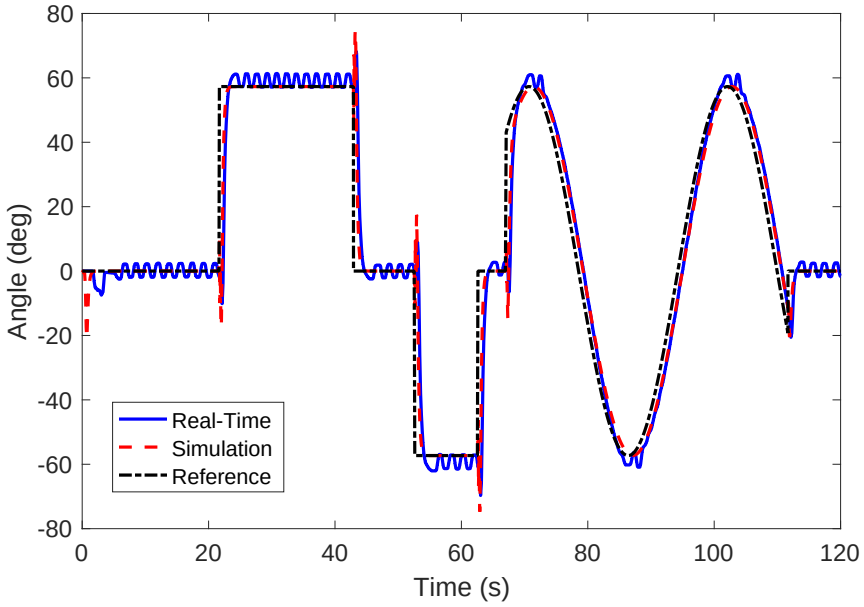

Figure 4.12: Rotary arm nonlinear optimal tracking control for θ over different references, then it tracks a time varying reference signal.

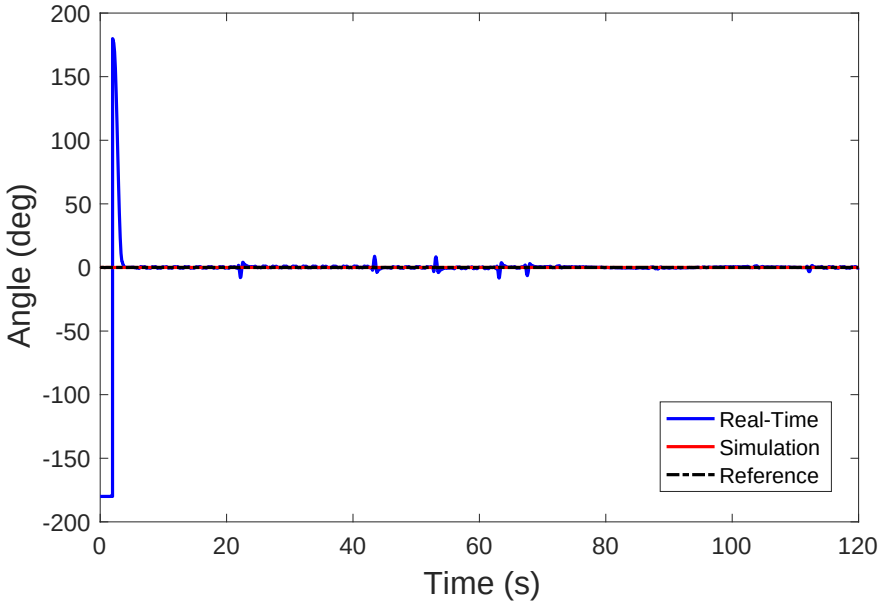

Figure 4.13: Pendulum stabilization

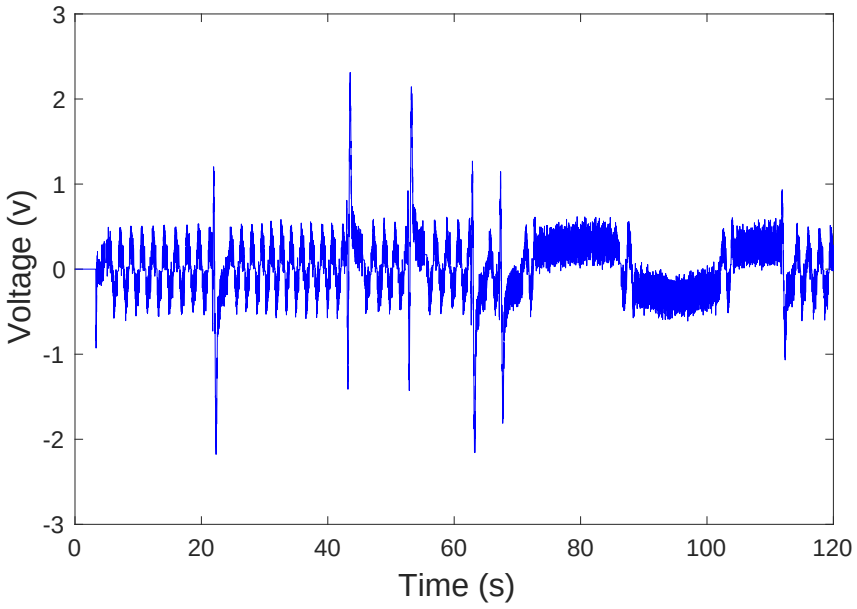

Figure 4.14: Applied voltage to servo-motor unit

4.2.2. Hardware Description and Data Acquisition

The rotary inverted pendulum physical system Figure 4.15, is located in the control laboratory of the graduated studies division of the Faculty of Electrical Engineering (UMSNH), which uses a Q8-USB Quanser® data acquisition device, and the servo amplifier voltPAQ-X1 from Quanser®. The motor is a Quanser® rotary servo unit base.

The rotary inverted pendulum physical prototype, is composed by the following components:

- ◇ The data acquisition device Quanser Q8-usb Figure 4.16, which is a measurement and control board with an extensive range of analog and digital input and output and encoders support, is used in order to measure the state variables of the system which are provided by encoder.

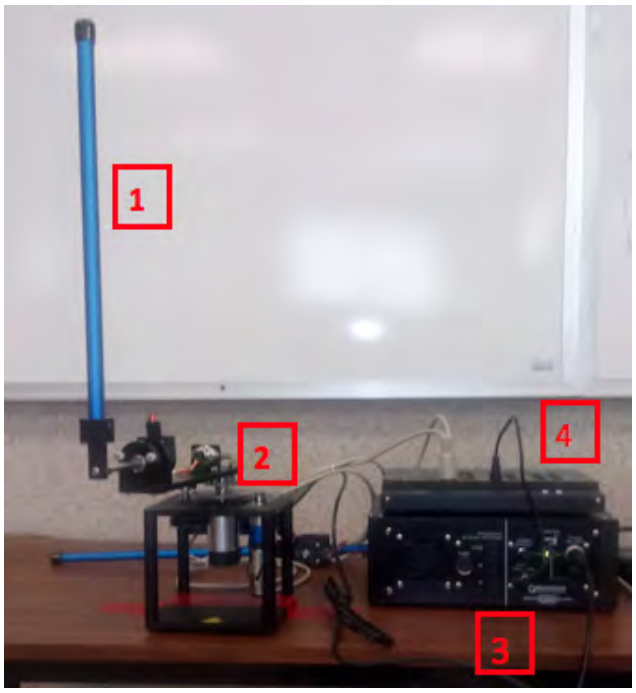

Figure 4.15: Complete rotary inverted pendulum system, which is composed by the following elements: 1) pendulum, 2) SRV02 rotary servo unit, 3) VoltPAQ-X1 power amplifier and 4) Q8-usb data acquisition device.

- ◇ The servo unit rotary base Figure 4.17, consists of a DC motor that is encased in a solid aluminum frame and equipped with a planetary gearbox. The system is equipped with three sensors: potentiometer, encoder, and tachometer. The potentiometer and encoder sensors measure the angular position of the load gear and the tachometer can be used to measured its velocity. Notice that for real time applications where the servo unit is used in order to drive the motion of a kinematic chain the servo unit model must be considered in the full model of the system.

- ◇ The VoltPAQ-X1 Figure 4.18, is linear voltage-controlled amplifier, pairing the VoltPAQ-X1 with Quanser data acquisition board it is possible to control physical systems as the rotary inverted pendulum.

- ◇ The Rotary Inverted Pendulum module attached to the Rotary Servo Base Unit

Figure 4.19.

The real time experiment carried out for the Rotary Inverted Pendulum can be found at:

http://dep.fie.umich.mx/~fornelas/data/uploads/video1.mov

https://www.youtube.com/watch?v=KiTNdwVf3p8&feature=youtu.be

4.3. Conclusions

In this chapter the effectiveness of the nonlinear optimal controller as well as the optimal sliding mode are proven via simulations for the Pendubot and both simulation and experimental results for the rotary inverted pendulum, which validates the models obtained from Chapter 2, and the controllers developed in Chapter 3. As a result of the simulation carried out for the Pendubot it was possible to appreciate that as the system reference approached the uncontrollable positions of the system, simulation errors were found mainly of numeric character, since the proposed controller has a wider tracking result in comparison with the controllers reported in the literature for the Pendubot, for instance [Rivera08],[Serrano-Heredia11],[Cai03]. It was considered that it is possible to check the advantage offered by the nonlinear optimal controller.

Figure 4.16: Quanser Q8-usb data acquisition device board

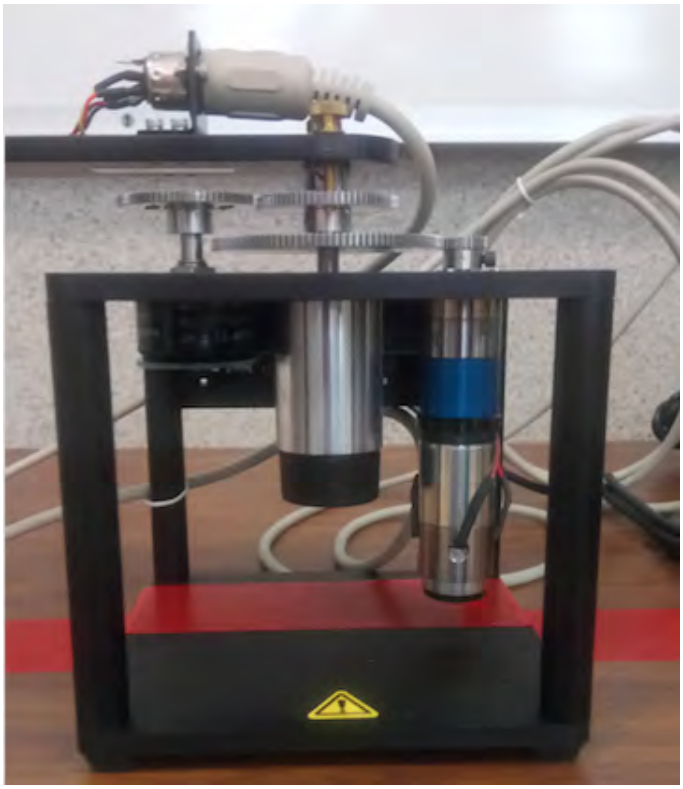

Figure 4.17: Servo motor gear-box

Figure 4.18: Quanser VoltPAQ-X1, power amplifier

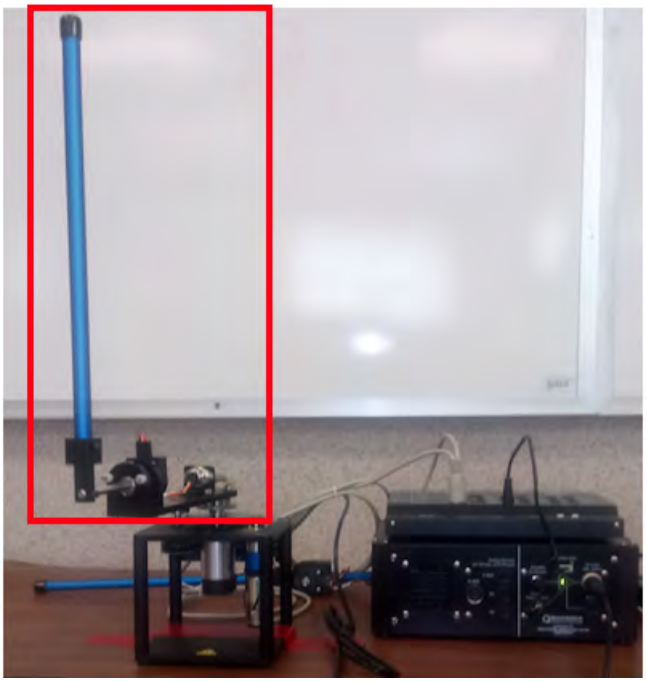

Figure 4.19: Rotary Inverted Pendulum, rotary arm and pendulum links

Figure 4.20: Real time experiment for the rotary inverted pendulum

Chapter 5

Conclusions and Future Work

5.1. General Conclusions

In this thesis the nonlinear optimal control techniques and the sliding modes, based on the SDCF representation, are applied for a class of mechanical systems. Derived on the research carried out together with the simulations and experimental results, the following facts can be concluded:

- ◇ The nonlinear optimal tracking control theory can be applied to general mechanical systems in order to be stabilized over a reference, or to track a time varying reference signal.

- ◇ Optimal control theory based on the SDCF can be used for the design of nonlinear controllers to directly handle with the non-minimum phase property associated with the underactuated mechanical systems. This result may be generalized for a class of systems which exhibits unstable internal dynamics.

- ◇ It is possible to combine nonlinear optimal control with sliding modes for a class of nonlinear systems, which can be represented into the so-called regular-form; by doing this, it is possible to take advantage of the optimality criterion derived

from the optimal control and the robustness properties from the sliding mode controller.

- ◇ Through the use of the nonlinear optimal control with sliding modes, it is possible to take advantage of the nonlinear regular form, in order to decouple the system into two different block, where the first block (which is considered to be a reduced order subsystem) controlled with an optimal control scheme, has a simpler structure that the second block, which is controlled by a robust controller, which do not require information of the parameters of the system. By doing so, it possible to have a robust nonlinear optimal controller able to reject parametric uncertainties and external disturbances.

- ◇ Nonlinear optimal control based on the SCDF is a suitable control scheme for real time applications without a great computational effort.

5.2. Future Work

This work represents the opportunity to continue investigating on the nonlinear optimal control systems and the sliding modes, as well as their properties and applications to mechanical systems, below are some proposals that could enrich the research within this area:

1. Obtain real-time experimental results for the nonlinear optimal sliding mode controller designed for the Pendubot.

2. Design state observers based on the SDCF.

3. Apply the nonlinear optimal control based on the SDCF to a different class of mechanical systems such as unmanned aerial vehicles (UAV), locomotive robotic systems, automotive mechatronic systems.

4. Apply nonlinear optimal control for disturbed nonlinear systems in the presence of unknown external disturbances.

5. Investigate methods in order to find the best factorization of the nonlinear system represented into the SCDF.

Appendix A

Nonlinear Optimal Stabilizing Controller Proof

Consider the following nonlinear system represented into the SDCF form

$$\dot{x} = A(x)x + B(x)u \tag{A.1}$$

Then the optimal control law u^* is applied where

$$u^* = -R^{-1}B^T(x)P(x)x \tag{A.2}$$

Therefore the behavior of the close loop system is given by

$$\dot{x} = \left(A(x) - B(x)R^{-1}B^T(x)P(x)\right)x \tag{A.3}$$

The stability of the system is proved in terms of the Lyapunov theory therefore the following Lyapunov candidate function is proposed

$$V(x) = x^T P x \tag{A.4}$$

$$\dot{V}(x) = x^T \dot{P} x + x^T P \dot{x} + \dot{x}^T P x \tag{A.5}$$

$$\begin{aligned}\dot{V}(x) = x^T\dot{P}x + x^T[PA(x) - PB(x)R^{-1}B^T(x)P(x) \\ +A^T(x)P - PB(x)R^{-1}B^T(x)P(x)]\end{aligned} \tag{A.6}$$

$$\dot{V}(x) = x^T\dot{P}x + x^T\left[PA(x) + A^T(x)P - 2PB(x)R^{-1}B^T(x)P(x)\right] \tag{A.7}$$

$$\dot{P} = -C(x)^TQC(x) + PB(x)R^{-1}B(x)^TP - A(x)^TP - PA(x) \tag{A.8}$$

$$-\dot{P} - C(x)^TQC(x) + PB(x)R^{-1}B(x)^TP = A(x)^TP + PA(x) \tag{A.9}$$

$$\dot{V}(x) = x^T\dot{P}x - x^T\left[\dot{P} + C(x)^TQC(x) + PB(x)R^{-1}B(x)^TP\right]x \tag{A.10}$$

$$\dot{V}(x) = x^T\dot{P}x - x^T\dot{P}x - \left[C(x)^TQC(x) + PB(x)R^{-1}B(x)^TP\right]x \tag{A.11}$$

$$\dot{V}(x) = -\left[C(x)^TQC(x) + PB(x)R^{-1}B(x)^TP\right]x \tag{A.12}$$

$$\dot{V}(x) < 0 \tag{A.13}$$

That is (A.1) with (A.2) has an asymptotically stable equilibrium point [Khalil02].

Appendix B

Nonlinear Optimal Tracking Controller Proof

Consider the following nonlinear system represented into the SDCF form

$$\dot{x} = A(x)x + B(x)u \tag{B.1}$$

Then the optimal control law u^* is applied where

$$u^* = -R^{-1}B^T(x)(P(x)x - z(x)). \tag{B.2}$$

Therefore, the behavior of the close loop system is given by

$$\dot{x} = \left[A(x) - B(x)R^{-1}B^T(x)P(x)\right]x + B(x)R^{-1}B^T(x)z(x). \tag{B.3}$$

System (B.3) can be analyzed as a dynamical system with a forcing term z, due to the fact that the solution of the SDRE does not depend on the solution of the differential vector z as seen in [Ornelas-Tellez13], the stability analysis for the nominal part can be established as

$$\dot{x} = \left[A(x) - B(x)R^{-1}B^T(x)P(x)\right]z \tag{B.4}$$

The stability of the system is proved in terms of the Lyapunov theory; therefore, the following Lyapunov candidate function is proposed

$$V(x) = x^T P(x) x \tag{B.5}$$

Taking the time derivate of $V(x)$ along the nominal system B.4, thus

$$\dot{V}(x) = x^T \dot{P}(x) x + x^T P(x) \dot{x} + \dot{x}^T P(x) x \tag{B.6}$$

By replacing (3.8) and (B.4) into (B.6) it follows that

$$\dot{V}(x) = x^T \dot{P}(x) x + x^T \left[P(x)A(x) + A^T P(x) - 2P(x)BR^{-1}B^T P(x) \right] x \tag{B.7}$$

from (3.8) it follows that

$$P(x)A(x) + A^T(x)P(x) = -\dot{P}(x) - C^T(x)QC(x) + P(x)B(x)R^{-1}B^T(x)P(x) \tag{B.8}$$

Equation (B.7) becomes

$$\begin{aligned} \dot{V}(x) &= x^T \dot{P}(x) x + x^T \left[-\dot{P}(x) - C^T(x)QC(x) - P(x)B(x)R^{-1}B^T(x)P(x) \right] x \\ &= -x^T \left[C^T(x)QC(x) + P(x)B(x)R^{-1}B^T(x)P(x) \right] x \end{aligned} \tag{B.9}$$

That is (B.1) with (B.2) has an asymptotically stable equilibrium point [Khalil02].

Appendix C

Super-Twisting Stability Proof

The super-twisting algorithm defined by

$$\begin{aligned} u(x) &= -M_1|\sigma|^{\frac{1}{2}}sign(\sigma) + u_1 \\ \dot{u}_1(x) &= -M_2 sign(\sigma), \quad M_1 > 0, \;\; M_2 > 0 \\ \sigma &= \lambda - \lambda_i \end{aligned} \tag{C.1}$$

with $M_1, M_2 > 0$ is able to drive the trajectories of the second order sliding mode on the sliding manifold in finite time.

The stability of the Super-Twisting algorithm (C.1) has been proven in [Moreno08] in the sense of Lyapunov theory by proposing the following candidate Lyapunov function

$$\begin{aligned} V(x) &= 2M_2|\sigma| + \frac{1}{2}u_1^2 + \frac{1}{2}\left(M_1|\sigma|^{\frac{1}{2}}sign\,(\sigma) - u_1\right)^2 \\ &= \xi^T P \xi \end{aligned} \tag{C.2}$$

where $\xi = \left(|\sigma|^{\frac{1}{2}}sign(\sigma)u_1\right)$ and

$$P = \frac{1}{2}\begin{pmatrix} 4M_2 + M_1^2 & -M_1 \\ -M_1 & 2 \end{pmatrix}. \tag{C.3}$$

The time derivate along the Super-Twisting algorithm (3.53) is given by

$$\dot{V}(x) = -\frac{1}{|\sigma^{\frac{1}{2}}|}\xi^T Q\xi + \frac{f(\sigma,t)}{|\sigma^{\frac{1}{2}}|}q_1^T\xi \tag{C.4}$$

where

$$Q = \frac{M_1}{2}\begin{pmatrix} 2M_2 + M_1^2 & -M_1 \\ -M_1 & 1 \end{pmatrix} \tag{C.5}$$

$$q_1^T = \left(2M_1 + \frac{1}{2}M_1^2 - \frac{1}{2}M_1\right). \tag{C.6}$$

According with the procedure described in [Moreno08], the expresion (C.4) can be reduced to

$$\dot{V}(x) = -\frac{M_1}{2|\sigma^{\frac{1}{2}}|}\xi^T\tilde{Q}\xi \tag{C.7}$$

where

$$\tilde{Q} = \frac{M_1}{2}\begin{pmatrix} 2M_2 + M_1^2 - \left(\frac{4M_2}{M_1} + M_1\right)\delta_1 - 2\delta_2 & \star \\ -\left(M_1 + 2\delta_1 + \frac{2\delta_2}{M_1}\right) & 1 \end{pmatrix} \tag{C.8}$$

There is exponential convergence if $(P_0 - \tilde{Q}) > 0$ if

$$\begin{aligned} M_2 &> 2\delta_3 \\ M_4 &> \frac{2\delta_3 M_2^3 + (\frac{1}{4}\delta_3^2 + 3\delta_4)M_2^2 + \delta_3\delta_4 M_2 + \delta_4^2}{M_2(M_2 - 2\delta_3)} \end{aligned} \tag{C.9}$$

Appendix D

Gear-Box Mathematical Modeling

Consider a DC motor armature circuit and a power train gear as seen in Fig. (D.1)

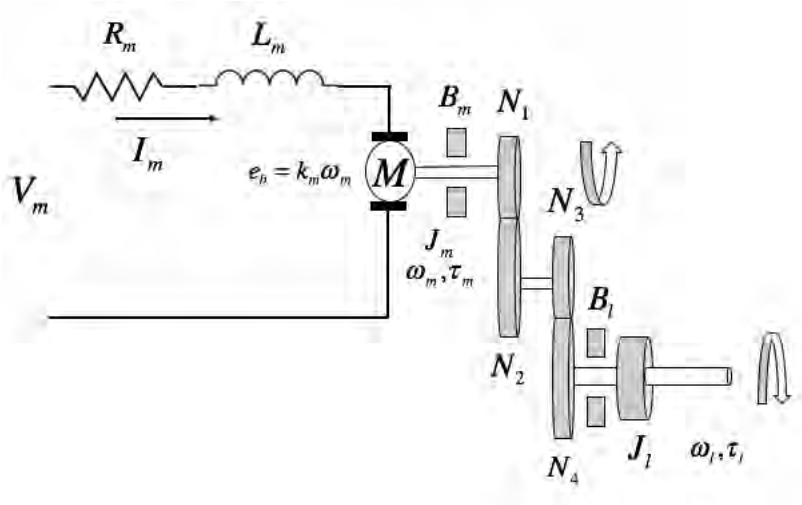

Figure D.1: Gear-box and DC motor

where R_m is the motor resistance, L_m is the inductance and k_m is the back-emf constant. The back-emf voltaje e_b depends on the motor speed shaft ω_m, which opposes the current flow, therefore the back emf voltage is given by:

$$e_b(t) = k_m\omega_m(t) \tag{D.1}$$

Analyzing the electrical circuit mesh, by using Kirchoff's voltage law

$$V_m(t) - R_m I_m(t) - L_m \frac{dI_m(t)}{dt} - k_m \omega_m(t) = 0 \tag{D.2}$$

Assuming that the motor inductance $L_m < R_m$, thus L_m can be ignored, therefore (D.2) becomes:

$$V_m - R_m I_m(t) - k_m \omega_m(t) = 0 \tag{D.3}$$

solving for I_m

$$I_m(t) = \frac{V_m(t) - k_m \omega_m(t)}{R_m} \tag{D.4}$$

Since the motor gear-box has one DOF, it is possible to apply the Newton's second law of motion described as

$$J\alpha = \tau \tag{D.5}$$

where J is the inertia moment of the body about its centroid, α is the angular acceleration of the system and τ is the sum of applied torques. Due to the fact that there are viscous frictional terms acting over the system, a viscous acting force on the motor shaft B_m and the load shaft B_l are considered, then (D.5) is expressed as

$$J_l = \frac{d\omega_l(t)}{dt} + B_l \omega_l(t) = \tau_l(t) \tag{D.6}$$

where J_l is the inertia moment of the load and τ_l is the applied torque to the load. Then the motor shaft equation is described as

$$J_m \frac{d\omega_m(t)}{dt} + B_m \omega_m(t) + \tau_{ml}(t) = \tau_m(t) \tag{D.7}$$

where J_m is the inertia moment of the motor shaft and τ_{ml} is the resulting torque acting on the motor shaft and the load. Where the torque applied to the load can be described by

$$\tau_l = \eta_g K_g \tau_{ml}(t) \tag{D.8}$$

where K_g is the gear ratio and η_g is the gear box efficiency, for planetary gearboxes the gear ratio is represented by N_1 and N_2 where

$$K_{g_{internal}} = \frac{N_2}{N_1} \tag{D.9}$$

which is the internal gearbox ratio, for the motor gear N_3 and the load N_4, the gear ratio is defined as

$$K_{g_{external}} = \frac{N_4}{N_3}. \tag{D.10}$$

Then from (D.9) and (D.10) the power train gear ratio is defined as:

$$K_g = K_{g_{external}} K_{g_{internal}}. \tag{D.11}$$

Therefore the applied torque at the motor shaft is expressed as

$$\tau_{ml} = \frac{\tau_l(t)}{\eta_g K_g}. \tag{D.12}$$

Assuming that the motor shaft must rotate K_g times for each output revolution, the the following expression can be obtained:

$$\theta_m(t) = K_g \theta_l(t). \tag{D.13}$$

Then the relationship between the angular speed of the motor shaft ω_m and the angular speed of the shaft can be found

$$\omega_m(t) = K_g \omega_l(t). \tag{D.14}$$

The differential equation which describes the gearbox motion is obtained by replacing (D.12),(D.14) and (D.7) into (D.6) where

$$J_m K_g \frac{d\omega_l(t)}{dt} + B_m K_g \omega_l(t) + \frac{J_l(\frac{d\omega_l(t)}{dt}) + B_l \omega_l(t)}{\eta_g K_g} = \tau_m. \tag{D.15}$$

Defining the terms

$$\begin{aligned} J_{eq} &= \eta_g K_g^2 J_m + J_l \\ B_{eq1} &= \eta_g K_g^2 B_m + B_l. \end{aligned} \tag{D.16}$$

Equation (D.15) derives in

$$J_{eq} \frac{d\omega_l(t)}{dt} + B_{eq} \omega_l(t) = \eta_g K_g \tau_m(t). \tag{D.17}$$

Considering that the motor torque is proportional to the applied torque the following expression is given

$$\tau_m(t) = \eta_t I_m(t) \tag{D.18}$$

expressing the motor torque in terms of the input voltage V_m and the load shaft speed ω_l and substituting the motor armature current (D.4) into the current torque relationship (D.18), the following expression is obtained

$$\tau_m = \frac{\eta_m k_t (V_m(t) - k_m \omega_m(t)}{R_m}. \tag{D.19}$$

Appendix E

Real-Time Software Installation

In order to have a correct operation of the system it is necessary to take care of the following indications

E.1. Step 1

It is necessary a personal computer running Microsoft-Windows® 7, Windows 8.1 or Windows 10, both 32 and 64 bit-version are supported, ensure the corresponding Matlab® *R*2014*b*, *R*2015*a* or *R*2015 version is installed on the computer. It is very important to ensure that the with Matlab installation the following add ons are accompanying the software:

- ◇ Simulink
- ◇ Simulink Coder
- ◇ Matlab Coder
- ◇ Control System Toolbox

Otherwise the system would no function

E.2. Step 2

Install a Microsoft Compiler, the Quaser-Software Quarc requieres a Matlab supported $C++$ compiler, ensure that only one of the following $c++$ compilers is installed:

- ◇ Microsoft Visual Studio Professional Edition 2012 (version 11.0) or 2013 (version 12.0).
- ◇ Microsoft Windows SDK 7.1.

Caveat if the Microsoft Windows SDK 7.1 is attempt to be installed, an installation failure may occur under two scenarios:

- ◇ If Microsoft Visual C++ 2010 SP1 (Express or Professional) is installed.
- ◇ If Microsoft Visual C++ 2010 redistributable packages (x64 or x86) are installed.

To avoid this issue:

1. Uninstall the Microsoft Visual $C++$ 2010 redistributable packages (both $x86$ as well as $x64$).
2. Install the Windows SDK 7.1. During installation, under the Installation Options menu, UNCHECK the "Visual $C++$ Compilers" and "Microsoft Visual $C++$ 2010" components.
3. Apply the SDK 7.1 patch from below:

   `http://www.microsoft.com/en-us/download/details.aspx?displaylang=en&id=4422`

4. Reinstall the Microsoft Visual C++ 2010 redistributable packages from

   `http://www.microsoft.com/en-us/download/details.aspx?id=14632`
   `http://www.microsoft.com/en-us/download/details.aspx?id=5555`

Appendix F

Matlab/Simulink® Simulation Codes

F.1. Pendubot's Simulink® Model

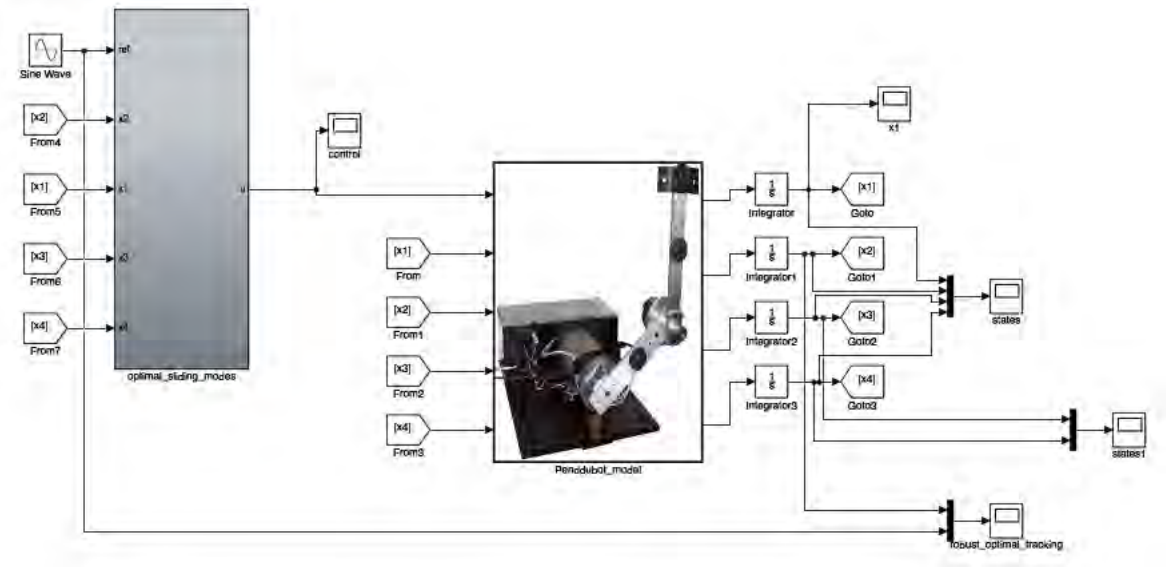

Figure F.1: Simulink® Pendubot's controller simulation model

F.1.1. Nonlinear Optimal Sliding Mode Controller

Simulink® Code

```
function [u,p11d,p12d,p13d,p21d,p22d,p23d,p31d,p32d,p33d,z1d,z2d,z3d,u1d,S,Ups]=
 fcn(ref,refd,x1,x2,x3,x4,p11,p12,p13,p21,p22,p23,p31,p32,p33,z1,z2,z3,u1)



th1 = 0.0399466;
th2 = 0.00952431;
th3 = 0.0113025;
th4 = 0.197753;
th5 = 0.0556227;
mu1 = 0.00545;
mu2 = 0.00047;
g = 9.8;

det = (1/((th2 + th3*cos(x2))*(th1*th2 - th3^2*cos(x2)^2)));

a11 = 0;
a12 = 0;
a13 = 1;

a21 = 0;
a22 = 0;
a23 = 0;

a31 = det*(sin(x1)/x1)*(-g*th1*th3*th5*cos(x2)^2 - g*th2*th3*th5*cos(x2)^2
- 2*g*th3^2*th5*cos(x2)^3);
a32 = det*(sin(x2)/x2)*(-g*th1*th3*th5*cos(x1)*cos(x2) - g*th2*th3*th5*cos(x1)*cos(x2)
- 2*g*th3^2*th5*cos(x1)*cos(x2)^2);
a33 = det*(th1*th3^2*x3*cos(x2)*sin(x2) + th2*th3^2*x3*cos(x2)*sin(x2)
+ 2*th3^3*x3*cos(x2)^2*sin(x2));

b1 = 0;
b2 = 1;
b3 = det*(mu2*th1*th3*cos(x2) + mu2*th2*th3*cos(x2) + 2*mu2*th3^2*cos(x2)^2);



A = [a11,a12,a13;a21,a22,a23;a31,a32,a33];
B = [b1;b2;b3];

C = [1,0,0;0,1,0;0,0,1];
X = [x1;x2;x3];

R = 1;
q1 = 100000;
q2 = 1/(0.5*abs(ref-x2)+1);
q3 = 1;

Q = [q1,0,0;0,q2,0;0,0,q3];

q3d = ref;
q4d = refd;
q2d = -refd;

r = [-q3d;q3d;q2d];

P = [p11,p12,p13;p21,p22,p23;p31,p32,p33];
z = [z1;z2;z3];
```

```
Pd = C'*Q*C-P*B*inv(R)*B'*P+A'*P+P*A;
zd =(A-B*inv(R)*B'*P)'*z+C'*Q*r;

p11d = Pd(1,1);
p12d = Pd(1,2);
p13d = Pd(1,3);
p21d = Pd(2,1);
p22d = Pd(2,2);
p23d = Pd(2,3);
p31d = Pd(3,1);
p32d = Pd(3,2);
p33d = Pd(3,3);
z1d = zd(1,1);
z2d = zd(2,1);
z3d = zd(3,1);
Ups = -inv(R)*B'*(P*X-z);
m1 = 10;
m2 = 0.8;
S = Ups -x4;
u1d = -m1*sign(S);
% Super Twisting
u = -m2*sqrt(abs(S))*sign(S)+u1;
```

F.1.2. Nonlinear Optimal Controller based on SDCF

Simulink® Code

```
function [p11d,p12d,p13d,p14d,p21d,p22d,p23d,p24d,p31d,p32d,p33d,p34d,p41d,p42d,p43d,p44d,z1d,z2d,z3d,z4d,U,e]=
fcn(p11,p12,p13,p14,p21,p22,p23,p24,p31,p32,p33,p34,p41,p42,p43,p44,z1,z2,z3,z4,x1,x2,x3,x4,ref,refd,ei)

q1 = 2000;
q2 = 1;
q3 = 1;
q4 = 10;
r1 = 1;

th1 = 0.0399466;
th2 = 0.00952431;
th3 = 0.0113025;
th4 = 0.197753;
th5 = 0.0556227;
mu1 = 0.00545;
mu2 = 0.00047;
g = 9.8;

q3d = ref;
q4d = refd;
q2d = -refd;


r = [-q3d;q3d;q2d;q4d];


a11 = 0;
a12 = 0;
a13 = 1;
a14 = 0;
a21 = 0;
a22 = 0;
```

```
a23 = 0;
a24 = 1;

det = (1/(-(th2 + th3*cos(x2))^2 + th2*(th1 + th2 + 2*th3*cos(x2))));

a31 = det*(sin(x1)/x1)*(g*th2*th4 - g*th3*th5*cos(x2)^2);
a32 = det*(sin(x2)/x2)*(th2*th3*x3^2 + 2*th2*th3*x3*x4 + th2*th3*x4^2 + th3^2*x3^2*cos(x2)
- g*th3*th5*cos(x1)*cos(x2));
a33 = det*(-mu1*th2);
a34 = det*(mu2*th2 + mu2*th3*cos(x2));

a41 = (sin(x1)/x1)*det*(-g*th2*th4 - g*th3*th4*cos(x2) + g*th1*th5*cos(x2)
+ g*th3*th5*cos(x2)^2);
a42 = (sin(x2)/x2)*det*(-th1*th3*x3^2 - th2*th3*x3^2 - 2*th2*th3*x3*x4 - th2*th3*x4^2
+ g*th1*th5*cos(x1)
- 2*th3^2*x3^2*cos(x2) - 2*th3^2*x3*x4*cos(x2) - th3^2*x4^2*cos(x2)
+ g*th3*th5*cos(x1)*cos(x2));
a43 = det*(mu1*th2 + mu1*th3*cos(x2));
a44 = det*(-mu2*th1 - mu2*th2 - 2*mu2*th3*cos(x2));

b3 = (th2)/(th1*th2 - th3^2*cos(x2)^2);
b4 = -(((th2 + th3*cos(x2)))/(th1*th2 - th3^2*cos(x2)^2));

A = [a11,a12,a13,a14;a21,a22,a23,a24;a31,a32,a33,a34;a41,a42,a43,a44];
B = [0;0;b3;b4];
C = [1,0,0,0;0,1,0,0;0,0,1,0;0,0,0,1];
Q = [q1,0,0,0;0,q2,0,0;0,0,q3,0;0,0,0,q4];
R = r1;

P = [p11,p12,p13,p14;p21,p22,p23,p24;p31,p32,p33,p34;p41,p42,p43,p44];
z = [z1;z2;z3;z4];
X = [x1;x2;x3;x4];

Pd = C'*Q*C-P*B*inv(R)*B'*P+A'*P+P*A;
zd =(A-B*inv(R)*B'*P)'*z+C'*Q*r;

p11d = Pd(1,1);
p12d = Pd(1,2);
p13d = Pd(1,3);
p14d = Pd(1,4);
p21d = Pd(2,1);
p22d = Pd(2,2);
p23d = Pd(2,3);
p24d = Pd(2,4);
p31d = Pd(3,1);
p32d = Pd(3,2);
p33d = Pd(3,3);
p34d = Pd(3,4);
p41d = Pd(4,1);
p42d = Pd(4,2);
p43d = Pd(4,3);
p44d = Pd(4,4);

z1d = zd(1,1);
z2d = zd(2,1);
z3d = zd(3,1);
z4d = zd(4,1);

U = -inv(R)*B'*(P*X-z);
```

F.2. RIP Simulink® Model

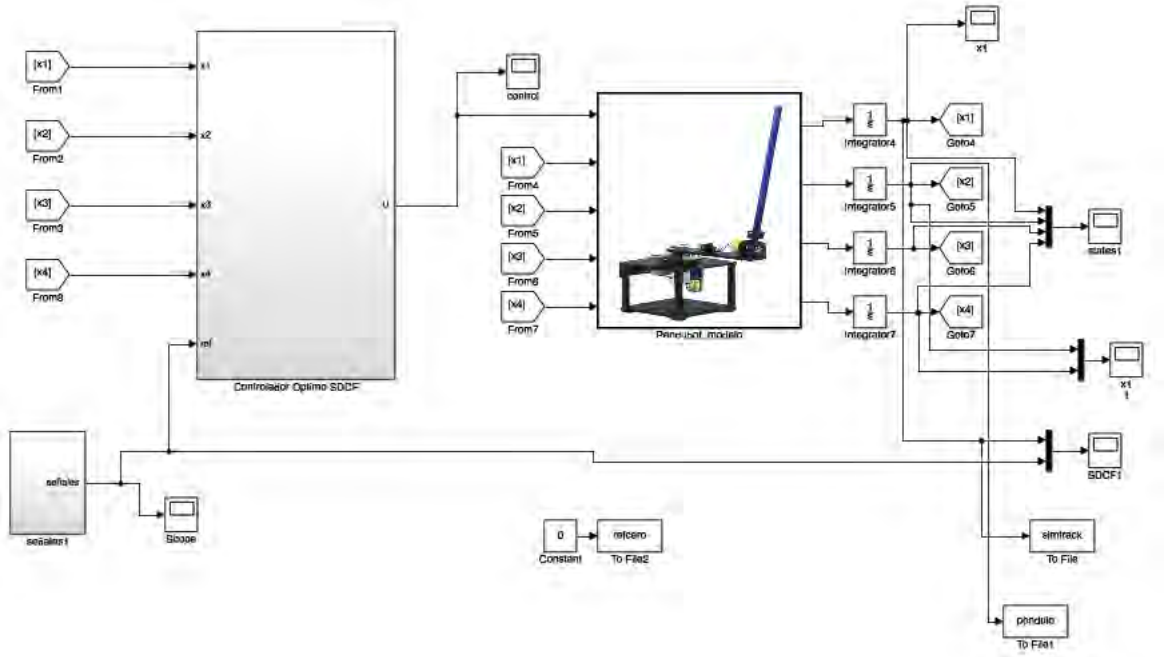

Figure F.2: Simulink® RIP controller simulation model

F.3. Nonlinear Optimal Controller based on SDCF

Simulink® Code

```
function [p11d,p12d,p13d,p14d,p21d,p22d,p23d,p24d,p31d,p32d,p33d,p34d,p41d,p42d,p43d,p44d,z1d,z2d,z3d,z4d,U]
=fcn(p11,p12,p13,p14,p21,p22,p23,p24,p31,p32,p33,p34,p41,p42,p43,p44,z1,z2,z3,z4,x1,x2,x3,x4,ref,refd)


q1 = 500;
q2 = 1000;
q3 = 10;
q4 = 10;

r1 = 30;

th1 = 0.00692521;
th2 = 0.00360582;
th3 = 0.00462229;
th4 = 0.00480772;
th5 = 0.0213995;
mu2 = 0.0005;
mu1 = .5;
```

```
g = 9.8;
Jt = 1.1883e-05;
Jr = 9.9829e-04;
Jp = 0.0012;
Mp = 0.1270;
Lp = 0.3365;
Lr = 0.2159;
g = 9.8100;
Dr = 0.0024;
Dp = 0.0024;
Kg = 70;
kt = 0.0077;
km = 0.0077;
Rm = 2.6000;


r = [ref;0;refd;0];


a11 = 0;
a12 = 0;
a13 = 1;
a14 = 0;

a21 = 0;
a22 = 0;
a23 = 0;
a24 = 1;

det = (1/((th1 + th2)*th4 - (th3^2 + th2*th4)*cos(x2)^2));


a31 = 0;
a32 = det*(sin(x2)/x2)*(-th3*th4*x4^2 + g*th3*th5*cos(x2) - 2*th2*th4*x3*x4*cos(x2)
 + th2*th3*x3^2*cos(x2)^2);
a33 = det*(-mu1*th4);
a34 = det*(-mu2*th3*cos(x2));

a41 = 0;
a42 = det*(sin(x2)/x2)*(g*th1*th5 + g*th2*th5 + th1*th2*x3^2*cos(x2) + th2^2*x3^2*cos(x2)
 - th3^2*x4^2*cos(x2) - g*th2*th5*cos(x2)^2 - 2*th2*th3*x3*x4*cos(x2)^2 - th2^2*x3^2*cos(x2)^3);
a43 = det*(-mu1*th3*cos(x2));
a44 = det*(-mu2*th1 - mu2*th2 + mu2*th2*cos(x2)^2);

b3 = (th4)/((th1 + th2)*th4 - (th3^2 + th2*th4)*cos(x2)^2);
b4 = (th3*cos(x2))/((th1 + th2)*th4 - (th3^2 + th2*th4)*cos(x2)^2);


A = [a11,a12,a13,a14;a21,a22,a23,a24;a31,a32,a33,a34;a41,a42,a43,a44];
B = [0;0;b3;b4];
C = [1,0,0,0;0,1,0,0;0,0,0,0;0,0,0,0];

A(3,3)= A(3,3)-Kg^2*kt*km/Rm*B(3);
A(4,3)= A(4,3)-Kg^2*kt*km/Rm*B(4);
B = Kg*kt*B/Rm;


Q = [q1,0,0,0;0,q2,0,0;0,0,q3,0;0,0,0,q4];
R = r1;

P = [p11,p12,p13,p14;p21,p22,p23,p24;p31,p32,p33,p34;p41,p42,p43,p44];
z = [z1;z2;z3;z4];
X = [x1;x2;x3;x4];
```

```
Pd = C'*Q*C-P*B*inv(R)*B'*P+A'*P+P*A;
zd =(A-B*inv(R)*B'*P)'*z+C'*Q*r;

p11d = Pd(1,1);
p12d = Pd(1,2);
p13d = Pd(1,3);
p14d = Pd(1,4);
p21d = Pd(2,1);
p22d = Pd(2,2);
p23d = Pd(2,3);
p24d = Pd(2,4);
p31d = Pd(3,1);
p32d = Pd(3,2);
p33d = Pd(3,3);
p34d = Pd(3,4);
p41d = Pd(4,1);
p42d = Pd(4,2);
p43d = Pd(4,3);
p44d = Pd(4,4);

z1d = zd(1,1);
z2d = zd(2,1);
z3d = zd(3,1);
z4d = zd(4,1);

U = -inv(R)*B'*(P*X-z);
```

Appendix G

List of publications

1. Nonlinear Optimal Control in Combination with Sliding Modes: Applied to the Pendubot, 2017 IEEE International Autumn Meeting on Power, Electronics and Computing (ROPEC 2017). Ixtapa, Mexico. (Under review)

References

[Anderson90] Anderson, B. D. *Optimal Control Linear Quadratic Methods*. Dover Publications, Englewood Cliffs, New Jersey, USA, 1990.

[Antsaklis07] Antsaklis, P. J. y Michel, A. N. *A Linear Systems Primer*. Birkhauser, Boston, USA, 2007.

[Athans07] Athans, M. y Falb, P. L. *Optimal Control an Introduction to the Theory and its Applications*. Dover, New York, USA, 2007.

[Bartolini98] Bartolini, G., Ferrara, A., y Usai, E. Chattering avoidance by second-order sliding mode control. *IEEE Transactions on Automatic Control*, 43(2):241–246, Feb 1998.

[Bellman57] Bellman, R. E. *Dynamic Programming*. Princeton University Press, Princeton, USA, 1957.

[Cai03] Cai, Z. y Su, C.-Y. Real-time tracking control of underactuated pendubot using takagi-sugeno fuzzy systems. *En Proceedings 2003 IEEE International Symposium on Computational Intelligence in Robotics and Automation. Computational Intelligence in Robotics and Automation for the New Millennium*, tomo 1, págs. 73–78 vol.1. July 2003.

[Carlson87] Carlson, D., Haurie, A., y Leizarowitz, A. *Infinite Horizon Optimal Control*. Springer-Verlag, Berlin, Germany, 1987.

[Chang12] Chang, X.-H. *Takagi-Sugeno Fuzzy Systems Non-fragile H-infinity Filtering*. Springler, Berlin, Germany, 2012.

[Cimen10] Cimen, T. Systematic and effective design of nonlinear feedback controllers via the state-dependent riccati equation (sdre) method. *Annual Reviews in Control*, 34(1):32 – 51, 2010.

[Cloutier97] Cloutier, J. R. State-dependent riccati equation techniques: an overview. *En Proceedings of the 1997 American Control Conference (Cat. No.97CH36041)*, tomo 2, págs. 932–936 vol.2. Jun 1997.

[Cloutier02] Cloutier, J. R. y Stansbery, D. T. The capabilities and art of state-dependent riccati equation-based design. *En Proceedings of the 2002 American Control Conference (IEEE Cat. No.CH37301)*, tomo 1, págs. 86–91 vol.1. May 2002.

[Dang14] Dang, Q. V., Allouche, B., Vermeiren, L., Dequidt, A., y Dambrine, M. Design and implementation of a robust fuzzy controller for a rotary inverted pendulum using the takagi-sugeno descriptor representation. *En 2014 IEEE Symposium on Computational Intelligence in Control and Automation (CICA)*, págs. 1–6. Dec 2014.

[Diaz-Sepulveda16] Diaz-Sepulveda, R., Ornelas-Tellez, F., y Sanchez, E. N. Real-time optimal tracking control for a three-phase inverter. *En 2016 13th International Conference on Electrical Engineering, Computing Science and Automatic Control (CCE)*, págs. 1–5. Sept 2016.

[Dorf08] Dorf, R. C. *Modern Control Systems*. Pearson Prentice Hall, USA, 2008.

[Edward98] Edward, C. y Spurgeon, S. *Sliding Mode Control*. Taylor and Francis, London, UK, 1998.

[Eom15] Eom, M. y Chwa, D. Robust swing-up and balancing control using a nonlinear disturbance observer for the pendubot system with dynamic friction. *IEEE Transactions on Robotics*, 31(2):331–343, April 2015.

[Erdem01] Erdem, E. B. y Alleyne, A. G. Experimental real-time sdre control of an underactuated robot. *En Proceedings of the 40th IEEE Conference on Decision and Control (Cat. No.01CH37228)*, tomo 3, págs. 2986–2991 vol.3. 2001.

[Farooq15] Farooq, U., Gu, J., El-Hawary, M. E., Balas, V. E., y Asad, M. U. Experimental study of optimal takagi sugeno fuzzy controller for rotary inverted pendulum. *En 2015 IEEE International Conference on Fuzzy Systems (FUZZ-IEEE)*, págs. 1–7. Aug 2015.

[Feng16] Feng, L., Ni, Q., Bai, Y., Chen, X., y Zhao, Y. Optimal sliding mode control for spacecraft rendezvous with collision avoidance. *En 2016 IEEE Congress on Evolutionary Computation (CEC)*, págs. 2661–2668. July 2016.

[Fridman02] Fridman, L. y Levant, L. *Sliding mode control in engineering*, cap. High-Order Sliding Modes. Marcel-Dekker, Manchester, UK, 2002.

[Fridman14] Fridman, L. y Poznyak, A. *Robust Output Lq Optimal Control Via Integral Sliding Modes*. Birkhauser, New York, USA, 2014.

[Friedland.96] Friedland., B. *Advanced Control Systems Design*. Prentice Hall, USA, 1996.

[Furuta93] Furuta, K., Yamakita, M., y and, K. N. Swing up control of a double pendulum. *En 1993 American Control Conference*, págs. 2229–2233. June 1993.

[Galicia12] Galicia, M., Loukianov, A., Rivera, J., y Utkin, V. I. Discrete-time sliding mode regulator for nonminimum phase systems. *En 2012 IEEE 51st IEEE Conference on Decision and Control (CDC)*, págs. 7708–7713. Dec 2012. ISSN 0191-2216. doi: 10.1109/CDC.2012.6425813.

[Gruebler17] Gruebler, M. *Getriebelehre*. Springler Verlag, Berlin, Germany, 1917.

[Hammett98] Hammett, D., Hall, C., y Ridgely, B. Controllability issues in nonlinear state-dependent riccati equation control. *Journal of guidance, control and dynamics*, 21:767–773, oct 1998.

[Hermann83] Hermann, R. Pfaffian systems and feedback linearization/obstructions. *En The 22nd IEEE Conference on Decision and Control*, págs. 119–121. Dec 1983.

[Isidori90] Isidori, A. y Byrnes, C. I. Output regulation of nonlinear systems. *IEEE Transactions on Automatic Control*, 35(2):131–140, Feb 1990.

[Isidori95] Isidori, A. *Nonlinear Control Systems*. Springler, Berlin, Germany, 1995.

[Isidori13] Isidori, A. The zero dynamics of a nonlinear system: From the

origin to the latest progresses of a long successful story. *European Journal of Control*, 19(5):369 – 378, 2013.

[J. Rivera08] J. Rivera, A. L. y Castillo-Toledo, B. Discontinuous output regulation of the pendubot. *Proceeding of the 17th world congress The international federation of automatic control Seoul Korea*, 2008.

[Jadlovská13] Jadlovská, S. y Sarnovský, J. Application of the state-dependent riccati equation method in nonlinear control design for inverted pendulum systems. *En 2013 IEEE 11th International Symposium on Intelligent Systems and Informatics (SISY)*, págs. 209–214. Sept 2013.

[Kalman59] Kalman, R. On the general theory of control systems. *IRE Transactions on Automatic Control*, 4(3):110–110, Dec 1959.

[Kathpal17] Kathpal, A. y Singla, A. Simmechanics; based modeling, simulation and real-time control of rotary inverted pendulum. *En 2017 11th International Conference on Intelligent Systems and Control (ISCO)*, págs. 166–172. Jan 2017.

[Khalil02] Khalil, H. K. *Nonlinear systems*. Prentice Hall, USA, 2002.

[Kirk04] Kirk, D. E. *Optimal Control Theory an Introduction*. Dover Publications, New York, USA, 2004.

[Kokotovic97] Kokotovic, P. *Constructive Nonlinear Control*. Springler-Verlag, Berlin, Germany, 1997.

[Levant93] Levant, A. Sliding order and sliding accuracy in sliding mode control. *International Journal of Control*, 1993.

[Loukianov80] Loukianov, V. U. Methods of reducing equations for dynamic systems to a regular form. *Institute of Control Problems, Avtomatika i Telemekhanika*, 1980.

[Moreno08] Moreno, J. A. y Osorio, M. A lyapunov approach to second-order sliding mode controllers and observers. *En 2008 47th IEEE Conference on Decision and Control*, págs. 2856–2861. Dec 2008.

[Moylan74] Moylan, P. Implications of passivity in a class of nonlinear systems. *IEEE Transactions on Automatic Control*, 19(4):373–381, Aug 1974.

[Mullhaupt98] Mullhaupt, P., Srinivasan, B., y Bonvin, D. On the nonminimum-phase characteristics of two-link underactuated mechanical systems. *En Proceedings of the 37th IEEE Conference on Decision and Control (Cat. No.98CH36171)*, tomo 4, págs. 4579–4583 vol.4. Dec 1998.

[Mullhaupt09] Mullhaupt, P. *Underactuated Mechanical Nonminimum-Phase Systems: Analysis and Control*. VDM Publishing, 2009.

[Nguyen03] Nguyen, H. *A First Course in Fuzzy and Neural Control*. Chapman and Hall, Florida, USA, 2003.

[Norton98] Norton, R. L. *Design of Machinery*. McGraw-Hill Series in Mechanical Engineering, New York, USA, 1998.

[Ornelas-Tellez13] Ornelas-Tellez, F., Rico-Melgoza, J. J., y Sanchez, E. N. Optimal tracking for a class of nonlinear systems based on the state-dependent riccati equation. *En 2013 10th International Conference on Electrical Engineering, Computing Science and Automatic Control (CCE)*, págs. 42–47. Sept 2013.

[Ornelas-Tellez14] Ornelas-Tellez, F., Graff, M., y Sanchez, E. N. Pso optimal tracking control for state-dependent coefficient nonlinear systems. *En 2014 World Automation Congress (WAC)*, págs. 588–592. Aug 2014.

[Ortega98] Ortega, R. y Sira-Ramirez, H. *Passivity-Based Control Of Euler-Lagrange Systems*. Springer, Berlin, Germany, 1998.

[Reinholtz98] Reinholtz, C. *Mecanismos y Dinámica de Maquinaria*. Limusa, Mexico, 1998.

[Rivera08] Rivera, J., Loukianov, A., y Toledo, B. C. Discontinuous output regulation of the pendubot. *En Proceedings of the 17th World Congress The International Federation of Automatic Control*. July 2008.

[Saber01] Saber, R. O. *Nonlinear Control of Underactuated Mechanical Systems with Application to Robotics and Aerospace Vehicles*. Tesis Doctoral, Massachusetts Institute of Technology, 2001.

[Serrano-Heredia11] Serrano-Heredia, J., Loukianov, A. G., y Bayro-Corrochano, E. Sliding mode block control regulation of the pendubot. *En 2011 50th IEEE Conference on Decision and Control and European Control Conference*, págs. 8249–8254. Dec 2011.

[Shamma03] Shamma, J. S. y Cloutier, J. R. Existence of sdre stabilizing feedback. *IEEE Transactions on Automatic Control*, 48(3):513–517, Mar 2003.

[Slotine91] Slotine, J.-J. E. *Applied Nonlinear Control*. Prentice Hall, New Jersey, USA, 1991.

[Spong95] Spong, M. y Block, J. The pendubot: a mechatronic system for control research and education. *En Proceedings of 1995 34th IEEE Conference on Decision and Control*, tomo 1, págs. 555–556 vol.1. Dec 1995.

[Su83] Su, R. y Meyer, G. Canonical forms for nonlinear systems. *NASA Technical Reports Server*, 1983.

[Utkin92] Utkin, V. I. *Sliding Modes in Control and Optimization*. Springer-Verlag, New Delhi, India, 1992.

[Utkin99] Utkin, V. I. *Sliding Modes Control in Electromechanical systems*. Taylor and Francis, 1999.

[Vidyasagar89] Vidyasagar, M. *Robot Dynamics and Control*. John Wiley & Sons inc., Canada, 1989.

[Wang11] Wang, Z. y Guo, Y. Unified control for pendubot at four equilibrium points. *IET Control Theory Applications*, 5(1):155–163, January 2011.

[Wernli75] Wernli, A. y Cook, G. Suboptimal control for the nonlinear quadratic regulator problem. *Automatica*, 11, 1975.

[Yang16] Yang, C. *Advanced Technologies in Modern Robotic Applications*. Springer, Beijing, China, 2016.